

11-1-2023

Controlling Guest Binding to Transition Metal Hosts Via Redox Stimuli

Jasmine S. Sanford

Louisiana State University and Agricultural and Mechanical College

Follow this and additional works at: https://repository.lsu.edu/gradschool_dissertations

 Part of the [Inorganic Chemistry Commons](#)

Recommended Citation

Sanford, Jasmine S., "Controlling Guest Binding to Transition Metal Hosts Via Redox Stimuli" (2023). *LSU Doctoral Dissertations*. 6324.

https://repository.lsu.edu/gradschool_dissertations/6324

This Dissertation is brought to you for free and open access by the Graduate School at LSU Scholarly Repository. It has been accepted for inclusion in LSU Doctoral Dissertations by an authorized graduate school editor of LSU Scholarly Repository. For more information, please contact gradetd@lsu.edu.

CONTROLLING GUEST BINDING TO TRANSITION METAL HOSTS VIA REDOX STIMULI

A Dissertation

Submitted to the Graduate Faculty of the
Louisiana State University and
Agricultural and Mechanical College
in partial fulfillment of the
requirements for the degree of
Doctor of Philosophy

in

The Department of Chemistry

by
Jasmine Shermaine Sanford
B.Sc. Louisiana State University, 2017
December 2023

Acknowledgements

First, I thank God for blessing me with this experience. I have gained wisdom and self-confidence throughout my Ph.D. journey. Thank you to my parents, Cornell and Stacey Sanford and for my brother and sister, Bryan and Toni, for their tremendous love, guidance, and support.

Thank you to my advisor, Dr. Maverick, for welcoming me into his group and for all of his advice and support in helping me becoming a better chemist and communicator throughout my graduate career. I am appreciative of him giving me the opportunities to present our research to other scientists in workshops and conferences.

I am also indebted to Dr. Frank R. Fronczek and Dr. Weiwei Xie for teaching me how to perform crystallography and for gladly volunteering to always educate me more on X-ray structures. Thank you to Dr. Thomas Weldeghiorghis and Dr. Zhang for instructing me on how to perform NMR studies and to Dr. Connie David and Dr. Fabrizio Donnarumma for aiding me to understand mass spectrometry data.

Thank you to my other committee members, Dr. Chambers, Dr. Haber, and my Dean's Representative, Dr. Constant for all of the advice and encouragement that they have given me throughout my time as a graduate student. Also, thank you to Dr. Tyrslai Williams for being a mentor to me and always motivating me to get out of my comfort zone to help me build my self-confidence.

I would also like to specifically thank my group members Takia Sultana, Ruchika Sharma, Kyron Thomas and my other friends in the Chemistry Department for their support and generosity throughout this experience. Thank you for your patience and navigating me throughout my experience as a graduate student.

Table of Contents

Acknowledgements.....	ii
List of Abbreviations.....	iv
Abstract.....	vi
Chapter 1. Introduction.....	1
Chapter 2. Interaction of Cu ^{II} -xpt hosts and Cl ⁻ Guests.....	18
Chapter 3. Ruthenium β -diketonate Hosts and Alkali-metal Guests.....	33
Chapter 4. Inducing Guest Binding with Cationic Ruthenium Hosts.....	71
Chapter 5. Facilitating Anion Guest Binding with Ruthenium Hosts.....	94
Chapter 6. Conclusions.....	107
Appendix A. X-ray Crystallography and Structure Refinement.....	109
Appendix B. Electrochemical and ¹ HNMR Analysis of Metal-Organic Hosts with Guests.....	116
Appendix C. Permission.....	123
List of References	125
Vita.....	134

List of Abbreviations

acac.....	acetylacetone
bpy.....	2,2'-bipyridine
BTAC.....	benzyltriethylammonium chloride
CV.....	cyclic voltammetry
Dabco.....	1,4-diazabicyclo[2.2.2]octane
dbm.....	dibenzoylmethane
dbm-2OMe.....	1,3-bis(2-methoxyphenyl)propane-1,3-dione
DMF.....	dimethylformamide
dmgH ₂	dimethylgloxime
DMSO.....	dimethyl sulfoxide
dpen.....	diphenylethylenediamine
d1nm.....	1,3-di(1-naphthyl)propane-1,3-dione
d2nm.....	1,3-di(2-naphthyl)propane-1,3-dione
en.....	ethylenediamine
ESI-MS.....	electrospray ionization-mass spectrometry
<i>fac</i>	facial
<i>m</i> -xpt.....	meta-xylylenebis(pyridyltriazole)
<i>mer</i>	meridional
NMR.....	nuclear magnetic resonance
rotovap.....	rotary evaporator
TBAF.....	tetrabutylammonium fluoride
TBAHSO ₄	tetrabutylammonium hydrogen sulfate

TBAPF₆.....tetrabutylammonium hexafluorophosphate
TTF..... tetrathiafulvalene
TLC.....thin-layer chromatography
OTs.....*p*-toluenesulfonate
TPPO.....triphenylphosphine oxide
UV/vis.....ultraviolet/visible
XRD.....X-ray diffraction

Abstract

Several metal complexes were investigated as potential hosts to execute controllable host-guest interactions using a redox stimulus. Previously, our group has synthesized new Cu^{II} *m*-xylylenebis(pyridyltriazole) (*m*-xpt) hosts and their redox properties were analyzed. In Chapter 2, we take advantage of the Cu^{II} host's ability to perform redox to investigate its interaction with chloride guest ions. This study was executed with two main Cu-xpt hosts: [Cu₂(*m*-xpt)₂(NO₃)₂](PF₆)₂ and [Cu₂(*m*-xpt)₂Cl₂]Cl₂. The host-guest interaction was analyzed with additions of Cl⁻ salt. Although there was evidence of redox-controlled binding of Cl⁻, the reactions could not be studied easily by electrochemistry.

In Chapter 3, we studied various ruthenium (III) β-diketonate complexes as potential hosts for alkali-metal ion guests. The cationic guests associate with the anionic Ru^{II} reduced host and are released upon oxidation to the neutral Ru^{III} host. This was observed through a positive shift in host's redox potential, [Ru(diket)₃]^{0/-}. In our work, we found that the Na⁺ association becomes stronger when the substituents on the diketone ligand increase in electron density. Three new ruthenium β-diketonate complexes are prepared as potential hosts with the intention of increasing Na⁺ affinity. Ru(dbm-2OMe)₃ displayed greater sensitivity to the Na⁺ guest compared than any known ruthenium beta-diketonates. This host's binding constant was determined to be two orders of magnitude higher than that of [Ru(dbm)₃]⁻. These findings were also evidenced by UV-Vis, ¹H NMR, spectroelectrochemistry, and crystallography analysis.

After the success of implementing host-guest interactions of anionic Ru hosts with guest cations, we decided to carry out analysis of several cationic Ru hosts with neutral and anionic guests in Chapters 4 and 5. These hosts will be oxidized in order to attract more anion guests. The guest interaction occurs through hydrogen bonding to the host's ligands. The [Ru(bpy)(en)₂](PF₆)₂,

fac-[Ru(pypz)₃](PF₆)₂, [Ru(bpy)(dpen)₂](PF₆)₂, and [Ru(dmgh₂)₃](PF₆)₂ hosts display increased affinity for the anions when they are oxidized to ruthenium (III).

Chapter 1. Introduction

1.1. Supramolecular Host-Guest Chemistry

Supramolecular chemistry has provided great potential to be utilized in many real-world applications, such as catalysis, ion exchange, drug delivery, gas storage, and achieving synthesis within a confined environment.¹⁻⁸ Fortunately, metal-organic hosts can accomplish these works using host-guest interactions. Researchers have begun to study these supramolecular systems that strongly interact with certain guests. Many of these hosts were discovered to bind to guests through hydrogen binding and π - π interactions.⁹⁻¹² Figure 1.1 displays a simple schematic of host-guest chemistry.

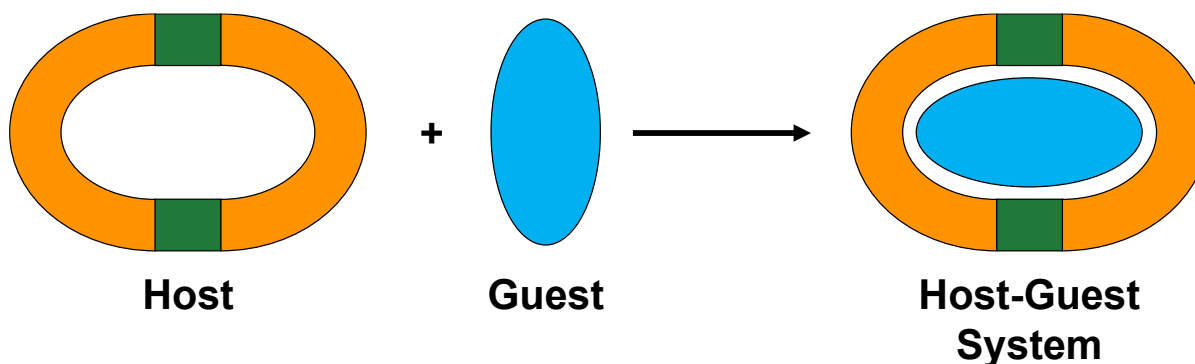


Figure 1.1. Diagram of host-guest interaction of a metal-organic host with a guest. Metal centers, green and ligands, orange.

Most host-guest systems are demonstrated through crystal structures however, these interactions display the host-guest binding without the ability to release the guest. Only a few known hosts are known to have controllable guest-binding. We decided to perform this by manipulating the metal-organic host, thus altering the binding constant between it and its guest. Some of the known methods to control host-guest interactions are through influencing the pH, light, or temperature of the system.¹³⁻¹⁶ However, changing the pH requires utilizing more chemicals that have potential to distort data. Using temperature can induce unwanted oxidation and light can deteriorate the analyte.¹⁷

A promising approach to executing controllable host-guest interaction without the interference of other factors is through electrochemistry. The oxidation state of the metal center of the host can be easily influenced by electrodes in solution. This aids in regulation of the guest bind and release process in real-time. Not many known studies have experimented with redox-controlled host-guest interaction. One of these works was performed by Croué and co-workers, where they permitted a Pt host to bind and release coronene using a four-electron transfer.¹⁸ They discovered that the organic guest was captured in the cavity of the neutral Pt host, but dissociate from the host when the cavity is oxidized to 4+. Figure 1.2 displays a schematic of this process.

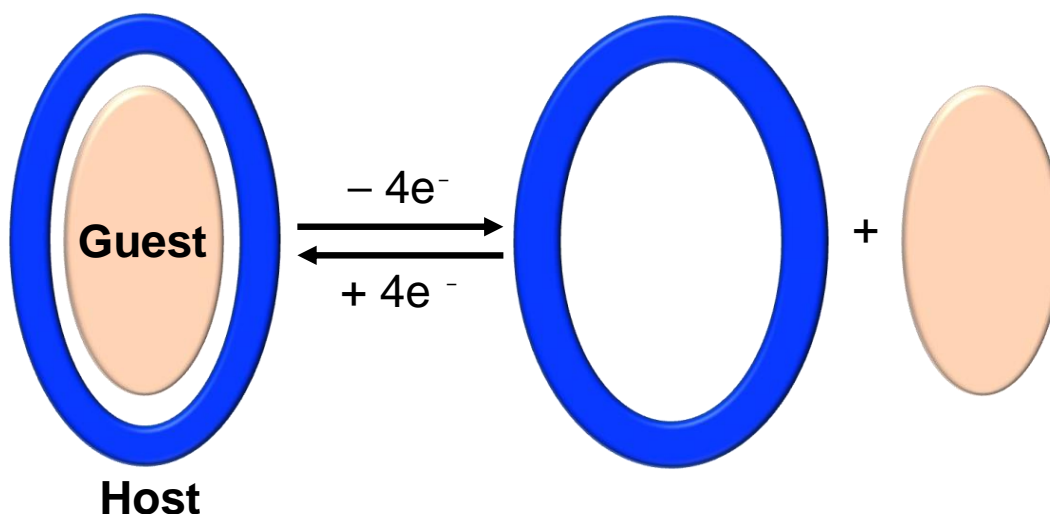


Figure 1.2. Simple diagram of using redox to manipulate the binding affinity between the host and guest.

Their control of the binding and release of coronene was confirmed using fluorescence, DFT calculations, ^1H NMR, and CV studies.¹⁸ Sunatsuki and co-workers also established host-guest binding using a single tripodal ligand (Figure 1.3) of the Mn host with different guest cations: Na^+ , K^+ , and NH_4^+ .¹⁹ They observed that the host's half-wave potential, $E_{1/2}$, is more positive when the guest cations are added. They also discovered that the Na^+ and K^+ ions bind to the phenolate and methoxy O atoms. The NH_4^+ attaches to the host via hydrogen bonding.

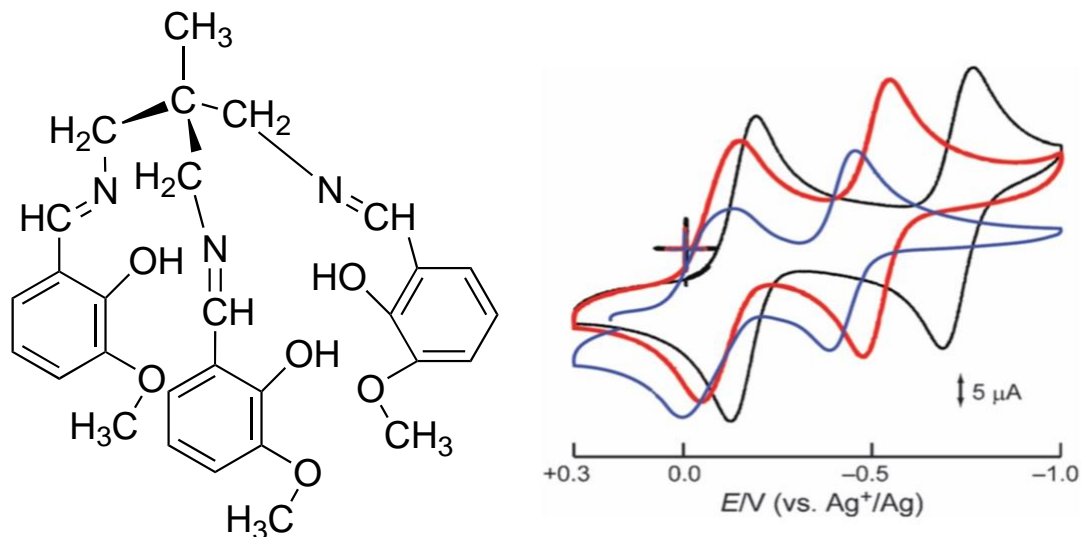


Figure 1.3. Structure of tripodal ligand, 1,1-tris[(3-methoxysalicylideneamino)methyl]ethane (left). Mn single-ligand hosts: $[\text{Mn}^{\text{III}}\text{L}]$, black, $[\text{Mn}^{\text{III}}\text{LK}(\text{PF}_6)]$, red, and $\text{NH}_4[\text{Mn}^{\text{II}}\text{L}]$, blue¹⁹ (right). Reprinted with permission from *Chemical Communications* **2011**, 47 (32), 9149-9151. Copyright 2011, Royal Society of Chemistry.

1.2. Square Planar Copper(II) Hosts and Metal-Guest Coordination

Square planar metal complexes, or molecular squares, have been utilized as hosts in examining host-guest interactions. Stang and co-workers accomplished this with Pd and Pt molecular square hosts.²⁰ These complexes captured aromatic guests through noncovalent interactions and σ - and π -donating Lewis bases. The Fujita Group also excelled in this by permitting neutral aromatic guest-binding to these hosts by exploiting the hosts' cavities.^{21,22}

Our group, in particular, has previously analyzed guest-binding using macrocyclic Cu^{II} tetradentate β -diketonate hosts, where the hosts differed by its spacer ligands.²³⁻²⁶ These macrocyclic hosts were found to have an attraction to N-donating organic guests. These compounds bind to the Cu metal centers inside the ring-structured host. The cofacial naphthylene-based $\text{Cu}_2(\text{NBA})_2$ host (Figure 1.4) displayed the ability to bind to Lewis bases such as Dabco and pyrazine inside.²³ Later, Davidson and co-workers used the same Cu^{II} square planar host template to create a new host with a larger m-terphenyl spacer to capture a bigger 4,4'-bipyridine guest.²⁷

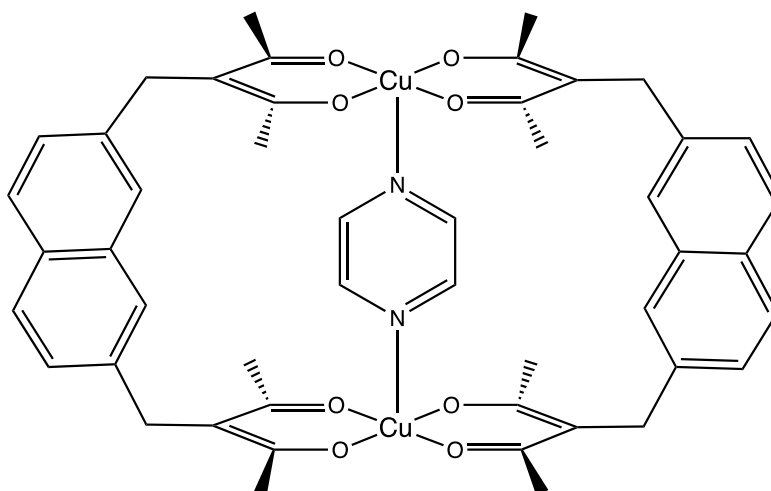


Figure 1.4. Copper(II) bis(β -diketonate) binding to pyrazine.²³

The binding process of this system worked exceptionally because of the stability of the Cu^{II} metal center in square-planar and square-pyramidal geometries. Nevertheless, because we want to explore manipulating the host-guest interactions using redox, these hosts are not desirable. This is because the less stable Cu^{I} metal center would not sustain redox reactions when connected to electron-deficient O atoms of the β -diketonate ligands.

Influenced by these findings, we ventured into studying Cu^{II} square planar hosts where the ligands are N-donor ligands due to their more predictable rigid structure. We decided to resort to using pyridyltriazole ligands instead of 2,2'-bipyridine for our Cu^{II} host to avoid repulsive $\text{H}\cdots\text{H}$ interactions distorting the square planar framework (Figure 1.5).¹²

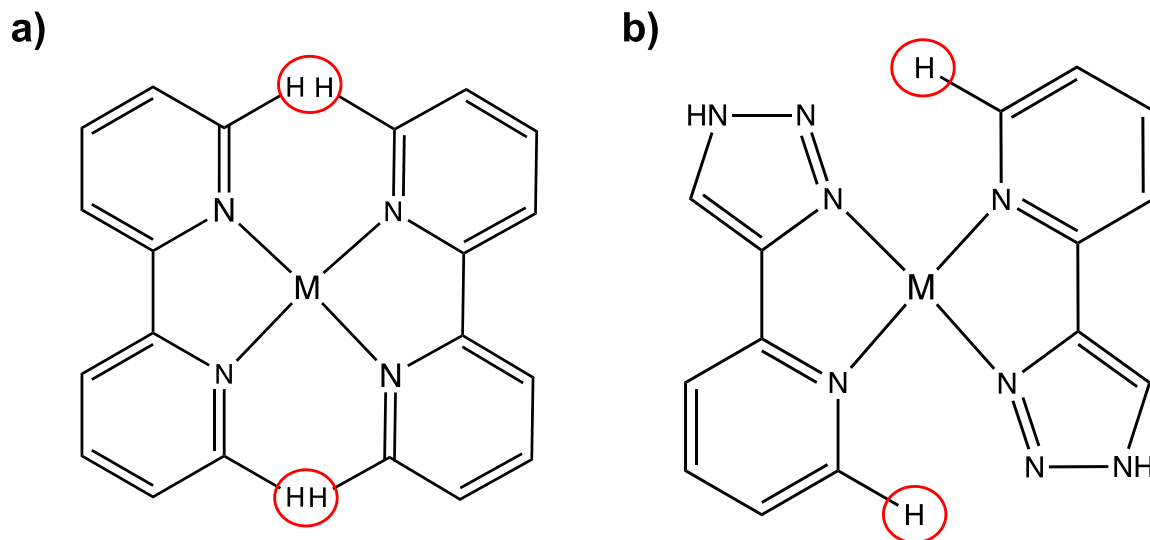


Figure 1.5. a) Framework of a metal complex with trans-bis(2,2'-bipyridine) ligands, which shows unfavorable H...H interactions, b) Metal trans-bis(pyridyltriazole) structure that avoids repulsive H...H interactions.

There is also a considerable history of the synthesis of metal-pyridyltriazole complexes.²⁸ Another benefit to selecting this N-donor ligand is that its stability would make the metal complex a practical choice for tunable guest-binding. Through this, our group has assembled a new ligand system where bis(pyridyltriazole) ligands are used to form a Cu^{II} dimer. One of these new bimetallic hosts is [Cu₂(npt)₂](PF₆)₄. The host-guest interaction between the Cu-npt host with Dabco was analyzed using UV-vis and was noted by a slight color change.¹² Figure 1.6 displays the host-guest system of the Cu-npt host with Dabco guest.

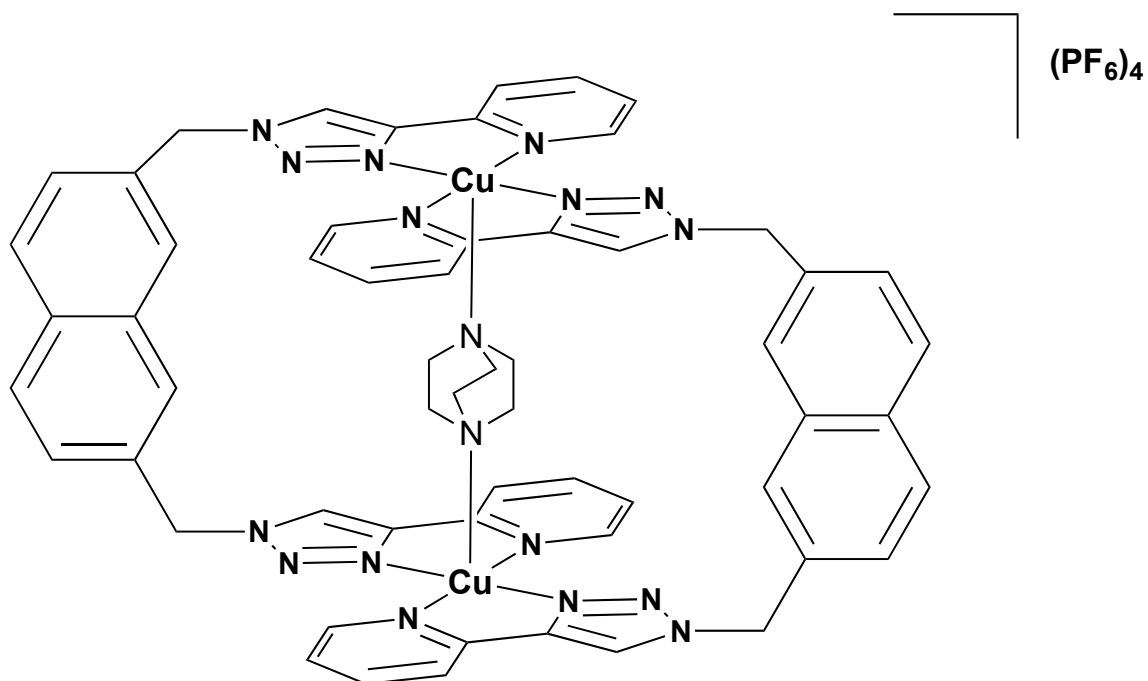


Figure 1.6. Structure of $[\text{Cu}_2(\text{npt})_2(\mu\text{-Dabco})](\text{PF}_6)_4$ host-guest system.

Later, our group investigated this host-guest chemistry using redox, but we discovered that this host did not display reversible bind and release behavior.²⁹ This indicates that Dabco is not a suitable guest for studying its bind and release process with the Cu-npt host through redox control. Fortunately, other pyridyltriazole complexes were synthesized and appear to be good candidates for host-guest chemistry: $[\text{Cu}_2(m\text{-xpt})_2(\text{NO}_3)_2](\text{PF}_6)_2$ and $[\text{Cu}_2(m\text{-xpt})_2\text{Cl}_2]\text{Cl}_2$ (Figure 1.7).

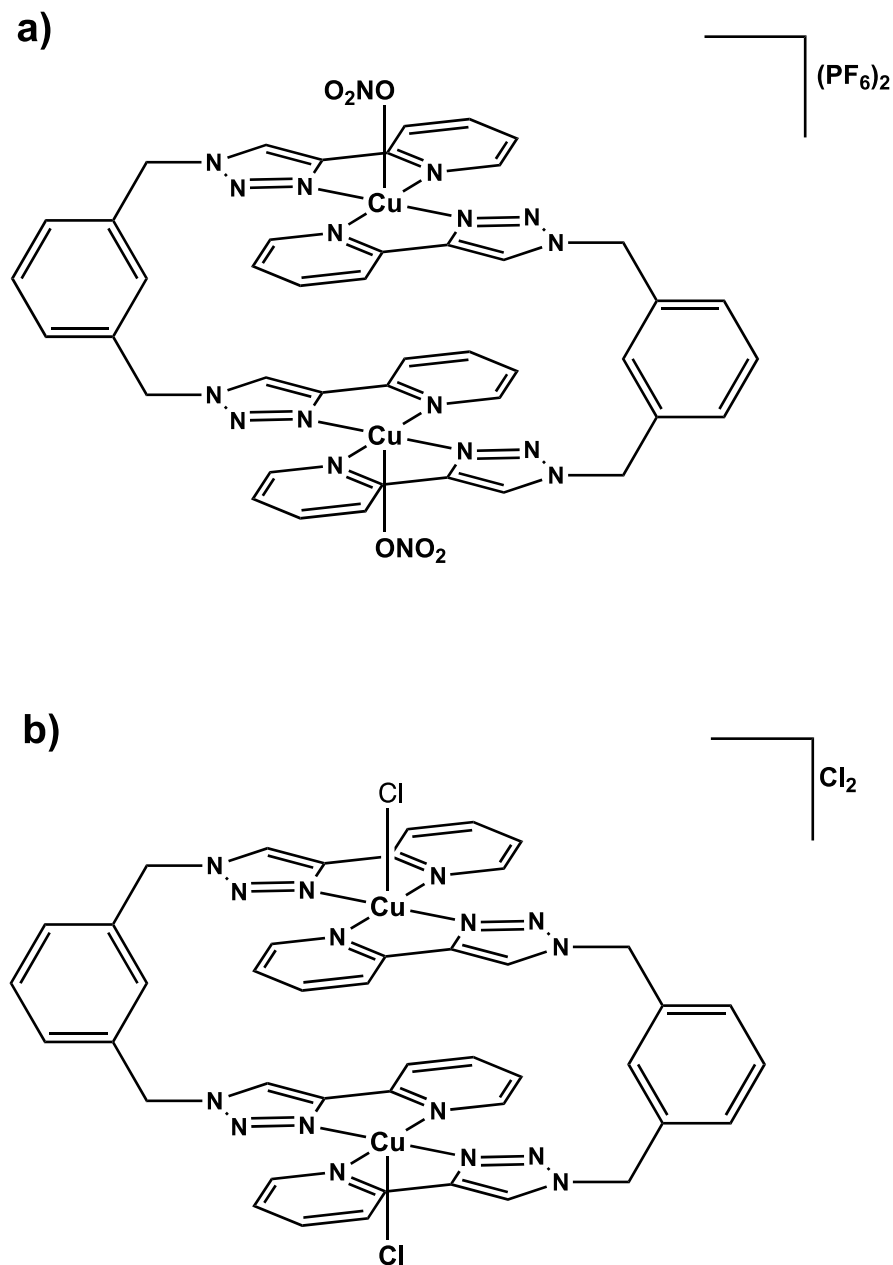


Figure 1.7. Structures of the Cu^{II}-xpt complexes: a) $[\text{Cu}_2(m\text{-xpt})_2(\text{NO}_3)_2](\text{PF}_6)_2$ and b) $[\text{Cu}(m\text{-xpt})_2\text{Cl}_2]\text{Cl}_2$.

Both Cu-xpt complexes were found to be redox-active³⁰, which led to our intrigue in finding out if they can perform controlled guest binding using cyclic voltammetry. Considering the Cu^{II} metal center has six coordination sites, this opens a great prospect that the remaining sites can be used for guest-binding. Because the cavity of Cu-xpt is much smaller than that of Cu-npt,

we decided to use Cl^- ions for guest-binding. We intend to analyze and manipulate its bind/release process of Cl^- using CV. The results of this experimentation are in Chapter 2.

1.3. Anionic Ruthenium(II) β -diketonate Hosts and Alkali Ion Guests

As mentioned, our group has great experience in working with stable Cu^{II} bis(β -diketonates) as molecular hosts. The open coordination sites and π interactions in the open cavity allows for promising guest-binding due to the stability of the Cu^{II} metal center.^{26,31} Nonetheless, because we intend to achieve manipulative host-guest interaction using redox, the Cu^{II} bis(β -diketonates) hosts would not be sufficient in this application.

For the sake of maintaining facile host-guest binding, we investigated similar frameworks as hosts with stable metal centers that can withstand redox control. This led to us focusing on Ru^{III} β -diketonate complexes. Previously, there have been analysis on the noticeable positive shift of the redox potential of metal-acetylacetonate hosts with alkali-metal perchlorate salts.^{32,33} The positive $\Delta E_{1/2}$ was determined to be too large to be due to electrostatic effects.³⁴ While examining crystal structures, Steinbach and Burns observed that the H atoms in solvent molecules interact with the O atoms of acetylacetonate metal complexes.³⁵ As a result of these studies, it became feasible that the O atoms in metal β -diketonate complexes may have an attraction to cations, which can be reflected in the positive shift of $E_{1/2}$.

It is well known that in chemical and biological redox systems there is a coupling between proton and electron transfer processes that can be controlled using pH manipulation.³⁶ The Meyer Group described that during oxidation, the sample becomes more acidic. This complements the allowance of proton transfer using redox (Figure 1.8a).³⁶ Lexa and co-workers studied this by analyzing the redox properties of an iron porphyrin undergoing redox and ligand exchange.³⁷ Thus,

we aim to perform controllable host-guest interaction by replacing the proton transfer aspect with guest bind or release. Figure 1.8b displays a simple square scheme of this process.

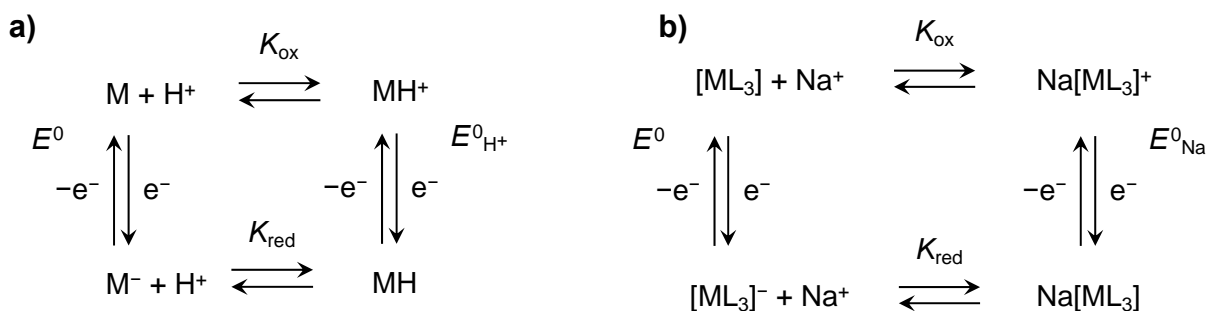


Figure 1.8. a) Simple proton-coupled electron transfer, b) Square scheme for the coupled redox and cation-binding reactions with the ML_3 host complex.

Using the ruthenium(III) acetylacetonate complexes, $[ML_3]$, as examples, guest-binding with Na^+ is controlled by adding or removing electrons. Once $[ML_3]$ is reduced to $[ML_3]^-$, the Na^+ guest has more affinity for the reduced host, allowing guest-binding to take place. On the other hand, when the host is oxidized to $[ML_3]$ again, guest-release occurs. The Na^+ guest having greater association with the reduced host than the oxidized host demonstrates that the binding constant, $K_{\text{red}} > K_{\text{ox}}$. With the addition of Na^+ guest, the host becomes easier to reduce, inducing the positive shift in the host's Ru^{II}/Ru^{III} redox potential. Therefore, the host's standard potential is less than the redox potential with added Na^+ , or $E^0 < E^0_{Na^+}$.

Various ruthenium β -diketonate complexes were investigated as well to see this effect in the presence of alkali-metal ions.³⁴ This experimentation displayed how the redox potential of these complexes were affected by the addition of Li^+ and Na^+ ions. The main focus was on $Ru(acac)_3$. This complex showed a greater positive shift in the redox potential than other ruthenium diketonates studied. In this paper, Endo proposed that the large $\Delta E_{1/2}$ is due to the electron-releasing nature of its methyl substituent. The electron-donating ability of the methyl substituent

increases the negative charge on the O atoms in the reduced complex, permitting greater attraction of the alkali guest ions.

Endo also performed UV-vis analysis of neutral $\text{Ru}(\text{acac})_3$ with tetraethylammonium perchlorate and with NaClO_4 . He discovered that both spectra looked identical, meaning that the change in the redox potential is mainly due to association of Na^+ to the Ru^{II} complex, not Ru^{III} . When $\text{Ru}(\text{acac})_3$ is reduced to $[\text{Ru}(\text{acac})_3]^-$, in the presence of Li^+ , an air-sensitive precipitate is formed in acetonitrile. Elemental analysis on the solid were consistent with $\text{Li}[\text{Ru}(\text{acac})_3]$ being the compound.³⁴ This finding was also evidence of host-guest binding occurring with the cation and the anionic host complex.

This conclusion was further supported by an earlier study by Patterson and Holm.³⁸ They noticed that $E_{1/2}$ is influenced by the substituent effect of a plethora of Ru tris(β -diketonato) complexes. The structures that have electron-donating substituents have more negative redox potentials than the electron-accepting substituents. Along with this, Endo also identified that the $\Delta E_{1/2}$ with Na^+ correlates to the binding constant of Na^+ to the β -diketonate host.³⁴ The hosts that had a greater binding constant with the cationic guests were the ones that had electron-releasing substituents. This discovery validated the inference that the inductive effect plays a part in how the cationic guest is attracted to the β -diketonates.

In Chapter 3, we discuss our target of constructing new ruthenium tris(β -diketonato) hosts with substituents that dispense a greater local negative charge to increase sensitivity for alkali-ion guests. With this work, we also want to maintain facile host-guest interaction. This creates a more positive $\Delta E_{1/2}$, along with the cyclic voltammogram of the host maintaining its reversibility with added guest. With the new host having reversibility and stronger association with Na^+ , this accomplishes more reliable guest bind and release using only a one-electron transfer. The proposed

new hosts we synthesized includes: $\text{Ru}(\text{d2nm})_3$, $\text{Ru}(\text{d1nm})_3$, and $\text{Ru}(\text{dbm-2OMe})_3$ (Figure 1.9). Along with cyclic voltammetry analysis, we aim to display evidence of host-guest binding through UV-vis spectroscopy, ^1H NMR, crystal structure analysis, and spectroelectrochemistry.

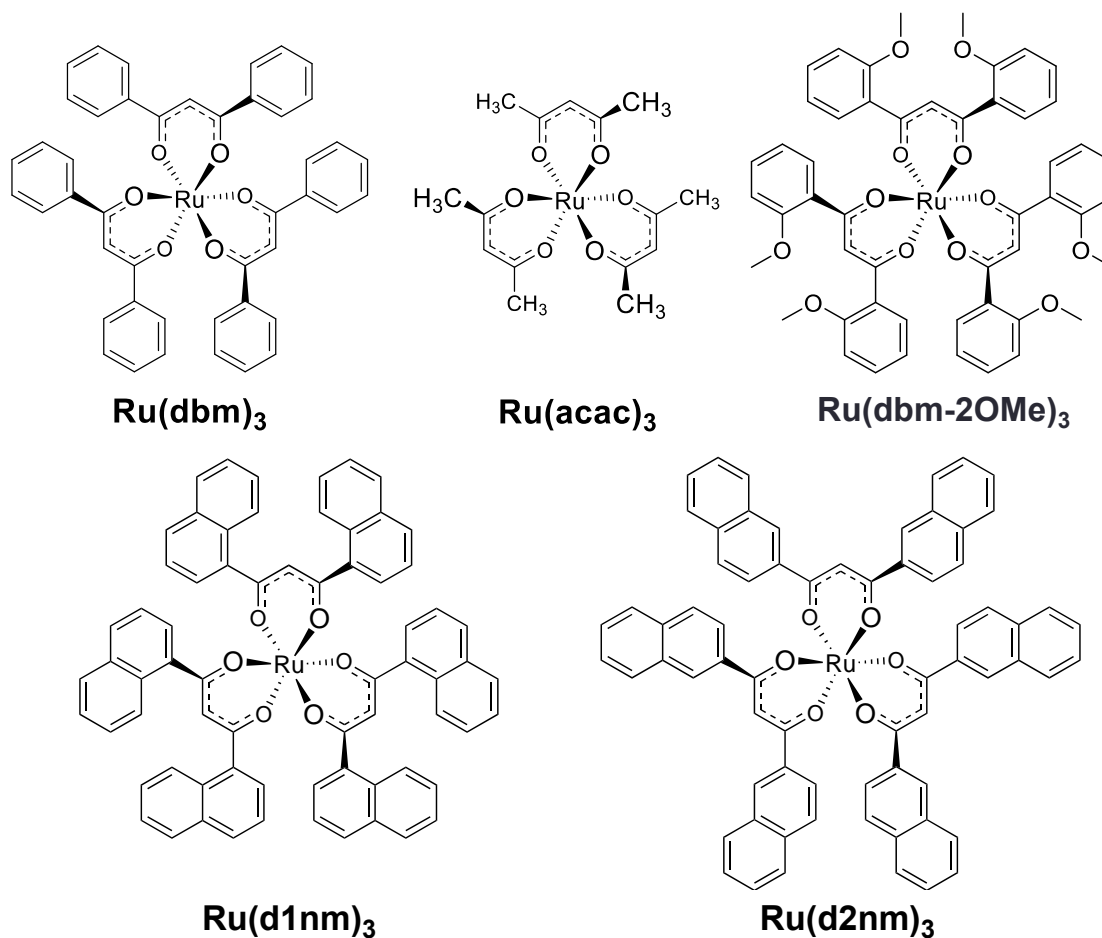


Figure 1.9. Ru β -diketonate hosts.

Spectroelectrochemistry permits us to have a qualitative and quantitative way to display that host-guest binding is occurring. Because the ruthenium(II) β -diketonate host is air-sensitive, it is difficult to accomplish UV-vis studies of the reduced host in a normal UV-vis setup. Fortunately, spectroelectrochemistry exhibits the UV-vis spectrum while performing redox, allowing us to see the change in the reduced host's spectrum when Na^+ guest is added, while under an inert gas. This experimentation is accomplished by using a quartz cuvette, instead of a normal electrochemical cell (Figure 1.10). The light source hits the sample through one of the holes in the

honeycomb working electrode, which allows the UV-vis data to be recorded as the specimen undergoes the redox process..

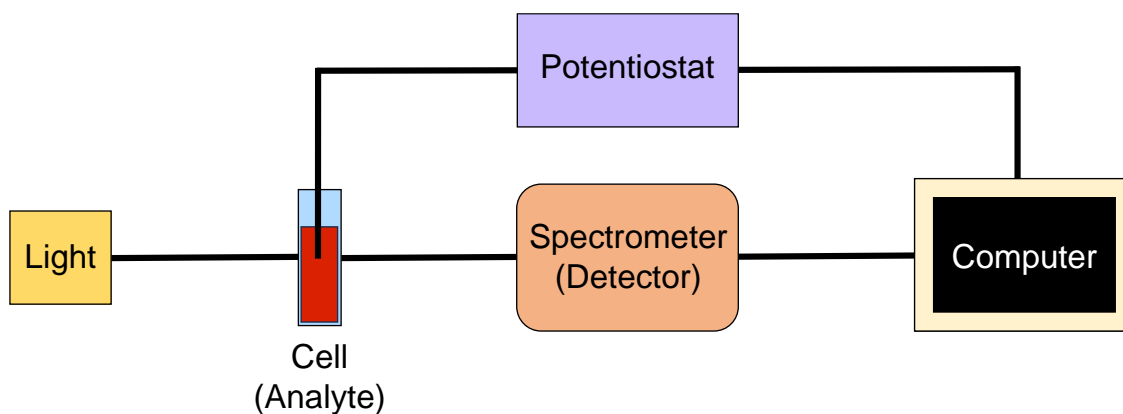


Figure 1.10. Simple schematic of spectroelectrochemistry setup.

1.4. Cationic Ruthenium Hosts and Hydrogen-binding Guests

Beforehand, we introduced the binding of Cl^- guests using Cu-xpt hosts. It was mentioned that the host-guest chemistry for this system was based on taking advantage of the open coordination sites of the metal center. Another way to manipulate host-guest interactions is by using a second coordination sphere, like what is discussed in Chapter 3. In Chapters 4 and 5, we intend to execute the same technique of increasing affinity of the host to guests. For this project, the guests are associating with the ligands of the host through hydrogen bonding and we are increasing the host's affinity for these guests by oxidizing the host.

Previously, Yoshikawa and co-workers displayed a crystal structure depicting the $[\text{Co}(\text{hexaen})]^{3+}$ host interacting with Cl^- guest through hydrogen-bonding with the en ligands.³⁹ The en ligands on the host would promote the $\text{NH}\cdots\text{A}^-$ guest-binding due to the ligand's acidity. From this, we looked into the $[\text{Co}(\text{en})_3]^{2+/3+}$ system. Though the $[\text{Co}(\text{en})_3]^{2+/3+}$ redox are both cationic hosts, it is still expected that the 3+ state would have better association with the A^- guest than 2+. Earlier, our group has attempted to measure whether the $[\text{Co}(\text{en})_3]^{2+/3+}$ host can withstand

host-guest control through redox, but the cyclic voltammogram was discovered to be irreversible likely due to ligand dissociation.⁴⁰

Turning to other metal-en complexes for potential hosts, we first considered 3d metal centers. The earlier 3d metals do not seem promising for our application because they favor O coordination instead of N, making the binding constant between metal and en ligand low, especially for redox. Other probable metals centers such as V⁴¹ and Cr are very air-sensitive in the 2+ oxidation state. The most stable M-en complexes of the 3d metals, other than Co, are Ni- and Cu-en. However, Ni^{II} is not redox-active⁴² and [Cu(en)₃]²⁺ may have difficulty in synthesizing due to the stability of the [Cu(en)₂]²⁺. Because of these reasons and the success of the Ru β-diketonate research, we decided to look into cationic Ru-en complexes as potential hosts for anionic guest ions.

The Ru metal center has great potential in the redox process due to it having more stability, which would prevent the ligand dissociation that occurs in the cobalt host. Another important aspect of the Ru(en)₃ host is that it can be synthesized in the [Ru(en)₃]²⁺ and [Ru(en)₃]³⁺ form. The 2+ structure, however, is air-sensitive. The 3+ host is also prone to undergo oxidation/deprotonation. The host is likely to have its en ligands undergo oxidation into imines (Figure 1.11).

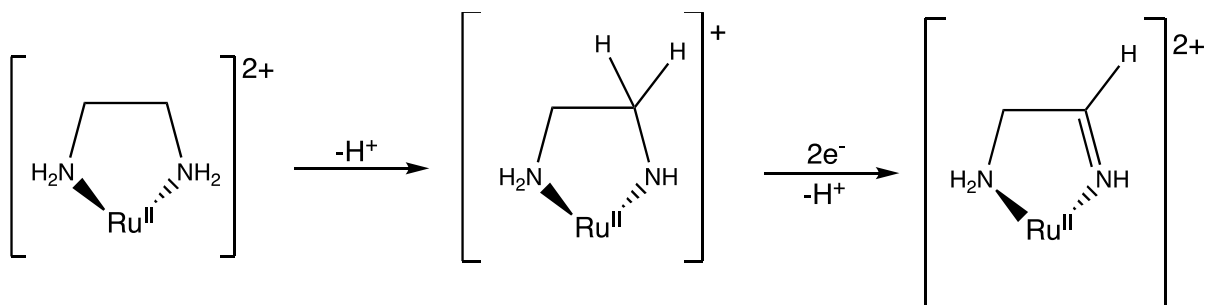


Figure 1.11. Ethylenediamine oxidation to imine of a ruthenium complex.

Because of the complexity of the $[\text{Ru}(\text{en})_3]^{3+/2+}$ system, we wanted to investigate host systems that integrate ethylenediamine, is air stable, and has facile synthesis.

Curtis et al. has made a few Ru-en complexes and studied their redox properties in acetonitrile, one of them being $[\text{Ru}(\text{bpy})(\text{en})_2](\text{PF}_6)_2$.⁴³ This host is promising for our application to perform host-guest binding with anions. It not only has stability in air and requires a simple synthesis for production, but it has a known redox potential that is not too positive for Cl^- guest-binding.⁴⁴ Even though this bpy host has one less en ligand for guest coordination, this host has two close-lying NH_2 groups that should be capable of binding to anions, while maintaining stable redox behavior. This host also has potential on inspiring a series of new hosts, such as $[\text{Ru}(\text{bpy})(\text{dpen})_2](\text{PF}_6)_2$.

Synthesizing the new $[\text{Ru}(\text{bpy})(\text{dpen})_2](\text{PF}_6)_2$ complex allows for the expansion of this host system to be used in future host-guest applications. The $[\text{Ru}(\text{bpy})(\text{en})_2](\text{PF}_6)_2$ structure is limited in being able to enhance its binding affinity with anionic guests. With the dpen host, the phenyl substituents on the ligands can be modified with groups such as OH^- or amide groups in order to increase the binding constant between the host and guest (Figure 1.12), much like what was accomplished with the $\text{Ru}(\text{dbm}-2\text{OMe})_3$ host in Chapter 3. Synthesizing this complex would lead to improvements in the host-guest association of this system. In Chapter 5, the host-guest chemistry of $[\text{Ru}(\text{bpy})(\text{dpen})_2](\text{PF}_6)_2$ with chloride ions were examined through cyclic voltammetry.

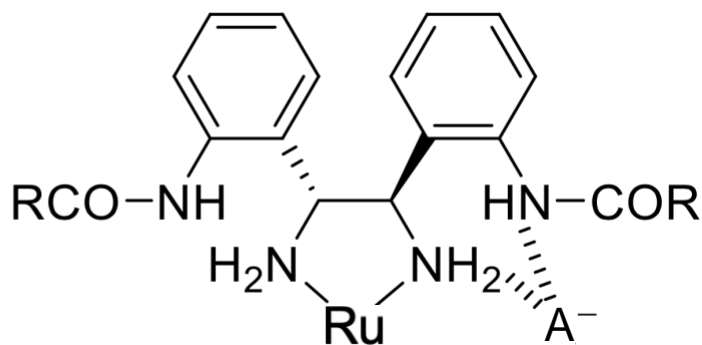


Figure 1.12. Chemical diagram of hydrogen bonding between amide-substituted (*R,R*)-1,2-diphenylethylenediamine ligand interacting with an anion guest, A⁻.

The potential in achieving host-guest interaction through NH \cdots A⁻ on the ligands encouraged us to test other reasonable host complexes for this application. For example, tris(dimethylgloxime) ruthenium complex was analyzed and discovered that the ligands' OH bond interacts with Cl⁻.⁴⁵ (Figure 1.13). This complex was analyzed as a potential host for chloride guest in Chapter 5. The Ru^{II} host being oxidized to a 3+ complex will also attract the guest even more than the starting 2+ host.

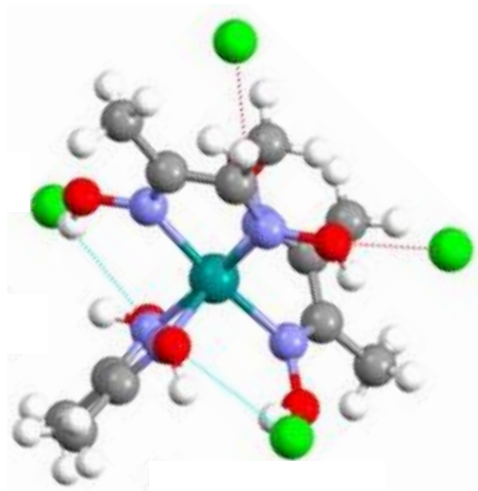


Figure 1.13. Cl⁻ guest ions (green) interacting with O \cdots H bonds of the [Ru(dmgh₂)₃]²⁺ host viewed down the c-axis.⁴⁵

Another technique that can be used to develop host-guest interaction is by constructing hosts that have a binding site for guests. Many researchers established host structures with H donor

sites in order to entice guest binding.⁴⁶⁻⁴⁹ The formation of these donor sites can be affected by what isomer the complex is. Octahedral complexes with three unsymmetrical bidentate ligands can be constructed as two types of isomers: *mer* and *fac*. The type of isomer makes a profound difference in the binding constant between the host and the guest due to how the ligand arrangement influences the development of the binding site.⁵⁰ For hydrogen binding, the *fac* form brings the H donors together and make a binding pocket for guest-binding.⁵¹

Previously, the Ward et al. examined a series of Ru^{II} tris(pyrazoyl-pyridine) hosts, one being [Ru(pypz)₃](PF₆)₂. These complexes displayed the importance of having either *mer* or the *fac* form in host-guest interactions using ¹H NMR studies.⁵¹ They showed that the *fac* host can bind to an electron-rich atom of the guest through hydrogen-bonding with the pyrazoyl-pyridine ligand.⁵¹ However, in the *mer* form, the donor groups are away from each other. This prevents the formation of the recognition site, making the guest-binding weaker.

We aim to increase the binding affinity of the host through redox by oxidizing it. This increases the positive charge of the cationic *fac* host and will entice guests to interact with it (Figure 1.14). Redox-controlled host-guest binding with ⁻O₃S(CF₂)₃CF₃, HF₂⁻, and TPPO is accomplished in Chapter 4.

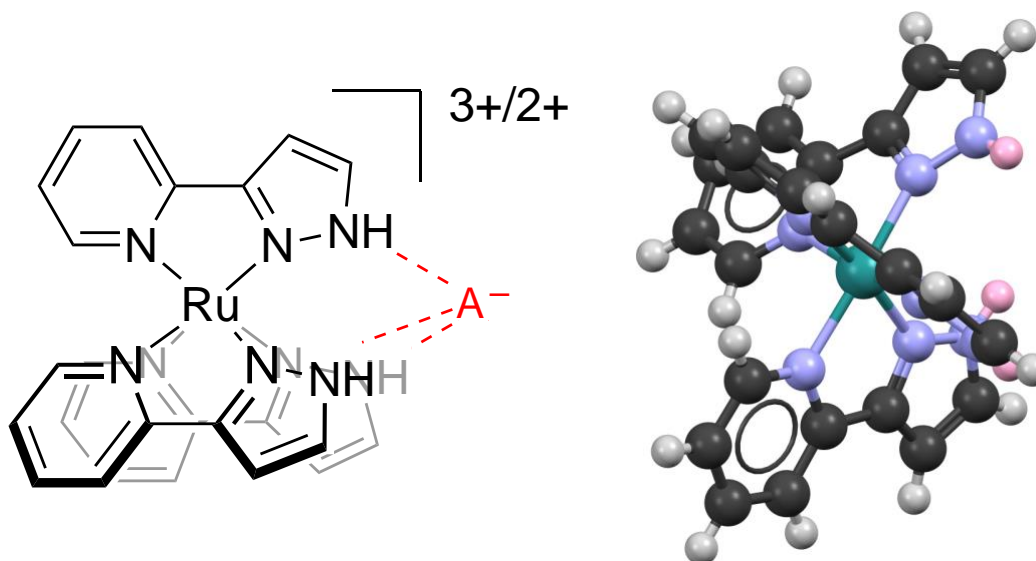


Figure 1.14. Chemical diagram of the *fac*-[Ru(pypz)₃](PF₆)₂ H donor site associating with an anionic guest, A⁻ (left). X-ray crystal structure of this cation, with the pyrazole NH protons shown in pink.⁵

This dissertation demonstrates multiple techniques in accomplishing redox-controlled host-guest chemistry of metal-organic complexes with guests. We discuss this application with Cu-*m*-xpt complexes and their ability to interact with chloride ions as guests using direct-metal coordination. The manipulation of the oxidation state of the metal centers influences the binding and release process of Cl⁻ due to the tuning of the open coordination sites on the metal center. We also analyze how the modification of the host's β-diketonate substituents affect the affinity of the host and alkali-ion guests using a redox stimulus. Chapters 4 and 5 examine how utilizing a second coordination sphere in the host can attract anions and organic guests through hydrogen bonding. This research exhibits how tuning the oxidation state of the host can increase its sensitivity to guests and be utilized in controlled host-guest chemistry.

Chapter 2. Interaction of Cu^{II}-xpt hosts and Cl⁻ Guests

2.1. Introduction

Among metal-organic host complexes, square planar geometries are one of the most analyzed. Previously, Pd and Pt molecular square hosts were discovered to bind to aromatic guests using σ - and π -donating Lewis bases and noncovalent interactions.⁵³ Other analysis have performed host-guest interactions with these macrocycles using guest-binding to the metal centers.^{21,22}

Previously, our group have observed guest-binding using Cu^{II} tetradentate β -diketonate hosts.^{24, 54-56} These dimeric hosts were discovered to interact with N-donating organic guests.^{27, 57} These guests bind to the Cu metal centers inside the macrocyclic host. The Cu₂(NBA)₂ host (Figure 2.1) associate with Lewis bases such as dabco and pyrazine inside its cavity.²⁴ Later, this host was used as a model host to build a new Cu^{II} square planar structure.²⁷ This new host has a larger *m*-terphenyl spacer than the naphthalene spacer in the Cu₂(NBA)₂ host. The larger spacer allows for the Cu^{II} complex to bind to the much larger 4,4'-bipyridine guest (Figure 2.1).²⁷

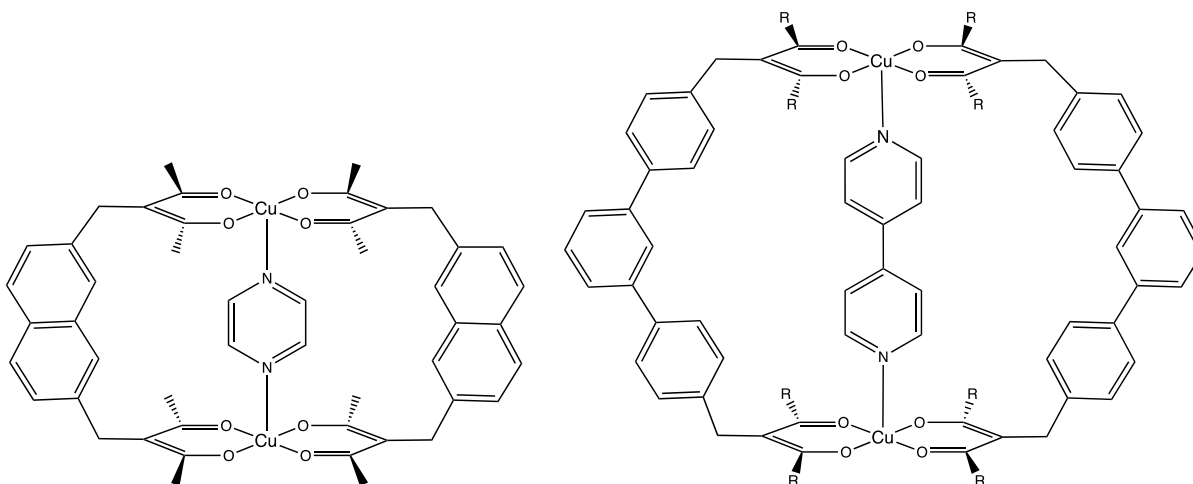


Figure 2.1. Cu₂(NBA)₂ host with pyrazine guest (left)²⁴, Copper(II) bis(β -diketonate) binding to 4,4'-bipyridine guest (right).²⁷

The exceptional binding these square planar hosts have with organic guests has inspired us to explore potential host-guest chemistry candidates. One of our methods in finding an applicable metal-organic host is selecting one that has ligands that make the square planar structure predictable.¹² With this, we examined possible frameworks that have rigid N-donor ligands, which are known to give complexes a more anticipated structure.

Metal-2,2'-bipyridine (bpy) complexes of the type $M(\text{bpy})_2$ are popular structures.^{43, 58-60} However, the bpy ligands are not appropriate for the square planar geometry that we desire. This is because the metal-bpy square planar framework would twist and distort due to the CH hydrogen atoms repulsing each other (Figure 2.2),⁶¹ making it unreliable for controllable guest-association.

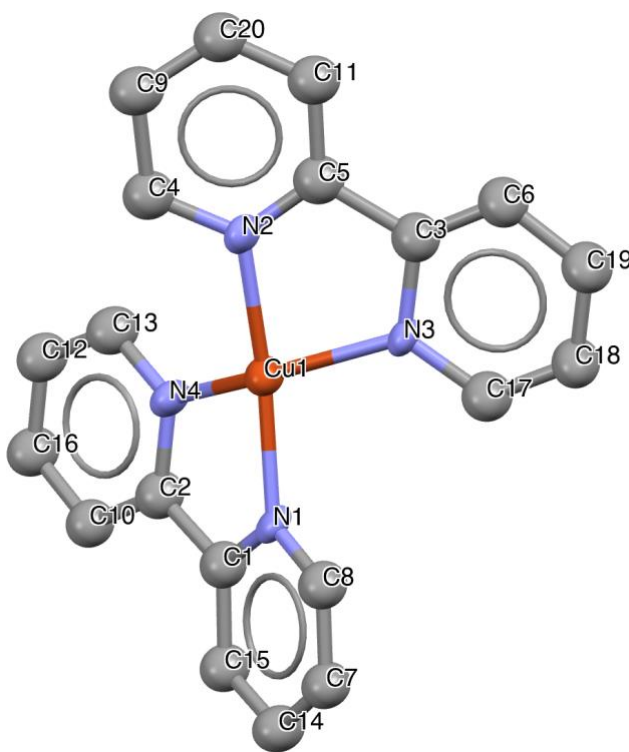


Figure 2.2. Crystal structure of $[\text{Cu}(\text{bpy})_2]^{2+}$.⁶² The two bpy ligands are not coplanar in this structure, because their CH hydrogen atoms interfere with one another.

We were inclined to research complexes that can retain the rigidity and geometry. This led us to focus on creating pyridyltriazole hosts. These structures maintain the advantage of having the N-donor ligand for redox reactions and potential association with organic guests without the

large distortion that bpy ligands can cause. The triazolyl-pyridine host is stabilized due to the N-donor and the framework of the ligand, which makes it a feasible host for controllable guest-binding.⁶³ These complexes are likely to not have the distortion problem of metal-bpy hosts because the pyridyltriazole structures does not have the interaction between hydrogens (Figure 2.3).¹²

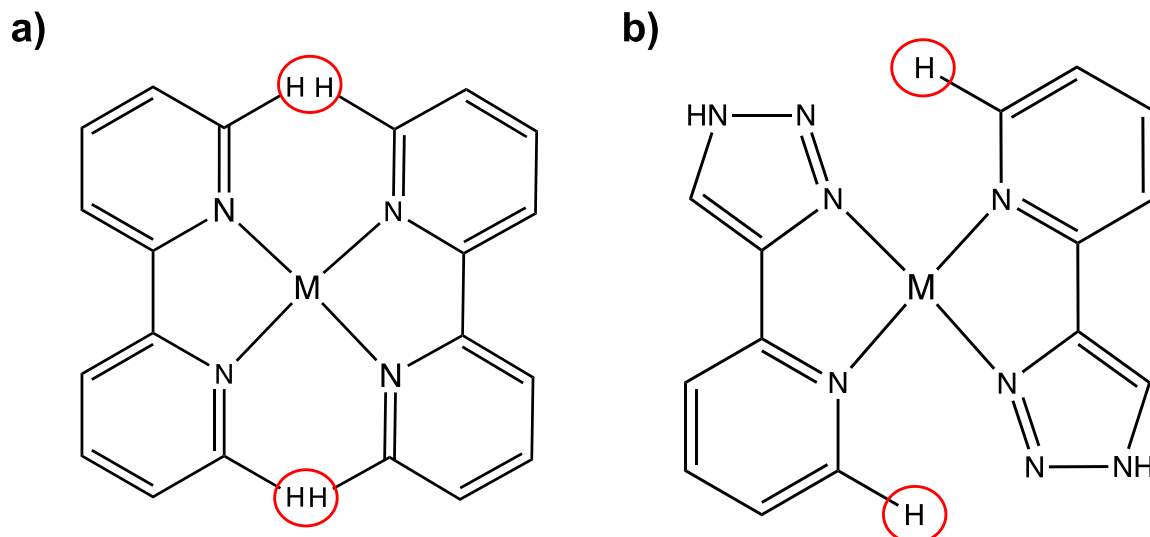


Figure 2.3. a) Framework of a metal complex with trans-bis(2,2'-bipyridine) ligands, which shows unfavorable H...H interactions, b) Metal trans-bis(pyridyltriazole) structure that does not have these repulsive interactions.

Another benefit of studying metal-pyridyltriazole complexes is that the synthesis of these ligands is carried out through the notorious click-reactions.⁶³ Our group has produced a new system of ligands where a Cu^{II} dimer is composed using two bis(pyridyltriazole) ligands. Throughout the years, these binuclear frameworks were utilized as hosts to bind to various guests.^{12,30} [Cu₂(npt)₂](PF₆)₄, for example, was studied to perform host-guest chemistry with 1,4-diazabicyclo[2.2.2]octane (Dabco)¹² shown in Figure 2.4.

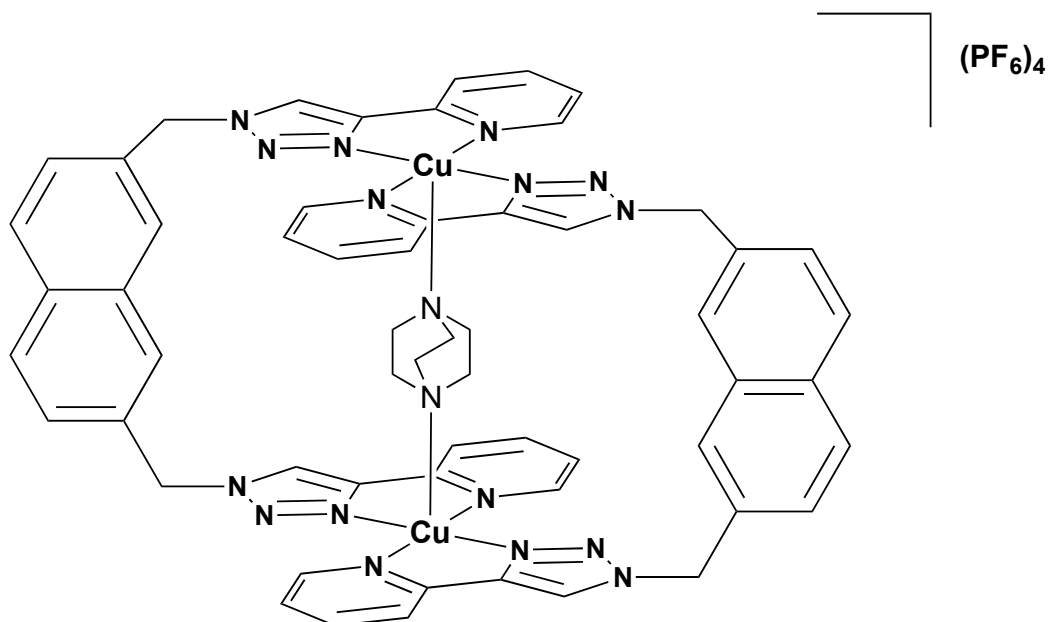


Figure 2.4. Structure of $[\text{Cu}_2(\text{npt})_2(\mu\text{-Dabco})](\text{PF}_6)_4$ host-guest system.

The host-guest association was observed using ultraviolet/visible (UV-vis) analysis, where the host-guest binding can be seen through a slight color change. When 5 equivalents of Dabco is added to the Cu-npt host-DMF solution, a 14 nm blue shift of the d-d absorption band is discovered from guest-binding.¹² Afterwards, our group decided to see if this host-guest chemistry can be controlled using redox. We expected the Cu^{II} -npt host to release Dabco upon reduction, because all the Cu^{I} center would not have any empty coordination sites. Then, it should bind to Dabco again when oxidized back to Cu^{II} . Sharma found a small effect of added Dabco on the Cu^{II} -npt/ Cu^{I} -npt redox potential,²⁹ indicating that the Cu^{II} form binds Dabco more strongly than the Cu^{I} . However, the voltammogram is not reversible and the cathodic peak potentials were shifting inconsistently with added Dabco.

Fortunately, our group has synthesized other Cu^{II} bis(triazoyl-pyridine) complexes that are potential good candidates for studying host-guest interactions: $[\text{Cu}_2(m\text{-xpt})_2(\text{NO}_3)_2](\text{PF}_6)_2$ and $[\text{Cu}_2(m\text{-xpt})_2\text{Cl}_2]\text{Cl}_2$ (Figure 2.5).

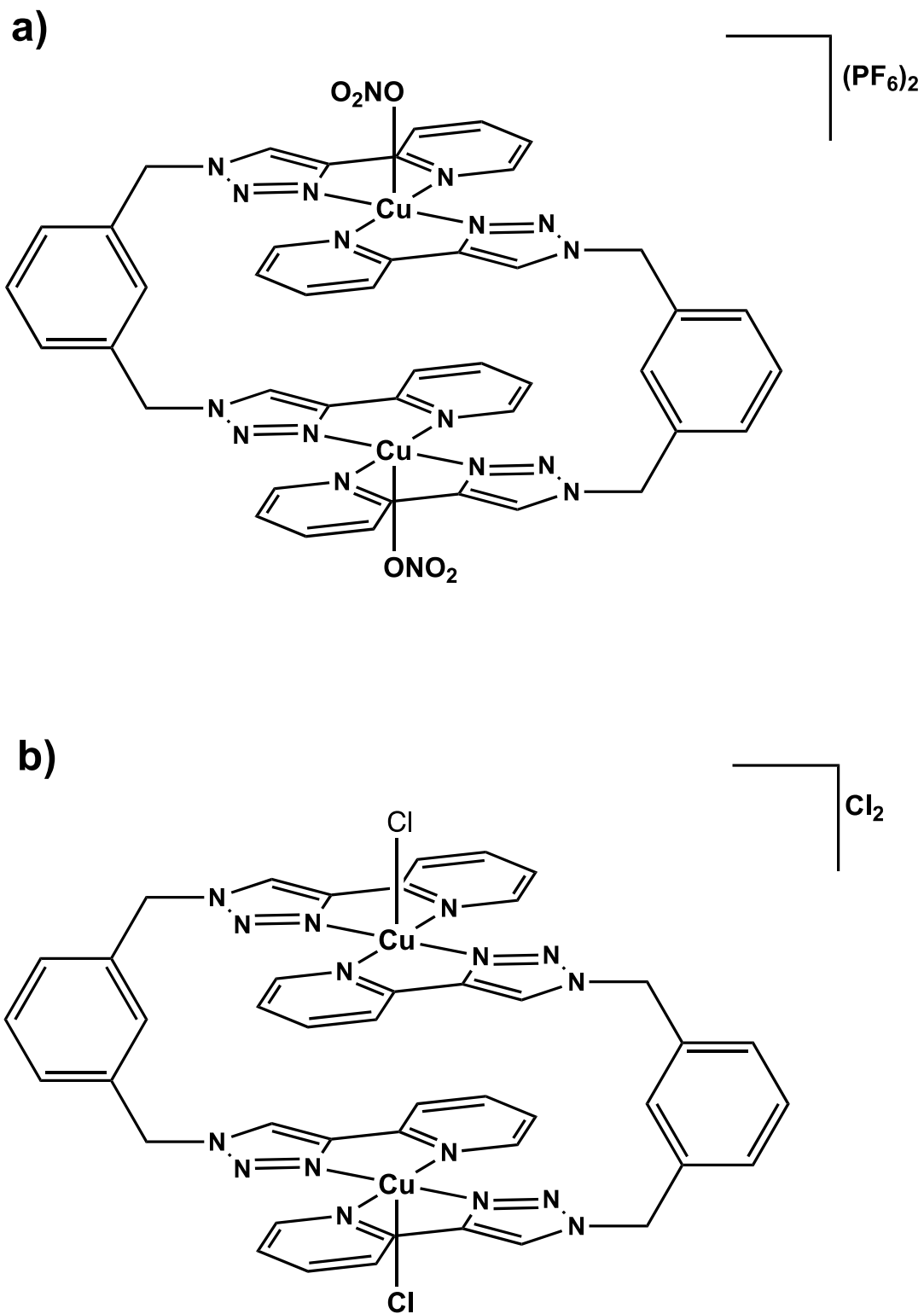


Figure 2.5. Structures of the Cu^{II} -xpt complexes: a) $[\text{Cu}_2(m\text{-xpt})_2(\text{NO}_3)_2](\text{PF}_6)_2$ and b) $[\text{Cu}(m\text{-xpt})_2\text{Cl}_2]\text{Cl}_2$.

Previously, our group has analyzed the redox properties of the above two Cu-xpt complexes through cyclic voltammetry and discovered that the complexes are redox-active. These structures were also found to act as hosts and bind to oxalate as a guest³⁰, which is shown in Figure 2.6.

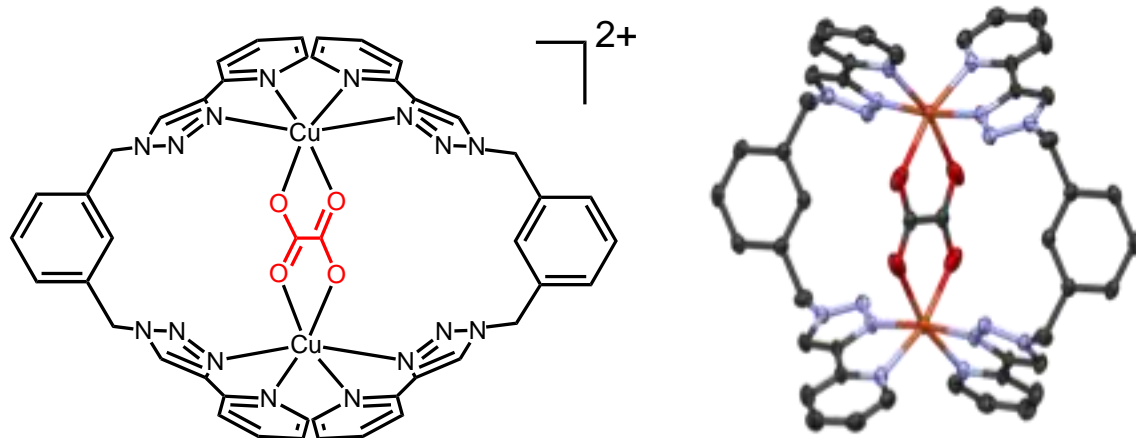
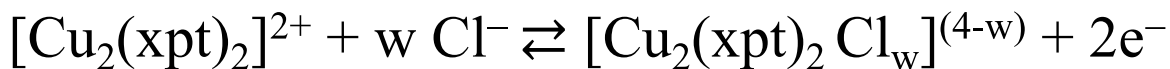


Figure 2.6. Chemical diagram and X-ray structure of $[\text{Cu}_2(m\text{-xpt})_2(\mu\text{-C}_2\text{O}_4)]^{2+}$ host-guest system. Counter-anions and hydrogen atoms are removed for clarity on X-ray framework.³⁰

These results inspired us to investigate if these complexes are capable of performing controlled host-guest chemistry through cyclic voltammetry. With the smaller cavity of the Cu-xpt complex compared to Cu-npt, we decided to see if this xpt host can bind to halide ions instead of organic guests. Similar to the Cu-npt with Dabco, our scheme of controlled guest-binding depends on the oxidation state of the Cu metal centers, which is displayed in Equation 1.



Equation 1. Redox reaction and bind/release process of the halide guest ion, Cl^- , to the $\text{Cu}^{\text{II}}\text{-xpt}$ host.

This method for the bind/release process begins with the behavior of the copper metal center. Because the Cu metal centers are in the 2+ oxidation state, they should be stable in coordination numbers of 5 or 6. This makes the $[\text{Cu}_2(m\text{-xpt})_2]^{4+}$ host a great prospect for guest to bind directly to the metal centers using the remaining open sites. When the Cu is in the 1+ oxidation

state, the metal center only has four coordination sites, which would all be used by the pyridyltriazole ligands. Since the halide guest is much more likely to dissociate from the metal center than the N-donating ligands, the guest is going to be released instead when the Cu^{II} is reduced to Cu^{I} . The guest-binding would be controlled when the Cu^{I} is oxidized back to Cu^{II} .

Taking advantage of the known favorable redox properties and the stability of these Cu^{II} bis(triazoyl-pyridine) frameworks, we decided to test whether the host-guest chemistry of these structures with chloride-ion guests can be controlled. At least one more Cl^- guest can promptly bind to each Cu^{II} metal center and be released efficiently due to Cu^{I} preferring only 4-coordination sites. Oxidation back to Cu^{II} would allow the chloride ions to directly coordinate to the host complex. We intend to analyze and manipulate its bind/release process of Cl^- using CV.

In order to prevent interference from other chemicals in our electrochemical system, we must use a chloride salt that is soluble in the appropriate solvent (DMF in this case). Also, its cation should not interact with our host. Thus, benzyltriethylammonium chloride (BTAC) was selected to provide the Cl^- guest in this study. The bulky cation of the salt inhibits any unnecessary associations with the host besides the proposed chloride ion guest.

We anticipated that the reduction of the Cu^{II} host would be increasingly more difficult as more halide guest ions are added. With a large concentration of Cl^- guests added, the host complex is inclined to stay in the 2+ oxidation state since reduction to Cu^{I} would be accompanied by dissociation of all Cl^- .

2.2. Results and Discussion

2.2.1. $[\text{Cu}_2(m\text{-xpt})_2(\text{NO}_3)_2](\text{PF}_6)_2$ Host with Cl^- ion Guest

The redox properties of the $[\text{Cu}_2(m\text{-xpt})_2(\text{NO}_3)_2](\text{PF}_6)_2$ host (Figure 2.8) was analyzed without any guest added. The voltammogram displayed quasi-reversible behavior that was in agreement with literature.³⁰ A slight positive shift in the reduction peak potential (E_{pc}) when 2 mM Cl^- (1:2 host/guest ratio) is added and a second oxidation peak (E_{pa2}) appears at 0.070 V (vs. $\text{Fc}^{0/+}$), displayed in Table 2.1.

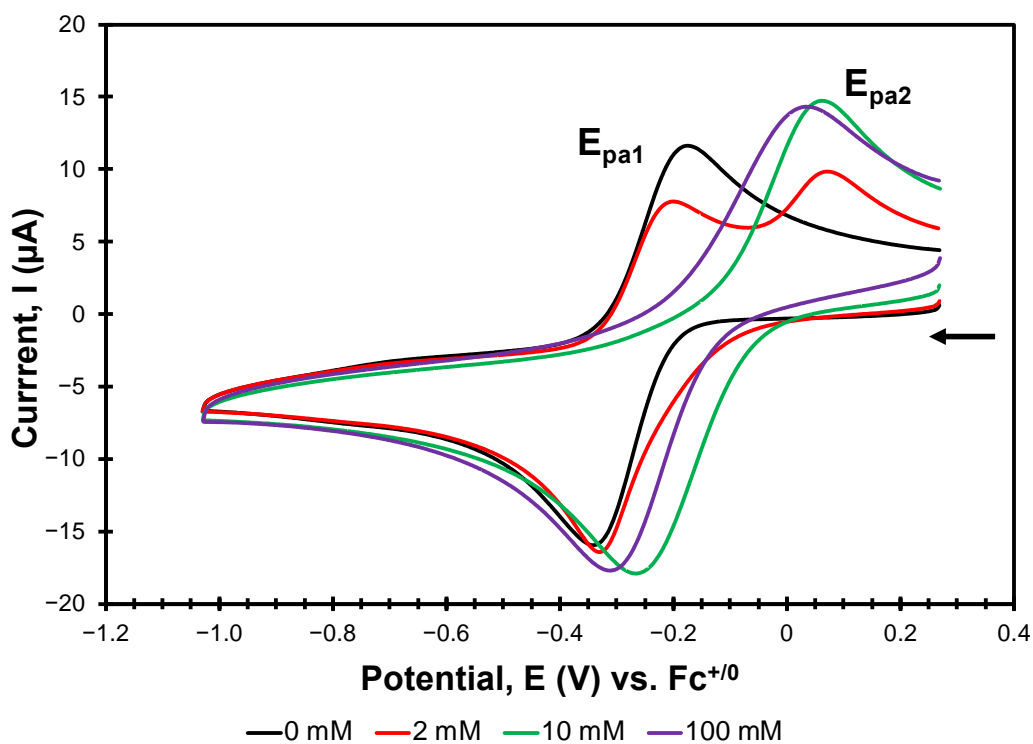


Figure 2.8. CV of $[\text{Cu}_2(m\text{-xpt})_2(\text{NO}_3)_2](\text{PF}_6)_2$ with BTAC (DMF, 0.1 M TBAPF₆, 0.1 Vs⁻¹). The data were measured using an Ag/AgCl reference electrode, glassy carbon working electrode, but plotted vs. $\text{Fc}^{+/0}$ reference redox couple, which has $E_{1/2} = 0.541$ V vs. Ag/AgCl under these conditions.

Table 2.1. Electrochemical parameters in volts (V vs. Fc⁺⁰) of [Cu₂(*m*-xpt)₂(NO₃)₂](PF₆)₂ with added BTAC.

[BTAC]	E _{pa1}	E _{pa2}	E _{pc}	ΔE _p ⁽¹⁾	E _{1/2} ⁽¹⁾
0 mM	-0.174	--	-0.342	0.168	-0.258
2mM	-0.199	0.071	-0.330	0.131	-0.265
10mM	--	0.062	-0.267	--	--
100mM	--	0.034	-0.313	--	--

The two anodic peaks found for the 2 mM concentration of added BTAC is likely from a mixture of the redox properties of the host complex, alone, and the host-guest redox. This is evidenced by E_{pa1} appearing at a similar peak potential as the host complex without any added chloride guest. This finding also suggests that the host complex would need more than a 1:2 host/guest ratio in order to observe complete host-guest binding.

The next addition is 10 mM Cl⁻ to the electrochemical system (1:10 host/guest ratio). E_{pa1} disappears and only E_{pa2} remains, which points to full conversion of the host complex. However, the E_{pc} shifts 0.063 V in the positive direction. This indicates that the reduction is becoming easier to perform with added Cl⁻, which is the opposite of what we expected. The redox behavior is also less reversible with added guest. The ΔE_p increases by 0.161 V, in comparison to the host complex. This led to our conclusion that our host is becoming a new complex when a large excess of guest Cl⁻ is added. When 100 mM of Cl⁻ is added, as with 10 mM Cl⁻, only the second oxidation wave is observed. There is a slight negative shift of both E_{pc} and E_{pa2} compared to the 10 mM data.

Another Cu^{II}-xpt structure has been synthesized in our group:³⁰ [Cu₂(*m*-xpt)₂Cl₂]Cl₂. It is feasible that this chloride host could be forming with the addition of BTAC to the PF₆ host electrochemical system. For example, adding Cl⁻ to a solution of the Cu-xpt complexes in DMF causes a color change from light blue to yellow-green. This color change could be a sign of a new chloride product being produced. Crystallization of the [Cu₂(*m*-xpt)₂(NO₃)₂](PF₆)₂ complex with BTAC (1:5 ratio) produces dark blue-green crystals that were characterized to be [Cu₂(*m*-

xpt)₂Cl₂]Cl₂. The redox properties of this complex have not been studied in the aforementioned literature. Nevertheless, [Cu₂(*m*-xpt)₂Cl₂](PF₆)₂ was analyzed through cyclic voltammetry (see Figure B1) and it was discovered that this structure has a more reversible voltammogram than [Cu₂(*m*-xpt)₂(NO₃)₂](PF₆)₂. Because the only disparity between these two frameworks is the [NO₃]⁻ and Cl⁻ ligands, this signifies that the Cu^{II}-xpt structure binds and releases chloride ions easier than nitrate ions. This finding also suggests that the Cu-xpt structure has a better binding affinity for chloride. We decided to explore the electrochemistry of [Cu₂(*m*-xpt)₂Cl₂]Cl₂ to analyze and compare the redox potential shifts of this complex to that of the PF₆ hosts.

2.2.2. [Cu₂(*m*-xpt)₂Cl₂]Cl₂ Host with Cl⁻ ion Guest

Cyclic voltammetry was executed with [Cu₂(*m*-xpt)₂Cl₂]Cl₂ in the same conditions as the [Cu₂(*m*-xpt)₂(NO₃)₂](PF₆)₂ host (Figure 2.9). The black trace shows the redox properties of the complex without any added chloride. The E_{pa}, 0.072 V, of this host (Table 2.2) is identical to the E_{pa2} of the 2 mM BTAC (Table 2.1) added in the [Cu₂(*m*-xpt)₂(NO₃)₂](PF₆)₂ experiment, 0.071 V. This is evidence of the PF₆ host being converted into the chloride salt as BTAC is added. The disappearance of E_{pa1} as BTAC is added in the [Cu₂(*m*-xpt)₂(NO₃)₂](PF₆)₂ studies reinforce this conclusion. The cathodic peak potentials of [Cu₂(*m*-xpt)₂(NO₃)₂](PF₆)₂ with the added Cl⁻ are also similar to the E_{pc} of [Cu₂(*m*-xpt)₂Cl₂]Cl₂ (Tables 2.1 and 2.2).

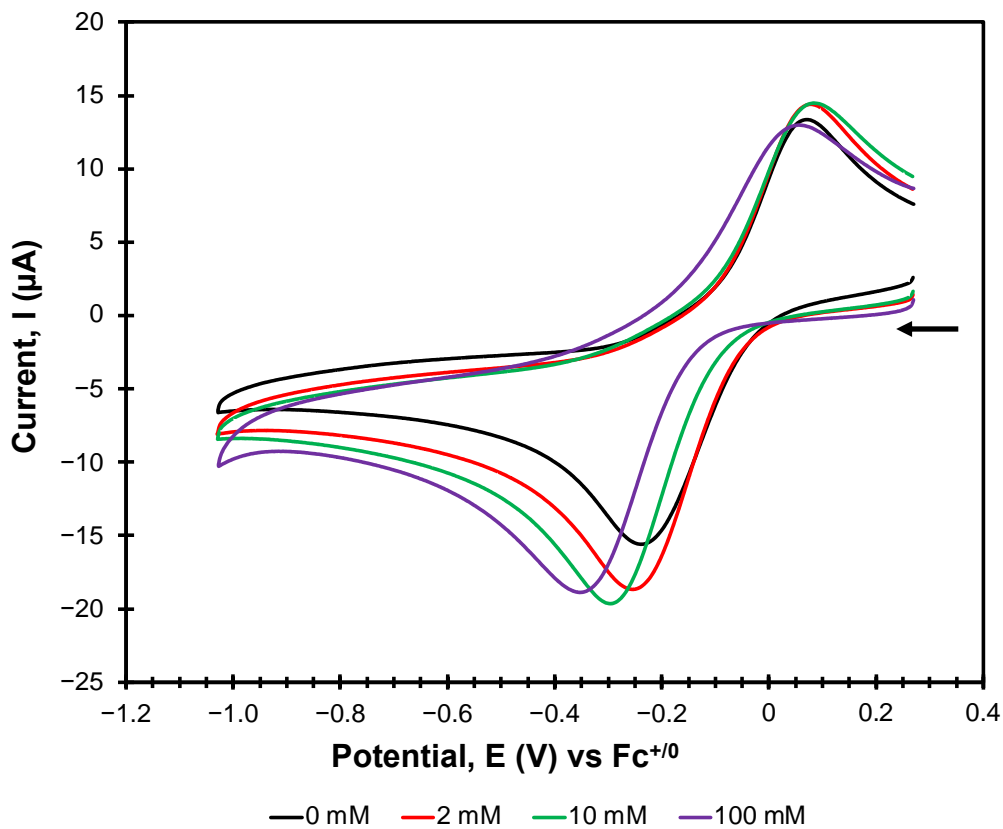


Figure 2.9. CV of $[\text{Cu}_2(m\text{-xpt})_2\text{Cl}_2]\text{Cl}_2$ with BTAC (DMF, 0.1 M TBAPF₆, 0.1 V s⁻¹).

Table 2.2. Electrochemical parameters in volts (V vs. Fc⁺⁰) of $[\text{Cu}_2(m\text{-xpt})_2\text{Cl}_2]\text{Cl}_2$ with added BTAC.

[BTAC]	E _{pa}	E _{pc}	ΔE _p	E _{1/2}
0 mM	0.072	-0.237	0.309	-0.083
2 mM	0.079	-0.253	0.332	-0.087
10 mM	0.085	-0.297	0.382	-0.106
100 mM	0.058	-0.353	0.411	-0.148

In the voltammogram of the $[\text{Cu}_2(m\text{-xpt})_2\text{Cl}_2](\text{PF}_6)_2$ host, a small shoulder appears at an approximate potential to the E_{pa2} and E_{pa} of the $[\text{Cu}_2(m\text{-xpt})_2(\text{NO}_3)_2](\text{PF}_6)_2$ and $[\text{Cu}_2(m\text{-xpt})_2\text{Cl}_2]\text{Cl}_2$ hosts, respectively (Figure B1). This suggests that the shoulder in the $[\text{Cu}_2(m\text{-xpt})_2\text{Cl}_2](\text{PF}_6)_2$ electrochemical data is from excess chloride.

Next, more chloride ions are added to the electrochemical system to observe the host-guest interaction of the $[\text{Cu}_2(m\text{-xpt})_2\text{Cl}_2]\text{Cl}_2$ host with Cl⁻. The negative shift of the redox potential as more Cl⁻ is added is the behavior we anticipated for anionic host-guest binding. However, the host

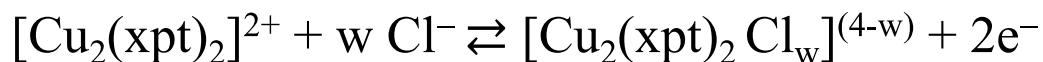
becomes less reversible throughout this process. This is due to E_{pc} shifting more negatively than the E_{pa} . This finding exhibits that $[Cu_2(m-xpt)_2Cl_2]Cl_2$ is not an applicable host for halide guest-binding.

Host-guest interaction is observed in this analysis, but the anodic peak potential shift is not as prominent as we desired. The oxidation peak potential requires a very large excess of chloride ions (1:100 host/guest ratio) to display a noticeable negative shift (Figure 2.9). This slight negative shift of E_{pa} discerned, even in the presence of a large surplus of guest, also is evidence of the binding of Cl^- to the Cu^{II} -xpt hosts is not as adequate as we aspired. This means that we would need to determine a better host in order to perform anion guest interaction. Our work in host-guest interaction with anionic guests is mentioned in Chapter 4 of this dissertation.

2.2.3. Calculation of the Number of Cl^- ion Guests Binding with $[Cu_2(m-xpt)_2Cl_2]Cl_2$

Pourbaix diagrams show changes in redox potentials with pH. These changes can be used to determine the number of protons involved in redox processes.^{64,65} In a one-electron/one-proton transfer reaction, the redox potential is expected to shift -0.0592 V per pH unit.

Redox potentials can also vary with concentration when species other than H^+ are involved in the reaction. In the present case, if a Cl^- ion binds in one oxidation state but not the other, the redox potential should also shift by 0.0592 V for each factor of 10 in $[Cl^-]$. The effects of guest binding on redox potential are further explained using the square schemes in Chapters 3 and 4 of this dissertation. We can utilize the same method to determine how many more guests bind to the targeted oxidized or reduced host than the starting state of the host. This can be measured using Equations 2 and 3.



$$E = E^\circ - \frac{0.0592 \text{ V}}{n} \log \frac{[\text{Cu}_2(\text{xpt})_2 \text{Cl}_w]^{(4-w)}}{[\text{Cl}^-]^w [\text{Cu}_2(\text{xpt})_2]^{2+}} \quad (\text{Equation 2})$$

At $E_{1/2}$, $[\text{Cu}_2(\text{xpt})_2]^{2+} = [\text{Cu}_2(\text{xpt})_2 \text{Cl}_w]^{(4-w)}$, so:

$$E_{1/2} = E^\circ - \frac{0.0592 \text{ V}}{n} \log \frac{1}{[\text{Cl}^-]^w} \quad (\text{Equation 3})$$

As mentioned, in a one-electron redox reaction, having a slope of 0.0592 means that one chloride would be binding in the Cu^{III} redox. However, the Cu-xpt redox involves a two-electron transfer. This means that $n = 2$ and that a slope of 0.0592 is indicative of two chloride ions binding. Because the host's cathodic peak potential, E_{pc} , has a reliable negative shift in the reduction peak potential, we decided to see how many Cl^- ions are released upon reduction of the complex (Figure 2.10).

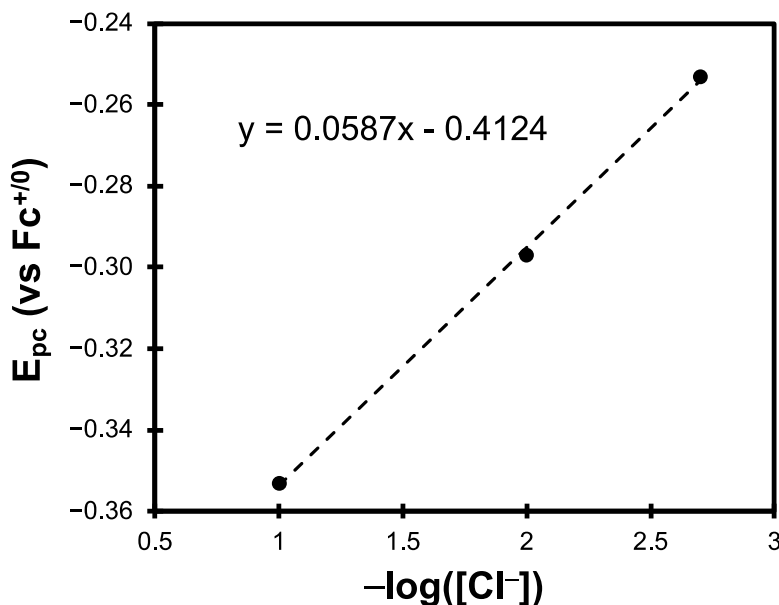


Figure 2.10. E_{pc} (vs. $\text{Fc}^{+/0}$) vs. $-\log([\text{Cl}^-])$ of 1 mM $[\text{Cu}_2(m\text{-xpt})_2\text{Cl}_2]\text{Cl}_2$. Slope for all concentrations.

Due to the irreversibility of the voltammograms, we elected to replace the $E_{1/2}$ in Equation 3 with E_{pc} . In our theory, we expected the reduction of the Cu-xpt host to release the two Cl^- ions and become a 4-coordinate $Cu_2(m-xpt)_2$ complex. The slope that was determined was 0.0587, which signifies that this is what is occurring. This also reinforces that the host is unreliable in binding back to the guest, likely due to its irreversible redox behavior.

2.3. Experimental

2.3.1. General

All commercially available chemicals were purchased from Aldrich, Alfa Aesar, BeanTown Chemicals, Sigma-Aldrich, Strem Chemicals, Fischer Scientific, J.T. Baker, and VWR Chemicals were utilized without further purification. All synthesis were executed in air.

Cyclic voltammetry of the metal-organic complexes was analyzed using an EC Epsilon Eclipse potentiostat/galvanostat (BAS Inc.) with Ag/AgCl reference electrode, a glassy carbon working electrode, and Pt wire counter electrode under nitrogen. All electrochemical experiments were performed using a 1 mM solution of the Cu-xpt host in DMF with 0.1 M tetrabutylammonium hexafluorophosphate (TBAPF₆). All scans were performed at 0.1 V s⁻¹. Additions of Cl^- through benzyltriethylammonium chloride were made throughout the experiment.

2.3.2. Synthesis of *m*-Xylylenebis(pyridyltriazole) (*m*-xpt)

The *m*-Xylylenebis(pyridyltriazole) (*m*-xpt) ligand were prepared using previous literature.²⁷ A white powder was collected and characterization was consistent with what was found in Crowley et al.²⁸

2.3.3. Synthesis of Cu^{II}-xpt complexes

The $[Cu_2(m-xpt)_2(NO_3)_2](PF_6)_2$, $[Cu_2(m-xpt)_2Cl_2](PF_6)_2$, and $[Cu_2(m-xpt)_2Cl_2]Cl_2$ complexes were prepared following the procedures in literature from our group.³⁰ A light blue

precipitate was formed for the $[\text{Cu}_2(m\text{-xpt})_2(\text{NO}_3)_2](\text{PF}_6)_2$ host, green-blue solid for $[\text{Cu}_2(m\text{-xpt})_2\text{Cl}_2](\text{PF}_6)_2$, and a light green precipitate for $[\text{Cu}_2(m\text{-xpt})_2\text{Cl}_2]\text{Cl}_2$. Ether vapor diffusion in DMF produced blue-green crystals of $[\text{Cu}_2(m\text{-xpt})_2\text{Cl}_2]\text{Cl}_2$.

Chapter 3. Ruthenium β -diketonate Hosts and Alkali-metal Guests

3.1. Introduction

Metal-organic supramolecular frameworks have been analyzed by researchers for decades. They have discovered that these metal-organic structures can be utilized as hosts that can bind to guests in a way that enzymes can associate with substrates. These interactions have opened a new way of exploring supramolecular complexes in a subject known as host-guest chemistry. Host-guest chemistry has allowed for scientists to investigate metal complexes that exhibit an affinity for certain guest ions or molecules.⁶⁶ They have found that these host complexes can interact with these guests through coordination to the metal center,^{21, 25, 27} π - π interactions,^{26, 67} or association with a second-coordination sphere.^{11, 68, 69}

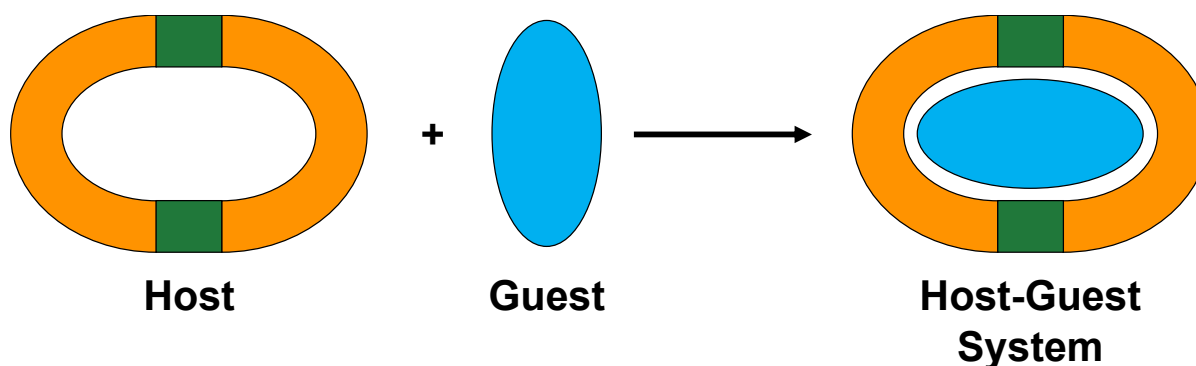


Figure 3.1. Diagram of host-guest interaction of a metal-organic host with a guest. Metal centers, green and ligands, orange.

Hydrogen binding⁹⁻¹¹ and π - π interactions are common methods of achieving host-guest association. These techniques have potential in being used for drug delivery. For example, the Therrien Group synthesized cationic ruthenium triangular metallo-prisms that interact with aromatic compounds through π -stacking.⁷⁰ Metal-organic hosts have also aided in advancing chemotherapeutics that only target cancer cells and reduce side effects. Mishra and co-workers were able to accomplish host-guest studies where a ruthenium complex was stronger against cancer cells than known anticancer drugs like doxorubicin.⁷¹ Heterometallic cobalt-ruthenium

frameworks were also executed as drugs that can mitigate gastric cancer.⁷² Although these studies are promising, a way to further progress research on host-guest chemistry is by developing modules where the bind and release of the guest can be controlled. However, for most systems, it is tasking to separate a guest from a host due to factors such as the binding constant being too strong. This suggests that in order to manipulate the binding constant between a host and guest, a stimulate is needed.

One technique of controlling host-guest chemistry is light. Through light, the binding affinity between a host and guest can be influenced by changing the intensity and wavelength.¹⁵ The Leung Group have analyzed host-guest therapeutics of iron oxide core silica nanoparticles and an antitumor drug and controlled it by using ultrasound.¹⁶ Other methods of controlling host-guest properties are through pH and temperature. Reversible guest-discharge of acids and bases from organometallic hosts was achieved by Chan et al. using pH-response.¹³ Heat-controlled host-guest chemistry has been admired by researchers as well due to temperature-sensitive ion channels occurring in nature. Wang and co-workers developed an artificial temperature-responsive nanochannel to transport ions using pillar[5]arene-based host-guest association.¹⁴ However, these forms of controlled host-guest interaction will lead to adversity for some systems. For example, temperature and light can cause deterioration of the analyte and pH-response studies involves using other reagents that can produce less reliable measurements.

One procedure that accomplished manipulative host-guest chemistry is redox stimulation. There is few known research done on utilizing redox to manipulate host-guest interactions. The Nitschke Group executed $[\text{PF}_6]^-$ guest-release by titrating an oxidant to a tetranuclear Fe^{II} host solution.⁷³ Unfortunately, this oxidation collapses the structure of the host, making it a mononuclear framework. To avoid the need for adding oxidizing and reducing agents to the

analyte, we decided to look into performing controlled host-guest association through redox using cyclic voltammetry (CV). Single tripodal ligand manganese hosts were studied electrochemically and they discovered that their redox potentials, $E_{1/2}$, shift in the positive direction with the addition of NH_4^+ , K^+ , and Na^+ .¹⁹ They have discovered that this $\Delta E_{1/2}$ is due the cations' interaction with the tripodal ligand's methoxy and phenolate O atoms from crystallography data.

Redox was implemented on Fe and Ni Schiff-based hosts with K^+ and Ba^{2+} ions using CV.⁷⁴ They found that the $E_{1/2}$ of the hosts had a large positive shift with the introduction of the guest ions. The alkali-metal ions were able to bind through the host's crown ether groups. They believe that the positive shift is due to the stabilization of the host's metal center.⁷⁵ The very large positive shift in the redox potential is indicative that the binding constant between the host and guest was very strong.

Also, a current study by Sallé and co-workers involved an extended tetrathiafulvalene Pt host and an organic coronene guest. This work was achieved without collapsing the structure of the host. Figure 3.2 displays a simple diagram of how oxidation of the host permits it to release a guest using a four-electron transfer.¹⁸

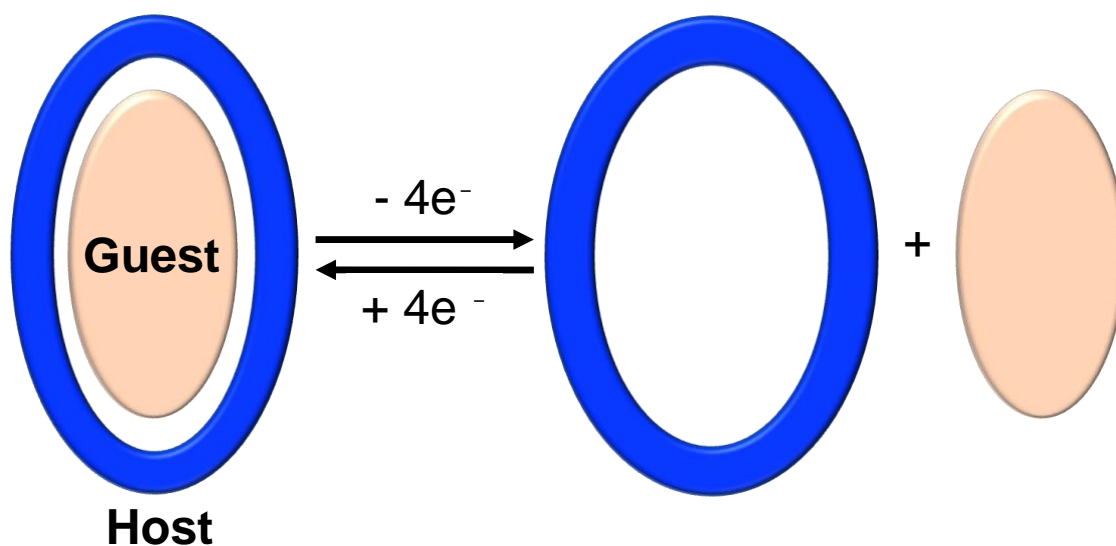


Figure 3.2. Schematic of using redox to manipulate the binding affinity between the host and guest.

For our research, we intend to control the cationic guest bind and release by tuning the redox properties of the metal-organic host complex. In order to observe this, we must choose a system where the binding constant between the host and guest is not too strong. A binding constant that is too large makes the release process very difficult. We also intend to analyze a host-guest system where the electron transfer is easy to accomplish. This is why we looked into a notable metal-diketonate host system with sodium ion guests. We took inspiration from proton and electron transfer coupling reactions to describe the control of the bind and release process using redox chemistry. We decided to replace the proton coupling with guest bind/release to create a square scheme (Figure 3.3).

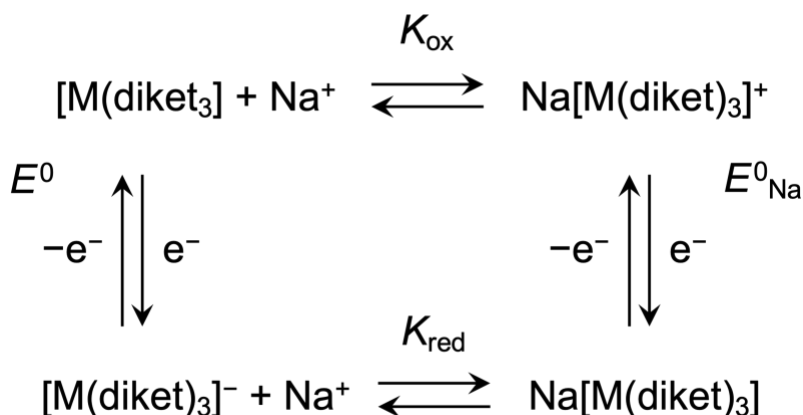


Figure 3.3. Square scheme for the coupled redox and cation-binding reactions with the $\text{M}(\text{diket})_3$ host complex.

The oxidation state of the host complex, $[\text{M}(\text{diket})_3]$, is influenced by adding or extracting electrons from the analyte. When the host is reduced, the Na^+ guest binds to it a lot better than the oxidized form, making the binding constant, K_{red} , greater than K_{ox} . When Na^+ is added, the reduction of $[\text{M}(\text{diket})_3]$ is easier to accomplish, which induces a positive shift in the $\text{M}^{\text{III/II}}$ redox potential. This signifies that the standard potential, E^0 , of $[\text{M}(\text{diket})_3]$ is less than E^0_{Na} , of $\text{Na}[\text{M}(\text{diket})_3]$. When $\text{Na}[\text{M}(\text{diket})_3]$ is oxidized, this triggers Na^+ guest release and the host is back to the original $[\text{M}(\text{diket})_3]$ host.

In the past, our group has studied metal-bis(β -diketonates) as potential hosts for guest molecules. We researched Cu^{II} diketonate complexes that were found to bind to guests using the available coordination sites of the metal center and through π -interactions.^{26,31} Nevertheless, the copper metal center would have difficulty binding and releasing these guest using electrochemistry. This is due to the instability of Cu^{I} with electron-deficient O diketonate ligands, which would affect the Na^+ guest binding. Because this host-guest chemistry requires a stable metal center, we determined to examine β -diketonate with a ruthenium metal center. Figure 3.4 illustrates the octahedral host framework. The Ru β -diketonate hosts vary by the R groups placed on the diketonate ligands.

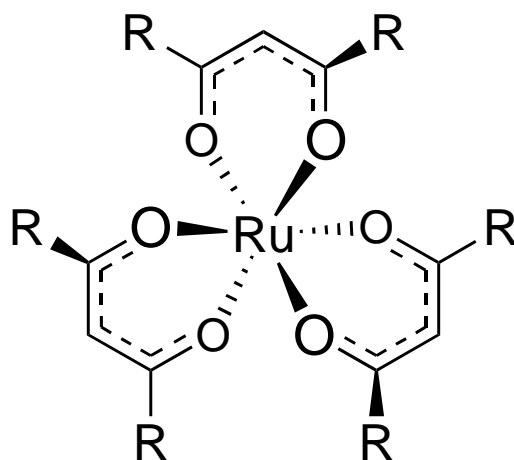


Figure 3.4. Structure of ruthenium β -diketonate host. Substituent of the β -diketonate ligand is represented by R.

Endo has studied the redox properties of various ruthenium(III) tris(β -diketonate) and its effect when Na^+ is added.³⁴ However, the main focus was on the $\text{Ru}(\text{acac})_3$ structure. This framework is a β -diketonate where the R groups are methyl substituents. $\text{Ru}(\text{acac})_3$ has a larger positive change in its redox potential than most of the other known β -diketonates. UV-vis studies of $\text{Ru}(\text{acac})_3$ were executed with tetraethylammonium (TEAP) and NaClO_4 separately and they discovered that both spectra are identical. This implies that the $\Delta E_{1/2}$ is due to the reduced host interacting with Na^+ , not the oxidized host. This was further evidenced by a precipitate formed

from the reduction of Ru(acac)₃ in the presence of Li⁺. Elemental analysis showed that the solid was discovered to be Li[Ru(acac)₃]. It is believed that the cation interacts with the O diketonate atoms of the host. Endo also deduced that the relationship between ΔE_{1/2} and K_{red} is linear. From the electrochemical analysis of all the Ru β-diketonates, it was concluded that the K_{red} is larger for hosts that have more electron-donating R groups.

Within the Ru β-diketonates Endo analyzed, Ru(dbm)₃ (dbm = dibenzoylmethane) was discovered to have a smaller binding constant to Na⁺ than Ru(acac)₃. It was concluded that the K_{red} of [Ru(dbm)₃]⁻ to Na⁺ to be 3.98 x 10², much less than that of 6.31 x 10³ for the acac host.³⁴ This is supported by the less positive ΔE_{1/2} when Na⁺ is introduced. It is likely this occurred due to the phenyl substituent not supplying as much electron density to the diketonate O atoms.

To advance the research done by Endo, we propose to use the Ru(dbm)₃ structure as a model host to synthesize new Ru β-diketonate hosts with greater sensitivity to alkali-metal ions. To succeed in this, we need to construct frameworks that provide a greater local negative charge to the diketonate O atoms. In turn, this will improve the binding affinity of the reduced dbm host, while maintaining the ability for the host to release the alkali-metal guest. The phenyl rings of dbm ligand were functionalized with attachments that would increase the affinity for cations. The new β-diketonate complexes prepared were: Ru(dbm)₃, Ru(acac)₃, Ru(d2nm)₃, Ru(d1nm)₃, and Ru(dbm-2OMe)₃ as shown in Figure 3.5.

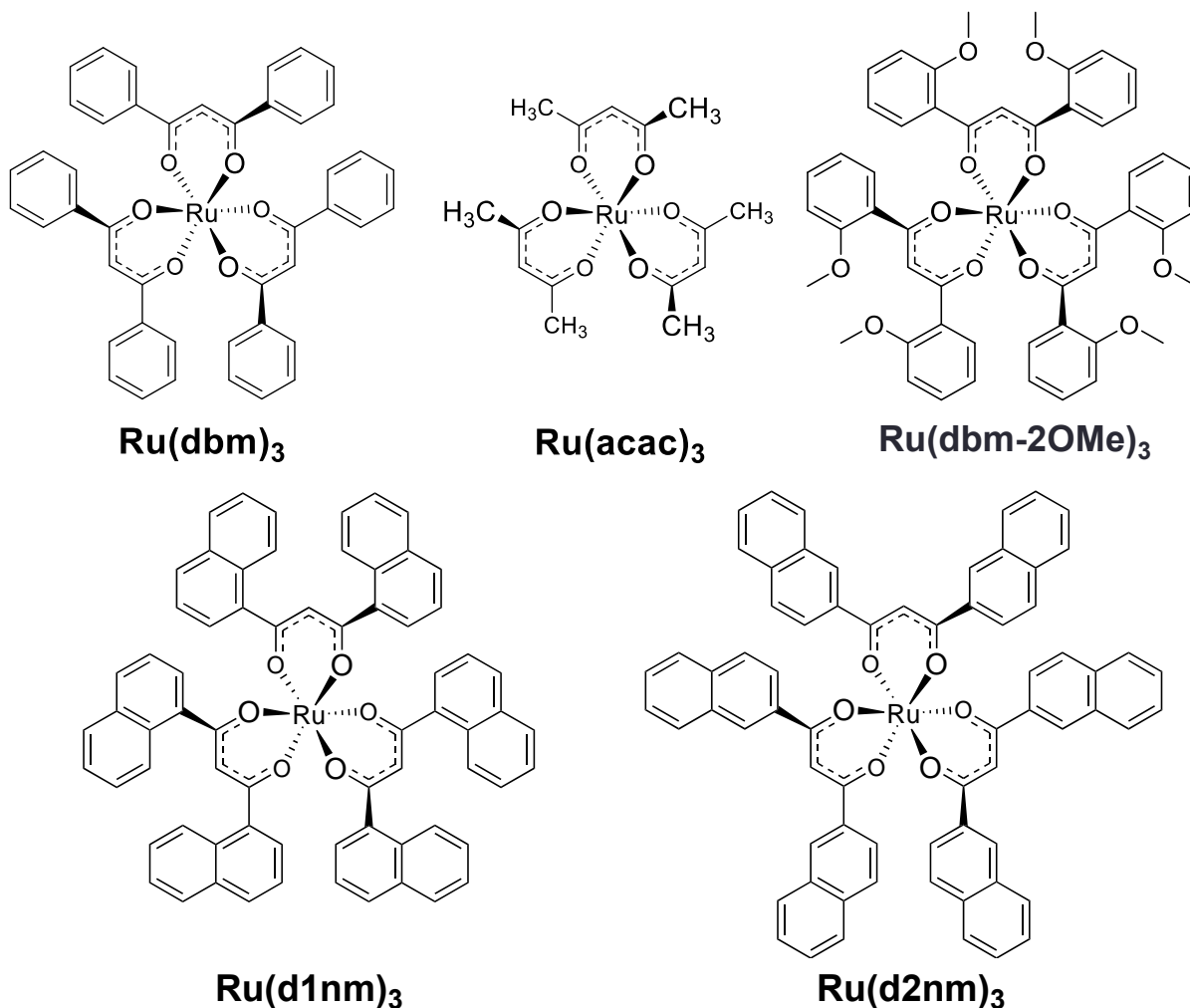


Figure 3.5. Ruthenium β -diketonate hosts.

The redox properties of the new ruthenium(III) tris(β -diketonate) complexes were examined using a one-electron transfer through CV. This one-electron transfer promotes more analysis on facile bind and release of host-guest systems. The guest-interaction of these new β -diketonates were observed using Na^+ and K^+ ions.

3.2. Results and Discussion

Host-guest properties of the Ru β -diketonates and Na^+ guests were observed using CV. The electrochemical measurements were analyzed in 0.1 M TBAPF₆ CH₃CN at 0.1 V s⁻¹ unless stated otherwise. The host was increasingly introduced to Na^+ , starting with 2 mM NaClO₄ (1:2 host/guest ratio) and ending with 100 mM (1:100 host/guest).

3.2.1. Interaction of Ru(acac)₃ Host with Na⁺ Guest

Because Endo researched the Ru(acac)₃ host, we elected to study it and compare it to the results of our new hosts. Figure 3.6 displays the voltammograms of the host complex for each of the corresponding guest concentration. The electrochemical parameters of Ru(acac)₃ at each concentration of guest added are labeled in Table 3.1. After 2 mM Na⁺ is added to the electrochemical solution, there is a +0.065 V $\Delta E_{1/2}$, which signifies the guest binding that Endo detected. After 100 mM Na⁺, the change in the redox potential is +0.264 V. It is notable that there is a larger positive shift when there is a high guest concentration. This suggests that [Ru(acac)₃]⁻ may need a higher amount of guest present in order to display more prominent guest binding.

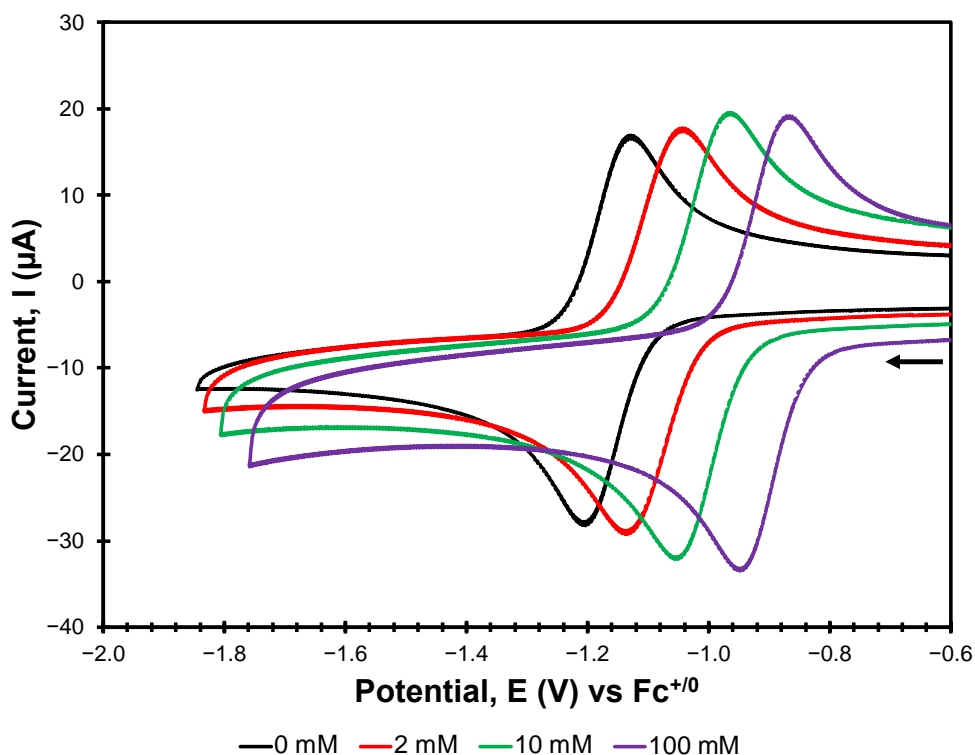


Figure 3.6. Cyclic Voltammetry of 1 mM Ru(acac)₃ with added NaClO₄, 0.1 M TBAPF₆ CH₃CN, 0.1 V s⁻¹. The data were measured using an Ag/AgCl reference electrode, glassy carbon working electrode, but plotted vs. Fc⁺⁰ reference redox couple, which has E_{1/2} = 0.445 V vs. Ag/AgCl under these conditions.

Table 3.1. Electrochemical parameters (V) of 1 mM Ru(acac)₃ with NaClO₄, 0.1 M TBAPF₆ CH₃CN, 0.1 V s⁻¹ against Fc⁺⁰.

[Na ⁺]	E _{pa}	E _{pc}	ΔE _p	E _{1/2}
0 mM	-1.138	-1.220	0.082	-1.179
2 mM	-1.067	-1.161	0.094	-1.114
10 mM	-0.989	-1.074	0.085	-1.032
100 mM	-0.868	-0.961	0.093	-0.915

In Chapter 2, we discussed the Nernstian method of using the E_{1/2} of the host to ascertain how many more guests bind to the oxidized or reduced host. Using this technique, the number of how many more Na⁺ are bound to the reduced state than the oxidized state is summarized by Equations 1 and 2.

$$E = E^\circ - \frac{0.0592 \text{ V}}{n} \log \frac{Na_w[Ru^{II}(\text{diket})_3]^{(w-1)}}{[Na^+]^w[Ru^{III}(\text{diket})_3]} \quad (\text{Equation 1})$$

At E_{1/2}, [Ru^{II}(diket)₃]⁻ = [Ru^{III}(diket)₃], so:

$$E_{1/2} = E^\circ - \frac{0.0592 \text{ V}}{n} \log \frac{1}{[Na^+]^w} \quad (\text{Equation 2})$$

We obtained the number of bound cations in the reduced form by calculating the slope of the E_{1/2} vs -log([Na⁺]) graph. Unlike the Cu-xpt host system in Chapter 2, [Ru(diket)₃]^{0/-} is a one-electron transfer, hence, one more Na⁺ binding would have a slope of -0.0592 V. Two ions binding would double this with a slope of -0.1184 V. Starting with the Ru(acac)₃ complex, the slope was determined to be ~0.12, which is indicative that this host is able to bind to two more Na⁺ ions when it is reduced (Figure 3.7). This analysis is consistent with what was found in Endo's studies.³⁴

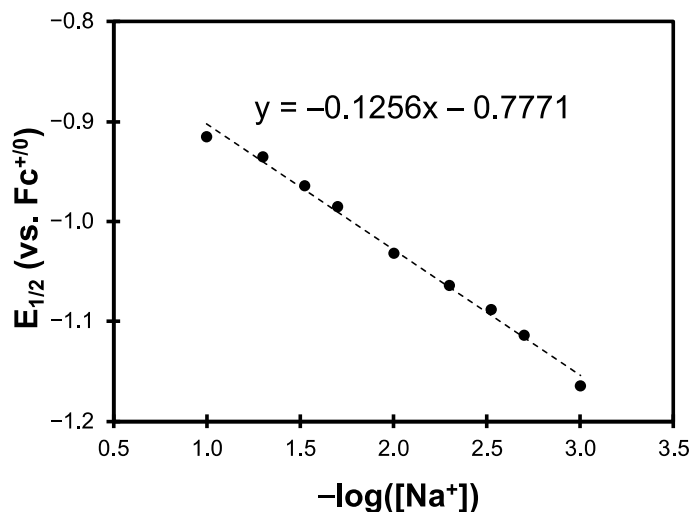


Figure 3.7. $E_{1/2}$ (vs. $Fc^{0/+}$) vs. $-\log([Na^+])$ of 1 mM $Ru(acac)_3$.

3.2.2. Interaction of $Ru(dbm)_3$ Host with Na^+ Guest

As founded in Endo's work, the $Ru(dbm)_3$ host did not display as much sensitivity to Na^+ as the acac host. Table 3.2 shows that the $\Delta E_{1/2}$ is very small (+0.012 V) at 1:2 host/guest ratio. At 100 mM Na^+ added, the overall change is +0.099 V. Figure 3.8 shows that the $\Delta E_{1/2}$ is not very noticeable until at least there is a 1:10 host/guest ratio.

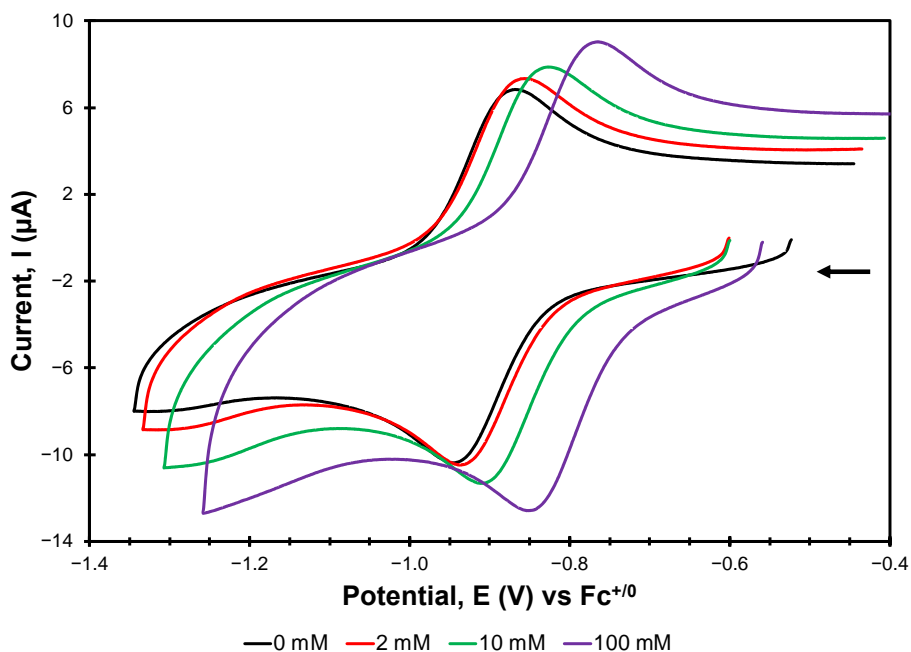


Figure 3.8. Cyclic Voltammetry of 1 mM $Ru(dbm)_3$ with added $NaClO_4$, 0.1 M $TBAPF_6$ CH_3CN , $0.1 V s^{-1}$.

Table 3.2. Electrochemical parameters (V) of 1 mM Ru(dbm)₃ with NaClO₄, 0.1 M TBAPF₆ CH₃CN, 0.1 V s⁻¹ against Fc⁺⁰.

[Na ⁺]	E _{pa}	E _{pc}	ΔE _p	E _{1/2}
0 mM	-0.868	-0.945	0.077	-0.907
2 mM	-0.855	-0.935	0.080	-0.895
10 mM	-0.827	-0.910	0.083	-0.869
100 mM	-0.765	-0.851	0.086	-0.808

Next, the number of bound Na⁺ was calculated for [Ru(dbm)₃]⁻. Because the binding affinity for this host is not as strong as [Ru(acac)₃]⁻, the data (Figure 3.9) is not linear when all concentrations are considered (black trace). Nevertheless, at higher concentrations, 10 – 100 mM, a linear slope is found and discovered to be -0.0606 (green trace). This signifies that one more Na⁺ binds to reduced host.

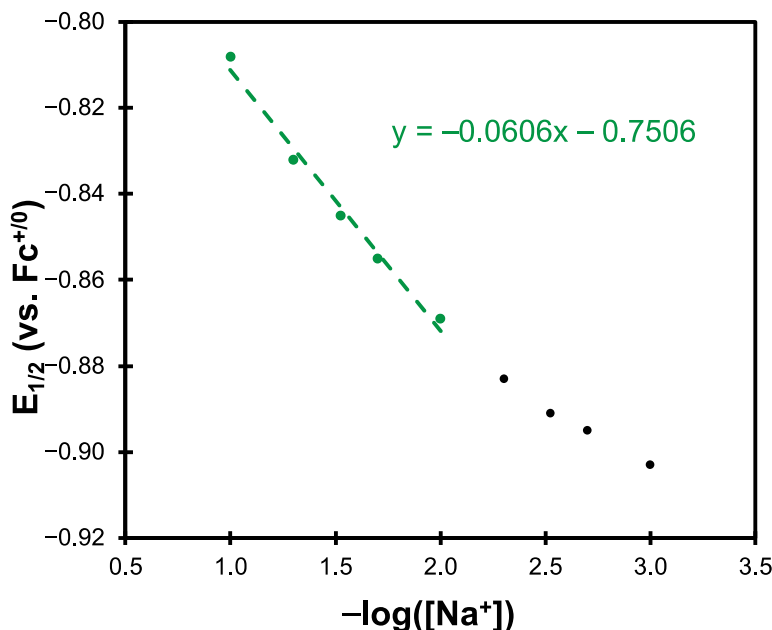


Figure 3.9. E_{1/2} (vs. Fc⁰⁺) vs. -log([Na⁺]) of 1 mM Ru(dbm)₃, 10 – 100 mM [Na⁺].

3.2.3. Interaction of Ru(d2nm)₃ and Ru(d1nm)₃ Hosts with Na⁺ Guest

The first R group we decided to attach to the phenyl ring of the Ru(dbm)₃ host is a second ring to create a naphthyl substituent. We elected to create a naphthyl β-diketonate host to induce Na⁺ binding by cation-π interaction.⁷⁶ Starting with the d2nm β-diketonate host, the ring is attached

in the 2' position. With this, we intended that the electron density in the second ring would be strong enough to attract Na^+ to the reduced host. We also synthesized the d1nm host as well and this host is expected to have a greater affinity with cations than the d2nm host. That is because in the d1nm host, the naphthyl ring is attached in the 1' position, which allows the second ring to be closer to the diketonate O atoms. Through this, the Na^+ would be attracted to the pi system in the second ring and thus, makes it easier for it to bind to the O atoms of the host.

First, the electrochemistry of the $\text{Ru}(\text{d2nm})_3$ was examined in DMF due to its better solubility than in acetonitrile. However, Figure 3.10 displays that the $\Delta E_{1/2}$ is low and noticeable until 100 mM Na^+ is added. Table 3.3 exhibits that the overall change in the redox potential is only +0.014 V. This signifies that this host does not have as much sensitivity to Na^+ ions as we anticipated. One reason for the lack of change in the redox potential is because this experiment was measured in DMF. In DMF, the host has competition with the oxygen atoms in the solvent, preventing some Na^+ from binding to the complex, which is not a problem in CH_3CN . This electrochemical study was also accomplished with $\text{Ru}(\text{dbm})_3$ in DMF to determine if the second ring enhanced the binding affinity of Na^+ (Figure B2). It was found that the $\Delta E_{1/2}$ is more distinct in $\text{Ru}(\text{dbm})_3$ than $\text{Ru}(\text{d2nm})_3$.

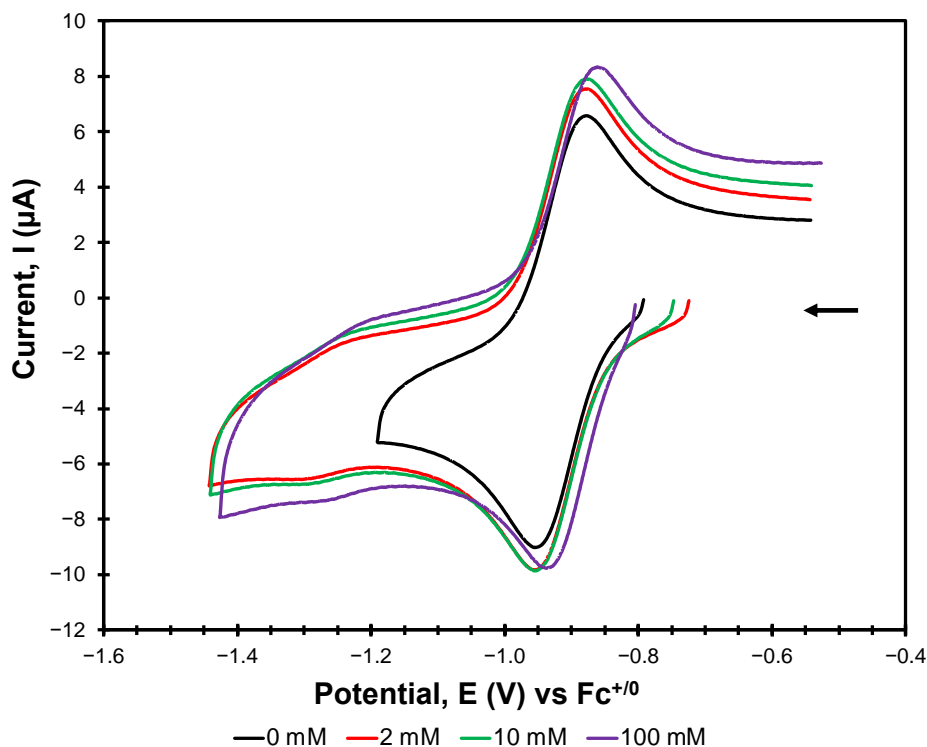


Figure 3.10. Cyclic voltammetry of 1 mM Ru(d2nm)₃ with NaClO₄ added, 0.1 M TBAPF₆ DMF, 0.1 V s⁻¹.

Table 3.3. Electrochemical parameters (V) of 1 mM Ru(d2nm)₃ with NaClO₄, 0.1 M TBAPF₆ DMF, 0.1 V s⁻¹ against Fc⁺⁰.

[Na ⁺]	E _{pa}	E _{pc}	ΔE _p	E _{1/2}
0 mM	-0.877	-0.953	0.076	-0.915
2 mM	-0.880	-0.950	0.070	-0.915
10 mM	-0.878	-0.952	0.074	-0.915
100 mM	-0.863	-0.938	0.075	-0.901

Afterwards, we analyzed the redox properties of Ru(d1nm)₃ in CH₃CN. After 50 mM NaClO₄ is added, the oxidation of the voltammogram becomes distorted. Table 3.4 demonstrates that the ΔE_{1/2} is smaller than [Ru(dbm)₃]⁻. This suggests that the sensitivity to Na⁺ is less than the dbm host. This is likely due to the lack of π-conjugation in the naphthyl group.⁷⁷ This substituent lacking conjugation prevents the pushing of electrons to chelating diketonate O atoms, reducing the ability for Na⁺ to bind. This also conveys that the cation-π interaction in the extra ring may

not be strong enough to attract Na^+ ions to the host. Nevertheless, this host does display the ability to bind to Na^+ guest when there is a large excess of guest (Figure 3.11).

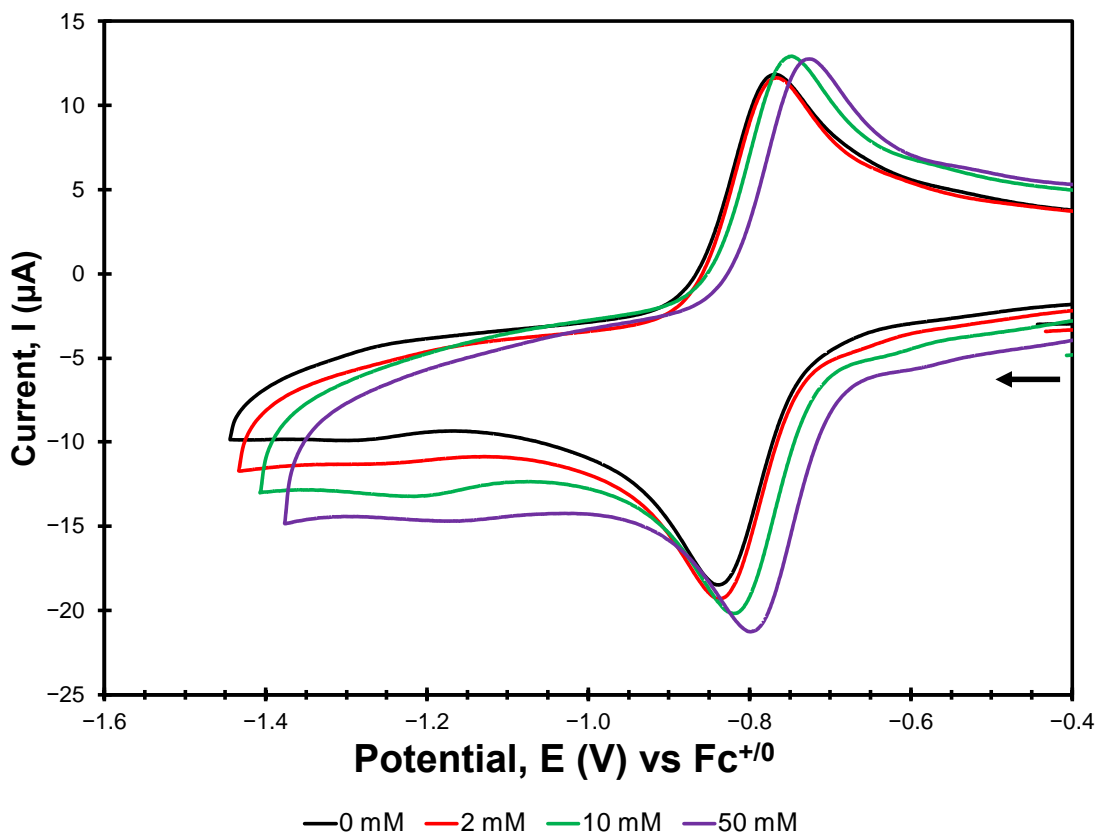


Figure 3.11. Cyclic voltammetry of 1 mM $\text{Ru}(\text{d}1\text{nm})_3$ with added NaClO_4 , 0.1 M TBAPF_6 CH_3CN , 0.1 V s^{-1} .

Table 3.4. Electrochemical parameters (V) of 1 mM $\text{Ru}(\text{d}1\text{nm})_3$ with NaClO_4 , 0.1 M TBAPF_6 CH_3CN , 0.1 V s^{-1} against $\text{Fc}^{+/0}$.

$[\text{Na}^+]$	E_{pa}	E_{pc}	ΔE_{p}	$E_{1/2}$
0 mM	-0.769	-0.841	0.072	-0.805
2 mM	-0.767	-0.837	0.070	-0.802
10 mM	-0.748	-0.820	0.072	-0.784
50 mM	-0.725	-0.797	0.072	-0.761

Afterwards, the number of bound Na^+ ions to $[\text{Ru}(\text{d}1\text{nm})_3]^-$ was determined using the redox potentials for each guest concentration. As seen for $[\text{Ru}(\text{dbm})_3]^-$, the graph for all concentrations does not display linear data due to the smaller binding constant between the reduced host and Na^+ . Figure 3.12 shows that the guest-binding behavior was detected in the 30 – 50 mM range and the

slope was discovered to be -0.0451 (green trace). This implies that some of this host can bind to one more Na^+ ion.

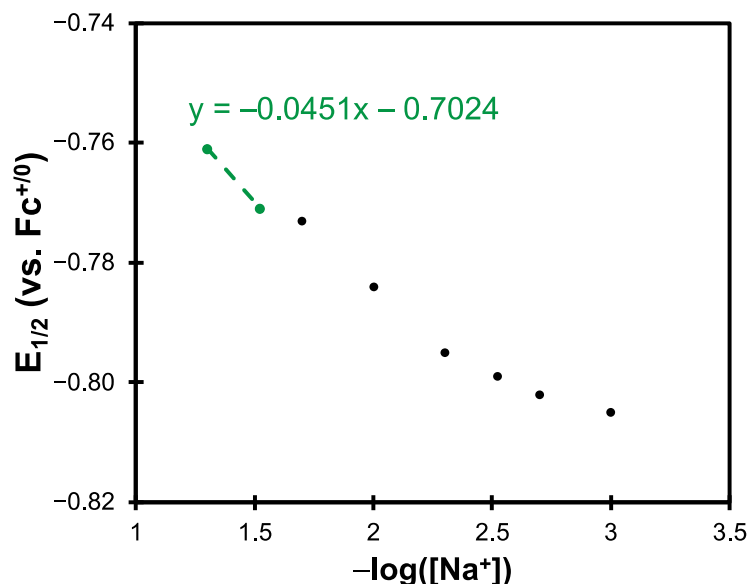


Figure 3.12. $E_{1/2}$ (vs. $\text{Fc}^{+/0}$) vs. $-\log([\text{Na}^+])$ of 1 mM $\text{Ru}(\text{d1nm})_3$, 30 – 50 mM $[\text{Na}^+]$.

3.2.4. Interaction of $\text{Ru}(\text{dbm-2OMe})_3$ Host with Na^+ Guest

Next, we aimed to construct the $\text{Ru}(\text{dbm-2OMe})_3$ host. This structure retains the phenyl substituent, but has a methoxy group placed in the 2'-position. This complex has great promise in being a considerable host for binding cations due to its inductive and chelating effects. The methoxy groups can induce electron density into the ring and thus, to the diketonate O atoms to attract Na^+ . Another benefit for this host is that the methoxy groups are near proximity to the diketonate O atoms, which means that Na^+ can also interact with the chelating methoxy O atom.

The host-guest properties of $[\text{Ru}(\text{dbm-2OMe})_3]^{0/-}$ in the presence of Na^+ was measured using the same experimental conditions. Table 3.5 displays the electrochemical parameters of the host after each addition of guest. After 2 mM is added, there is a large positive shift in the host's redox potential by +0.126 V. This $\Delta E_{1/2}$ can be visually seen in Figure 3.13 when comparing the black trace (host) and the red trace (host with 2 mM Na^+). This change is nearly twice the effect

seen for the acac host. This result also exhibits that the 2'-methoxy host does not require a large amount of guest added in order to notice its guest binding affinity. This emphasizes that this host has more distinguished sensitivity to Na^+ than any known ruthenium β -diketonate.

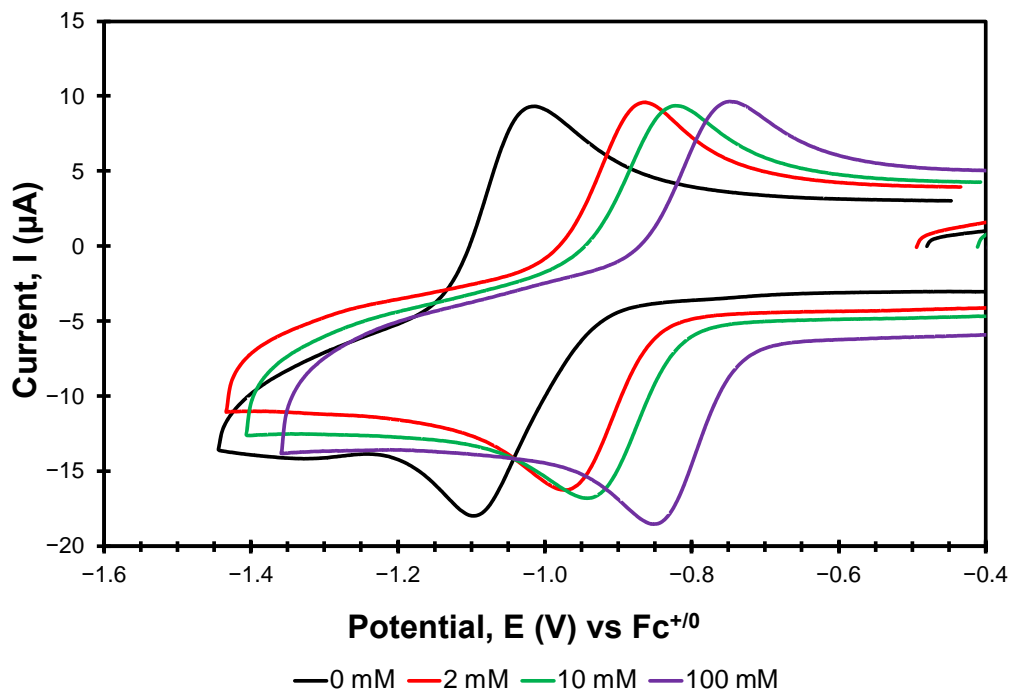


Figure 3.13. Cyclic voltammetry of 1 mM $\text{Ru}(\text{dbm}-2\text{OMe})_3$ with added NaClO_4 , 0.1 M TBAPF_6 CH_3CN , 0.1 V s^{-1} .

Table 3.5. Electrochemical parameters (V) of 1 mM $\text{Ru}(\text{dbm}-2\text{OMe})_3$ with NaClO_4 , 0.1 M TBAPF_6 CH_3CN , 0.1 V s^{-1} against $\text{Fc}^{+/0}$.

$[\text{Na}^+]$	E_{pa}	E_{pc}	ΔE_{p}	$E_{1/2}$
0 mM	-1.016	-1.098	0.082	-1.057
2 mM	-0.871	-0.990	0.119	-0.931
10 mM	-0.822	-0.941	0.119	-0.882
100 mM	-0.735	-0.841	0.106	-0.788

Figure 3.14 displays that the $[\text{Ru}(\text{dbm}-2\text{OMe})_3]^-$ complex can bind to two more Na^+ ions with a slope of -0.1048 . This finding indicates that the binding affinity of $[\text{Ru}(\text{dbm})_3]^-$ was improved by the addition of the methoxy groups.

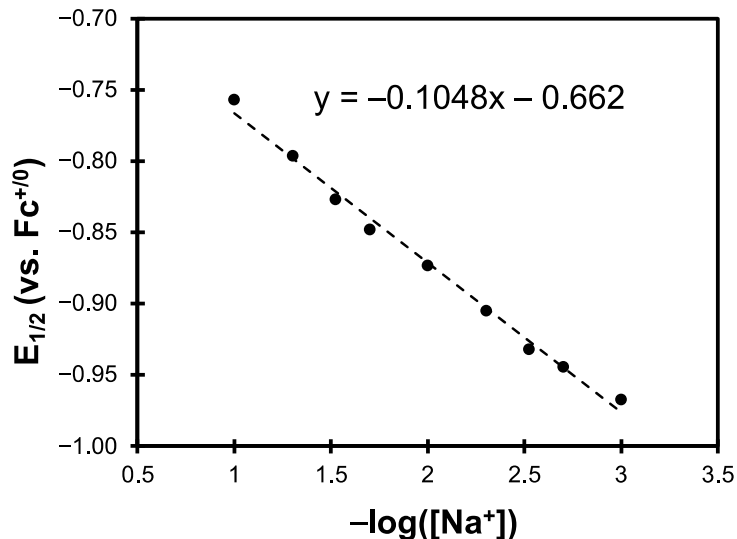


Figure 3.14. $E_{1/2}$ (vs. $\text{Fc}^{0/+}$) vs. $-\log([\text{Na}^+])$ of 1 mM $\text{Ru}(\text{dbm}-2\text{OMe})_3$, 1 – 100 mM $[\text{Na}^+]$.

3.2.5. Interaction of $\text{Ru}(\text{acac})_3$ and $\text{Ru}(\text{dbm}-2\text{OMe})_3$ Hosts with K^+ Guest

After studying the binding affinities of these Ru β -diketonates with Na^+ ions, we decided to examine how other alkali-metal ions influence the redox chemistry of these hosts. Hence, we looked into analyzing how these hosts associate with K^+ ions using CV. Because KClO_4 has poor solubility in CH_3CN , we elected to use $\text{KOSO}_2(\text{CF}_2)_3\text{CF}_3$ as our K^+ source. We implemented this inquiry using the $\text{Ru}(\text{acac})_3$ and $\text{Ru}(\text{dbm}-2\text{OMe})_3$ hosts due to their prominent sensitivity to Na^+ .

In the presence of K^+ , both hosts exhibit the same behavior that was seen with Na^+ . Figures 3.15 and 3.16 demonstrates that the acac host showed a greater positive shift at high concentrations and the 2'-methoxy did at low concentrations. There is a positive $\Delta E_{1/2}$ occurs after each addition of K^+ guest, however, the change is not as salient as what was discovered with Na^+ . This is likely because the K^+ ion is larger than Na^+ , which can reduce the ability for the guest to bind. Tables 3.6 and 3.7 quantifies these findings of $\text{Ru}(\text{acac})_3$ and $\text{Ru}(\text{dbm}-2\text{OMe})_3$, respectively. At 100 mM K^+ added, the $[\text{Ru}(\text{acac})_3]^{0/-}$ redox potential was +0.202 V, in comparison to the +0.264 V for Na^+ . In correlation, the $[\text{Ru}(\text{dbm}-2\text{OMe})_3]^{0/-}$ redox changes by +0.217 V with 100 mM K^+ added, indicating that K^+ has better affinity with the 2'-methoxy complex.

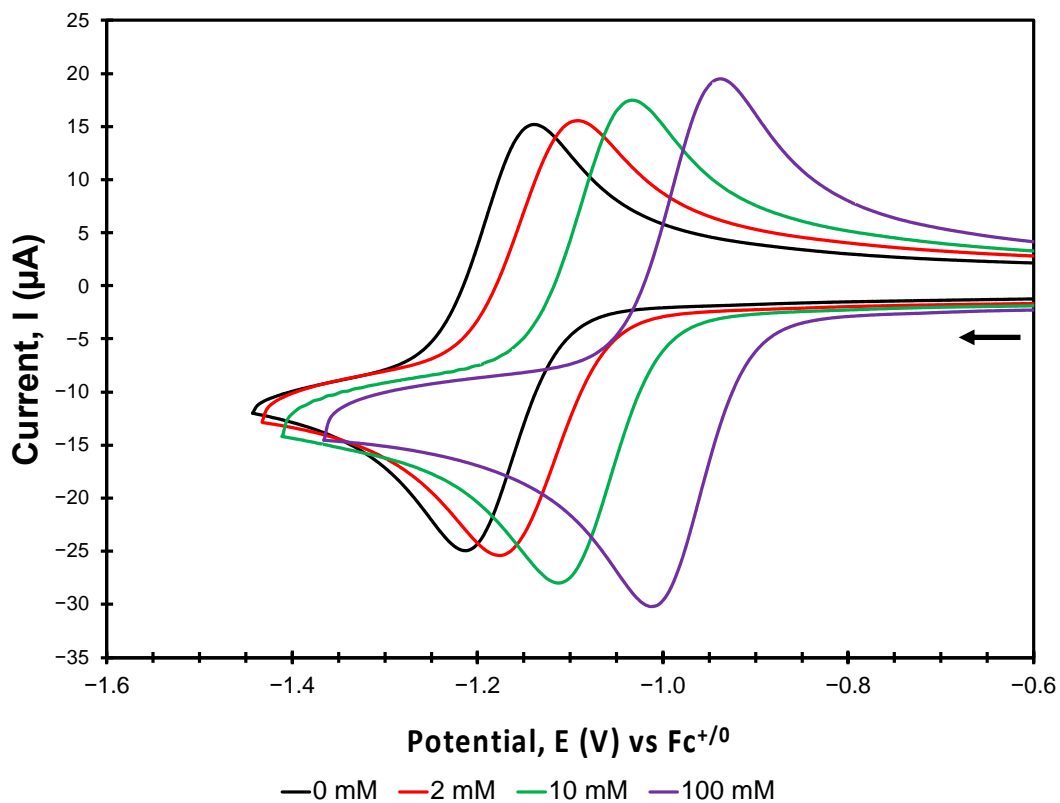


Figure 3.15. Cyclic voltammetry of 1 mM Ru(acac)₃ with KOSO₂(CF₂)₃CF₃, 0.1 M TBAPF₆ CH₃CN, 0.1 V s⁻¹.

Table 3.6. Electrochemical parameters (V) of 1 mM Ru(acac)₃ with KOSO₂(CF₂)₃CF₃, 0.1 M TBAPF₆ CH₃CN, 0.1 V s⁻¹ against Fc⁺⁰.

[K ⁺]	E _{pa}	E _{pc}	ΔE _p	E _{1/2}
0 mM	-1.139	-1.213	0.074	-1.176
2 mM	-1.091	-1.176	0.085	-1.134
10 mM	-1.034	-1.112	0.078	-1.073
100 mM	-0.937	-1.011	0.074	-0.974

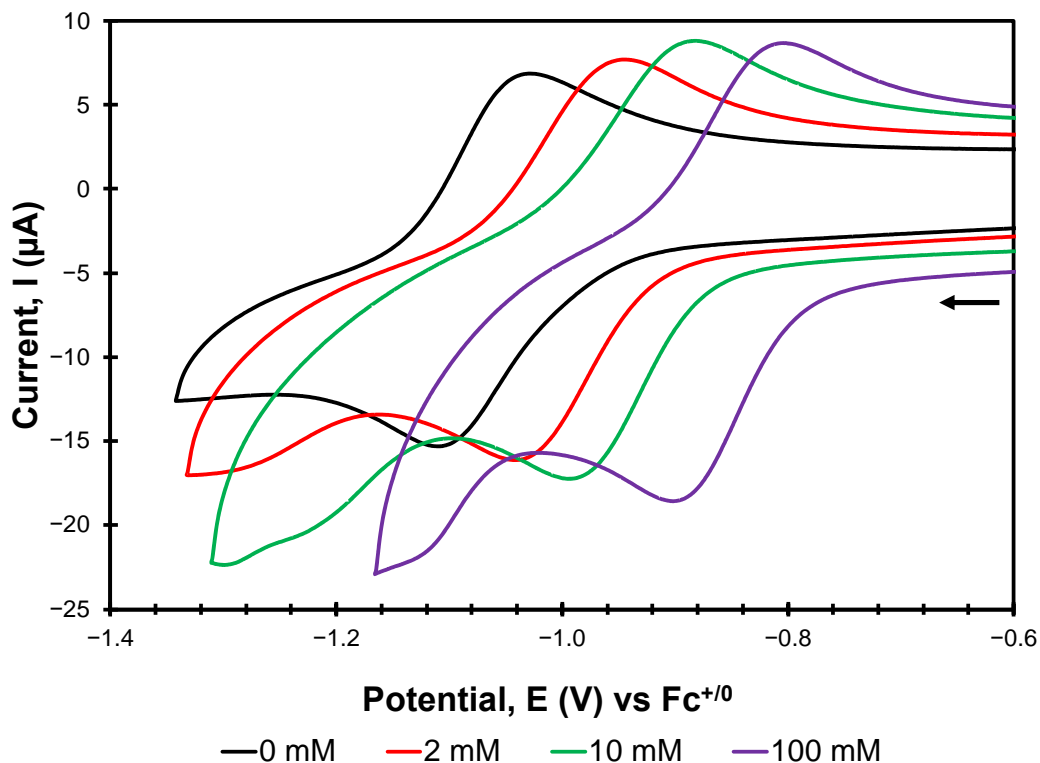


Figure 3.16. Cyclic voltammetry of 1 mM Ru(dbm-2OMe)₃ with KOSO₂(CF₂)₃CF₃, 0.1 M TBAPF₆ CH₃CN, 0.1 V s⁻¹.

Table 3.7. Electrochemical parameters (V) of 1 mM Ru(dbm-2OMe)₃ with KOSO₂(CF₂)₃CF₃, 0.1 M TBAPF₆ CH₃CN, 0.1 V s⁻¹ against Fc⁺⁰.

[K ⁺]	E _{pa}	E _{pc}	ΔE _p	E _{1/2}
0 mM	-1.111	-1.028	0.083	-1.069
2 mM	-0.945	-1.041	0.096	-0.993
10 mM	-0.881	-0.994	0.113	-0.938
100 mM	-0.802	-0.901	0.099	-0.852

Next, the number of bound K⁺ ions were ascertained from the electrochemistry data (Tables 3.8 and 3.9) using the same method as the Na⁺ ions. It was discovered that the [Ru(dbm-2OMe)₃]⁻ host binds to one more K⁺ (slope = -0.06) between guest concentrations 1 – 3 mM and [Ru(acac)₃]⁻ between 1 – 5 mM K⁺ added. At high concentrations, both hosts achieve slopes of -0.08 and -0.09 for [Ru(dbm-2OMe)₃]⁻ and [Ru(acac)₃]⁻, respectively. This signifies that both hosts are capable of binding to two more K⁺ ions, but not as facile as they can with Na⁺.

Table 3.8. Electrochemistry of Ru(acac)₃ in CH₃CN with KO₃S(CF₂)₃CF₃ (0.1 M TBAPF₆) at 0.1 V s⁻¹.

[K ⁺]	-log([K ⁺])	E _{1/2} (vs. Fc ^{0/+})
0	----	-1.176
0.001	3.	-1.145
0.002	2.70	-1.134
0.003	2.52	-1.119
0.005	2.30	-1.102
0.01	2	-1.073
0.02	1.70	-1.046
0.03	1.52	-1.020
0.05	1.30	-0.979
0.1	1	-0.974

Table 3.9. Electrochemistry of Ru(dbm-2OMe)₃ in CH₃CN with KO₃S(CF₂)₃CF₃ (0.1 M TBAPF₆) at 0.1 V s⁻¹.

[K ⁺]	-log([K ⁺])	E _{1/2} (vs. Fc ^{0/+})
0	----	-1.069
0.001	3	-1.011
0.002	2.70	-0.993
0.003	2.52	-0.983
0.005	2.30	-0.965
0.01	2	-0.938
0.02	1.70	-0.915
0.03	1.52	-0.899
0.05	1.30	-0.877
0.1	1	-0.852

As studied previously in literature,^{34,38} the inductive effect of the diketonate ligands is an indication of the sensitivity the host will have to the guest. The complex with the more electron-donating substituent will have a more negative E_{1/2}. This finding implies that Ru(acac)₃ has the most negative E_{1/2} because it has the greatest ligand-to-metal charge-transfer due to its methyl substituent and thus, have the most sensitivity to the cation. However, the new 2'-methoxy host demonstrates the importance of the chelating effect in the β-diketonate host framework. Despite

having a more positive $E_{1/2}$ than the acac host, the methoxy O atom chelating with the diketonate O atom enhances the binding affinity to the alkali-metal ion.

3.2.6. Evaluating Host-Guest Chemistry with ^1H NMR Analysis

Another technique of examining the host-guest properties of systems is by observing the chemical shifts in NMR when the host or guest is being slowly titrated. We elected to investigate the effects of adding Na^+ on the ^1H NMR spectra of Ru^{III} (Figures B3 and B6) and Ru^{II} β -diketonate complexes. In order to study the ^1H NMR spectrum of the $[\text{Ru}^{\text{II}}(\text{diket})_3]^-$, the Ru^{III} host was reduced using Cp_2Co . This reducing agent is great for this experimentation because it has a very negative redox potential of -1.33 V (vs. $\text{Fc}^{0/+}$),⁷⁸ meaning that it is strong enough to reduce all the Ru β -diketonates. Also, Cp_2Co has a known ^1H NMR signal at ~ 4.8 and Cp_2Co^+ at ~ 5.7 ppm.⁷⁹ The analysis of the $[\text{Ru}^{\text{III}}(\text{diket})_3]$ hosts were done with excess Na^+ added and the $[\text{Ru}^{\text{II}}(\text{diket})_3]^-$ complexes had a 1:1 host/guest ratio.

No change was observed in the $[\text{Ru}^{\text{III}}(\text{diket})_3]$ - CD_3CN solutions when Na^+ is added. After the ^1H NMR spectrum of the $[\text{Ru}^{\text{II}}(\text{acac})_3]^-$ solution was analyzed (Figure B4), Na^+ was added. A precipitate is produced from the formation of $\text{Na}[\text{Ru}^{\text{II}}(\text{acac})_3]$. This solid is only a little soluble in CD_3CN , so only a minimal amount was examined for ^1H NMR. However, for the $\text{Na}[\text{Ru}^{\text{II}}(\text{acac})_3]$ sample, the ^1H NMR data (Figure B5) is not clear enough to determine what happened to the chemical shifts when Na^+ is guest binding. This is likely due to the compound not being soluble enough in CD_3CN . When $[\text{Ru}^{\text{III}}(\text{dbm}-2\text{OMe})_3]$ is reduced to Ru^{II} , the brown solution turns blue and when Na^+ is added, the blue solution turns purple, with no precipitate formed.

The ^1H NMR spectra for Ru^{III} β -diketonates did not change when excess Na^+ is added. This suggests that the association of the cationic guest is due to the host's reduced state. This is further demonstrated in the changes in the signals for when Na^+ is added to the $[\text{Ru}^{\text{II}}(\text{dbm}-2\text{OMe})_3]^-$

solutions (Figures B7 and B8). There is a clear change in the $[\text{Ru}^{\text{II}}(\text{dbm}-2\text{OMe})_3]^-$ spectra when Na^+ is added, however, because the Ru^{II} , and $\text{Na}[\text{Ru}^{\text{II}}(\text{dbm}-2\text{OMe})_3]$ complexes are soluble in CD_3CN , it was difficult to achieve clear data of the ^1H NMR signals.

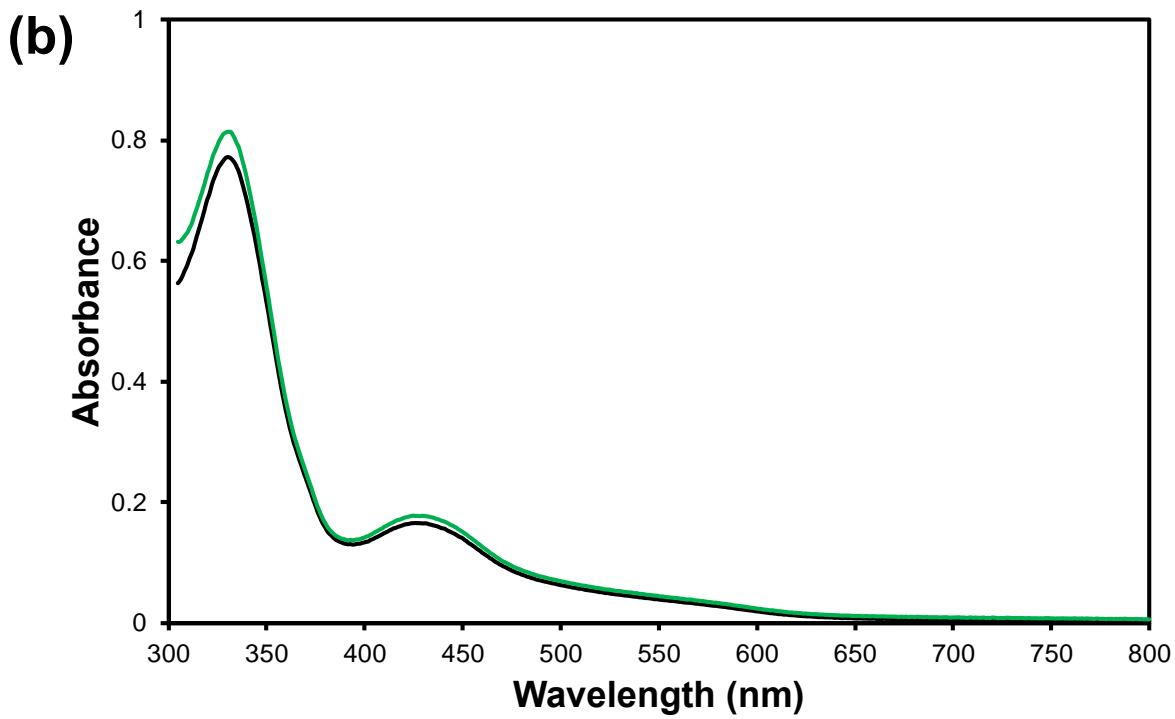
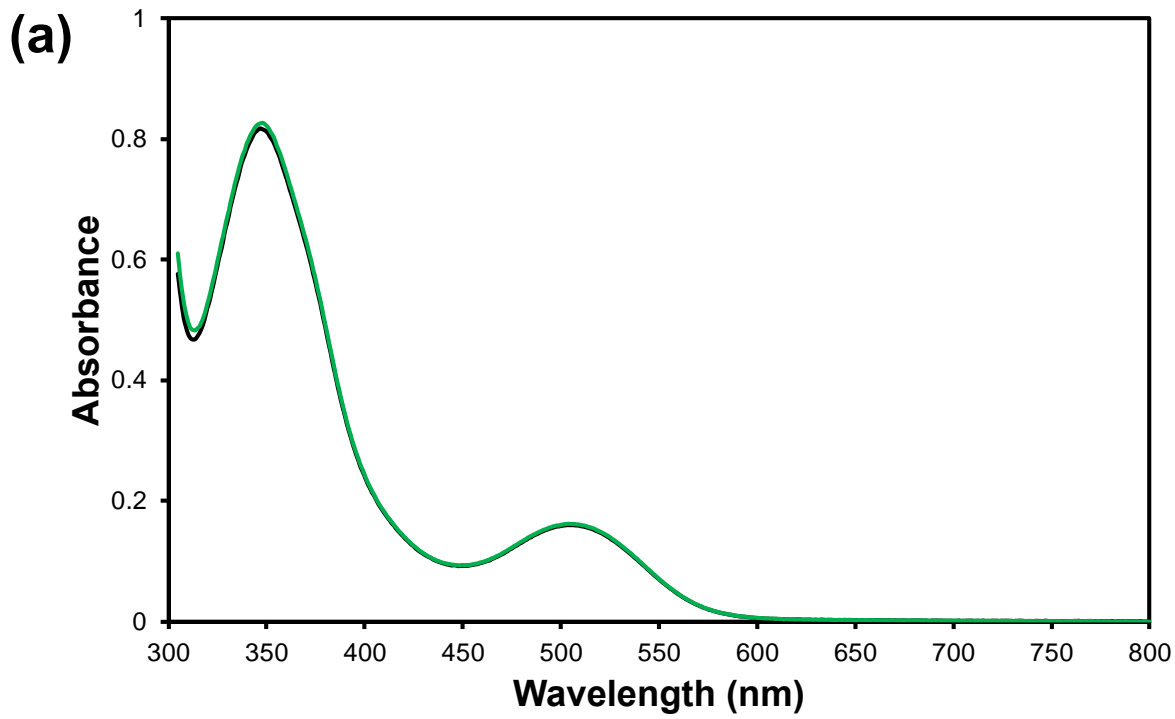
3.2.7. Inquiring the Na^+ Interaction on Ru^{III} β -diketonates using UV-vis Spectroscopy

All UV-vis studies were executed in CH_3CN . The $\text{Ru}(\text{acac})_3$, $\text{Ru}(\text{dbm})_3$, and $\text{Ru}(\text{dbm}-2\text{OMe})_3$ complexes were investigated for this evaluation. The concentrations of the hosts used were 0.1, 0.03, and 0.025 mM, respectively. The $[\text{Ru}^{\text{III}}(\text{diket})_3]$ samples were measured alone and with 20 mM NaClO_4 . This was investigated to observe the interaction between the Ru^{III} complex and Na^+ .

Our $[\text{Ru}^{\text{III}}(\text{acac})_3]$ spectrum is in agreement with what was reported in literature.⁸⁰ Figure 3.17(a) displays its UV-vis in spectrum and it has a UV λ_{max} at 347 nm and visible λ_{max} at 504 nm, black trace. When Na^+ is added to the solution (green trace) and measured, its UV-vis spectrum does not change.

The same procedure was executed with $[\text{Ru}^{\text{III}}(\text{dbm})_3]$ and its data is consistent with what was found in the literature's data in DCM.⁸¹ Figure 3.17(b) shows that $\text{Ru}(\text{dbm})_3$ has a λ_{max} of UV and visible absorbance at 330 and 427 nm, respectively (black trace). The $[\text{Ru}^{\text{III}}(\text{dbm})_3]$ host also has a charge transfer band ~ 550 nm. The addition of Na^+ did not affect the spectrum of the Ru^{III} host as well.

For $[\text{Ru}^{\text{III}}(\text{dbm}-2\text{OMe})_3]$ (Figure 3.17(c)), the UV and visible λ_{max} for this host is 338 and 417 nm, respectively with a charge transfer absorbance at ~ 550 nm. Adding the Na^+ ions did not change this spectrum. This study displayed that the binding affinity between Na^+ and the Ru^{III} β -diketonates is, at best, very weak.



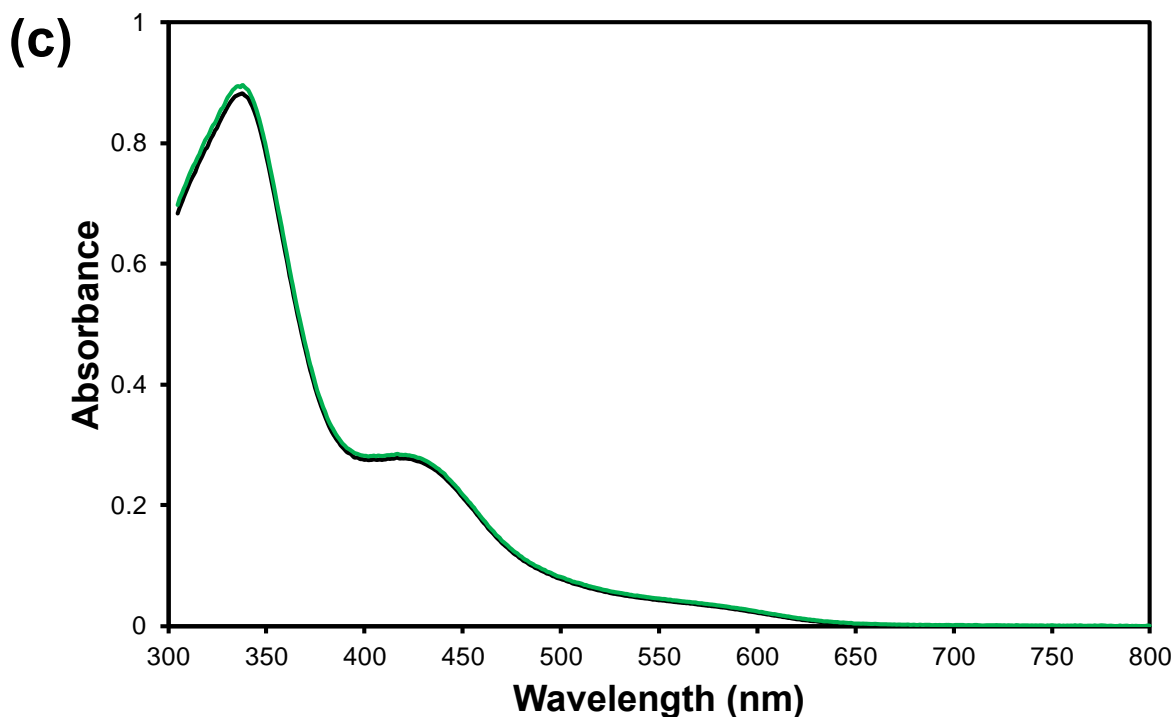


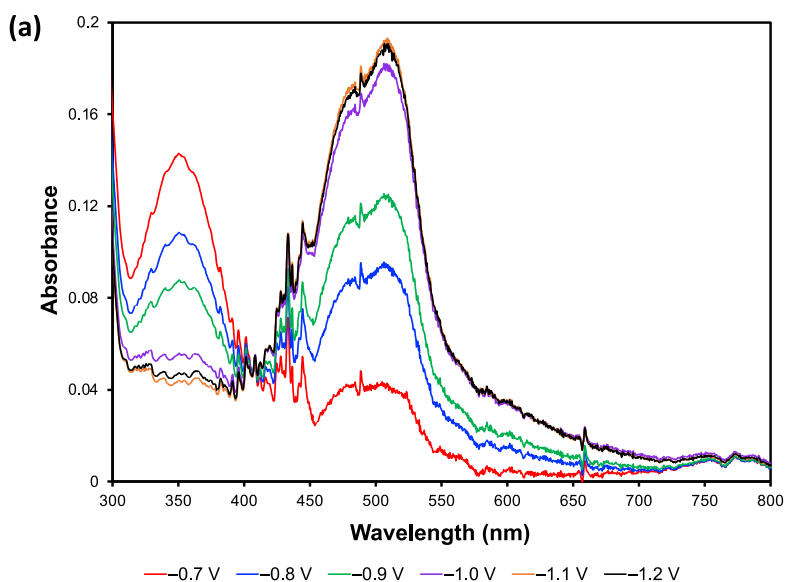
Figure 3.17. UV-vis spectra of Ru^{III}(diket)₃ hosts without NaClO₄ (black) and with 20 mM NaClO₄ (green) in CH₃CN with 1 cm pathlength: a) 0.1 mM Ru^{III}(acac)₃, b) 0.03 mM Ru^{III}(dbm)₃, c) 0.025 mM Ru(dbm-2OMe)₃.

3.2.8. Spectroelectrochemistry of Na⁺ with Ru^{II} β-diketonates

To observe how Na⁺ associates with the reduced host, negative potentials were applied to the Ru(diket)₃ electrochemical solutions to reduce the host. Certain potentials were implemented and after each application, the UV-vis spectrum was recorded. This procedure was done with the Ru β-diketonates alone and with 20 mM NaClO₄. The potentials were selected based on when each host undergoes reduction so that we can inspect the changes in the spectra as [Ru^{III}(diket)₃] is converted to [Ru^{II}(diket)₃]⁻.

First, this analysis was performed with the Ru(acac)₃ host (Figure 3.18). To reduce the host, the potentials applied decreases from -0.4 to -1.2 V. The UV-vis spectrum from [Ru^{III}(acac)₃] to [Ru^{II}(acac)₃]⁻ changes as more negative potentials are applied and the UV λ_{max} decreases in intensity and the visible λ_{max} increases. The [Ru^{II}(acac)₃]⁻ UV-vis spectrum produced

is in agreement with literature.⁸⁰ This same behavior is noticed with the addition of Na⁺ as well. Nevertheless, the main difference between the [Ru^{II}(acac)₃]⁻ and [Ru^{II}(acac)₃]⁻ with 20 mM Na⁺ is that the visible λ_{max} blue shifts from 505 to 484 nm due to interaction of Na⁺ to Ru^{II} host. It is also discerned that the transition of the Ru^{III} to the Ru^{II} host occurs at -1.0 V, which is where the E_{pc} of the acac host occurs. The change in the Ru^{III} spectrum with Na⁺ happens at a more positive potential (-0.8 V). This indicates that the UV-vis and electrochemistry data are congruent with each other.



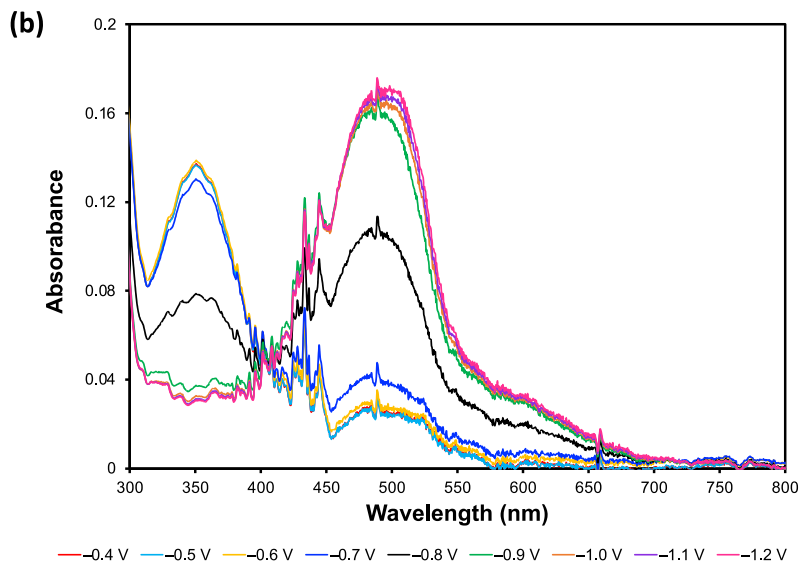
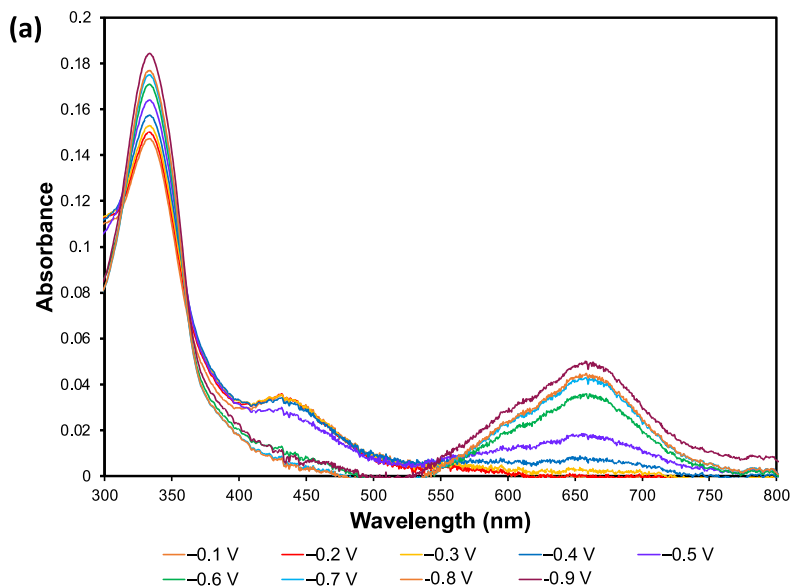


Figure 3.18. UV-vis spectra of 0.1 mM Ru^{II}(acac)₃ host a) without NaClO₄, b) with NaClO₄.

For the Ru(dbm)₃ host, the potentials used to reduce the complex was from -0.1 to -0.9 V (Figure 3.19). As the cathodic potentials are applied, the UV λ_{max} intensity increases and the visible λ_{max} decreases. The charge transfer absorbance increases and develops a λ_{max} at 658 nm. In the presence of Na⁺, the Ru^{II} host's charge transfer λ_{max} shifts from 658 to 622 nm. This large change indicates guest binding to the reduced host that is not found in the Ru^{III} host.



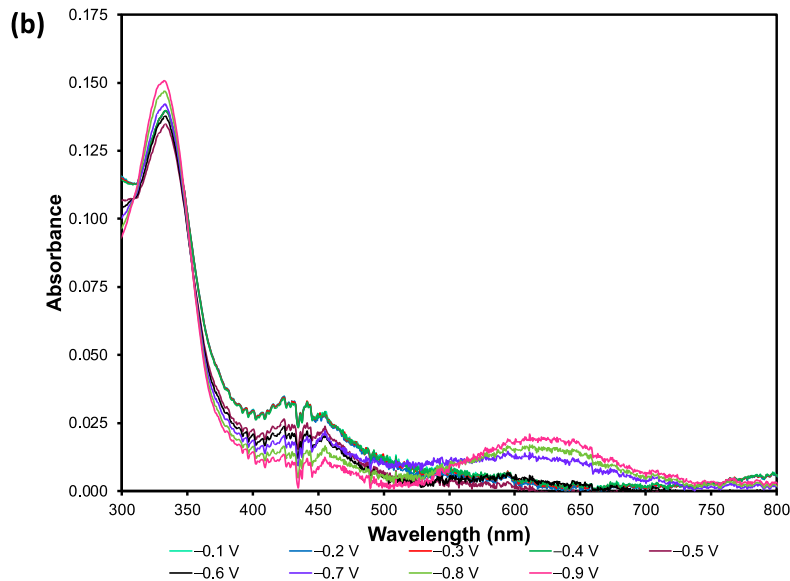


Figure 3.19. UV-vis spectra of 0.03 mM Ru^{II}(dbm)₃ host a) without NaClO₄, b) with NaClO₄.

Exceptionally, the [Ru^{II}(dbm-2OMe)₃]⁻ spectrum displayed the most change with the addition of Na⁺ (Figure 3.20). Applying potentials -0.3 to -0.9 V, the Ru^{III} was reduced to Ru^{II}. When the -0.7 V potential is applied, the visible λ_{max} absorbance decreases and the charge transfer band increases at a λ_{max} of 615 nm. There is also a blue shift in the UV λ_{max} from 338 to 329 nm and it also intensifies in absorbance. This large change in the spectrum is testified by the great color change from brown to blue. When the Na⁺ guest is added, the UV λ_{max} shifts to 324 nm and the charge transfer λ_{max} shifts to 548 nm. That large change in the spectrum is evidence by the color change from blue to purple.

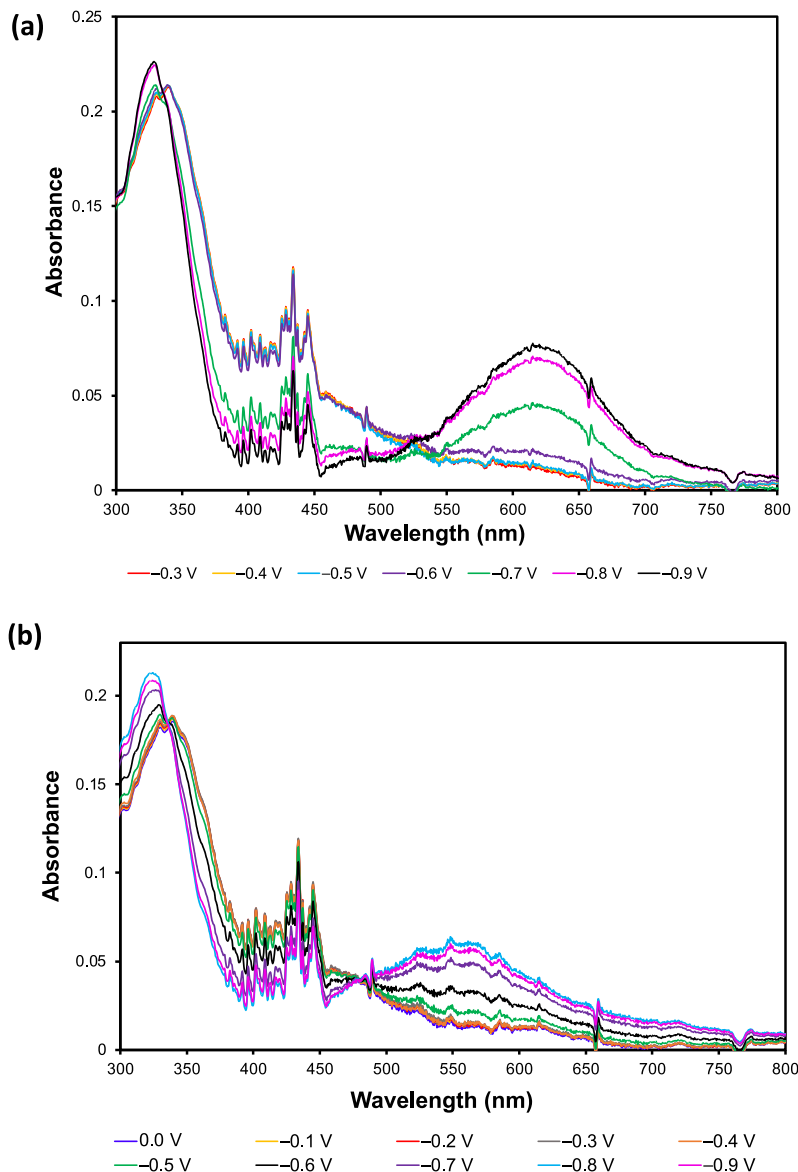


Figure 3.20. UV-vis spectra of 0.025 mM $\text{Ru}^{\text{II}}(\text{dbm-2OMe})_3$ host a) without NaClO_4 , b) with NaClO_4 .

Accomplishing spectroelectrochemistry with the Ru^{III} β -diketonates has permitted us to analyze the air-sensitive Ru^{II} compounds and its interaction with Na^+ guests. The difference in the spectra of the Ru^{II} complexes when Na^+ is added that is not seen in the Ru^{III} spectra signifies that the $\Delta E_{1/2}$ is due to the Na^+ association with the Ru^{II} host. The $[\text{Ru}^{\text{II}}(\text{dbm-2OMe})_3]^-$ spectrum had the most significant change when Na^+ is added. This is evidence that this new Ru β -diketonate has the most sensitivity to the Na^+ .

3.2.9. Crystal Analysis of the $\text{Na}_2[\text{Ru}^{\text{II}}(\text{dbm}-2\text{OMe})_3]$ Host-Guest System

After achieving quantitative data of host-guest binding of $[\text{Ru}^{\text{II}}(\text{dbm}-2\text{OMe})_3]^-$, we decided to attain a depiction of the host-guest system using crystallography. Due to the $[\text{Ru}^{\text{II}}(\text{dbm}-2\text{OMe})_3]^-$ host being air-sensitive, the sample must be prepped inside a glovebox. The $\text{Ru}(\text{dbm}-2\text{OMe})_3$ was dissolved in degassed CH_3CN and then reduced using excess Cp_2Co , producing a dark blue solution. Afterwards, NaClO_4 is added (1:5 host/guest ratio) and the blue solution turns dark purple. The sample was sealed and placed under a very low flow of nitrogen gas to execute slow evaporation. After 4 days, dark purple crystals were developed.

Figure 3.21 demonstrates the $\text{Na}_2[\text{Ru}^{\text{II}}(\text{dbm}-2\text{OMe})_3]$ host-guest system. This crystal structure shows that this host is able to bind to two Na^+ ions, which was indicated by the large positive shift in the redox potential and from the Nernstian calculations. The host being able to bind to two Na^+ ions is also a testament of how important the size of the host is. The $[\text{Ru}^{\text{II}}(\text{dbm}-2\text{OMe})_3]^-$ is large enough to be able to bind to two Na^+ ions. The methoxy groups in the 2'-position aided in greater Na^+ interaction as well. The crystal structure displays the importance of the chelating and inductive effects in improving the binding affinity of the reduced host and Na^+ .

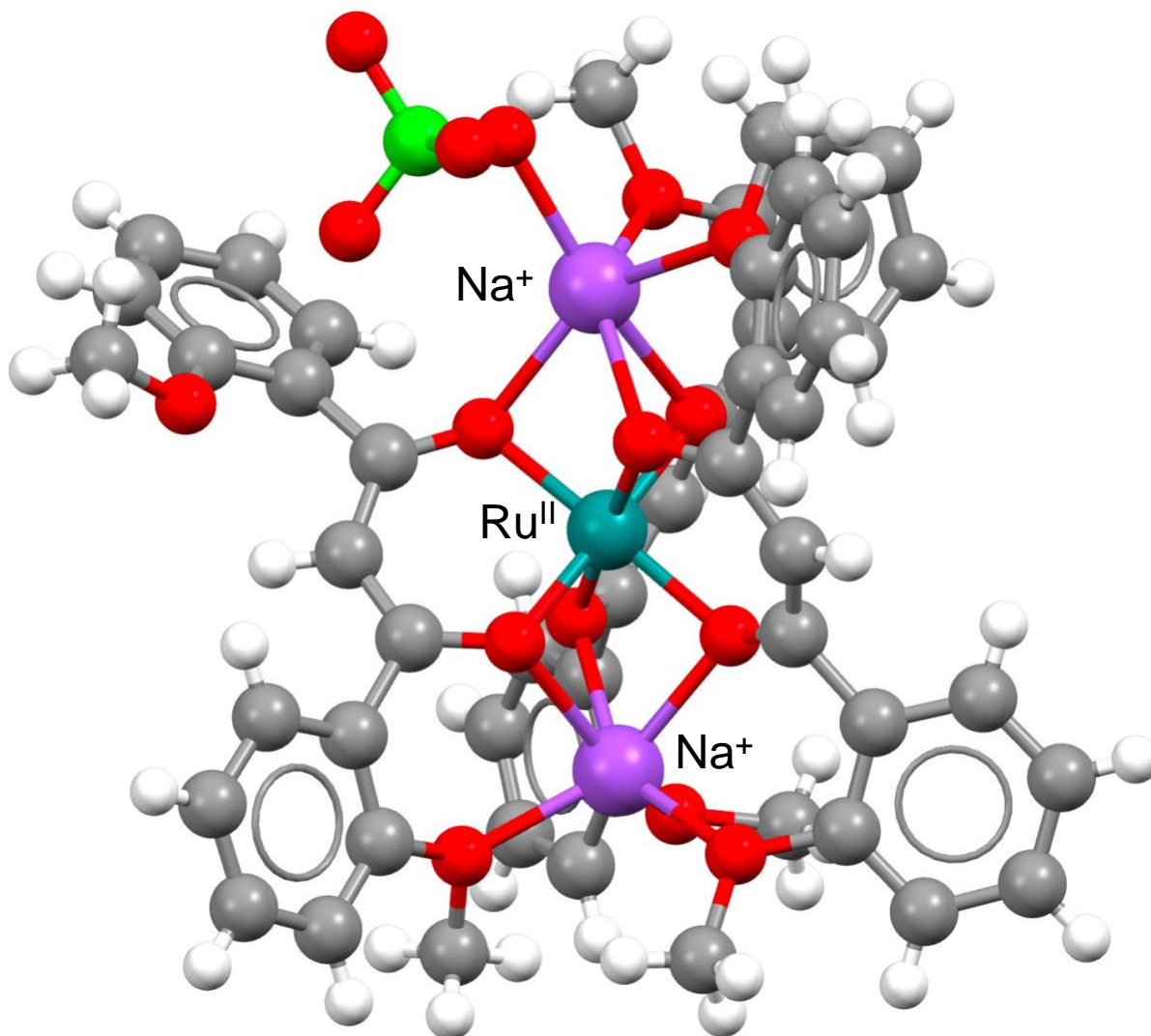


Figure 3.21. Crystal structure of the new $\text{Na}_2[\text{Ru}^{\text{II}}(\text{dbm-2OMe})_3]\text{ClO}_4$ host-guest system.

3.2.10. Calculation of the Binding Constant of Ru^{II} β -diketonates

Nernstian calculations were accomplished to obtain the binding constant of the Ru^{II} β -diketonates to Na^+ . This is measured by utilizing the $\Delta E_{1/2}$ from the electrochemical studies. Equation 3 has been used previously in literature⁸² to determine binding constants of host-guest systems using the change in redox potentials:

$$\Delta E_{1/2} = 0.0592 \log(K_{1\text{Na}}) + q \cdot 0.0592 \log([\text{Na}^+]), \quad q \text{ is the number of } \text{Na}^+ \text{ binding} \quad (\text{Equation 3})$$

With $K_{1\text{Na}}$ being the binding constant of Na^+ to $[\text{Ru}(\text{diket})_3]^-$, the $\log(K_{1\text{Na}})$ for the $[\text{Ru}^{\text{II}}(\text{d1nm})_3]^-$ host was calculated to be ca. 2.0. The $K_{1\text{Na}}$ of $[\text{Ru}^{\text{II}}(\text{dbm-2OMe})_3]^-$ host was determined to be ca. 4.5. For $[\text{Ru}^{\text{II}}(\text{dbm-2OMe})_3]^-$, this yields an approximate value of $K_{1\text{Na}}$ of ~30000. This value is approximately five times as high as the K_1 for $[\text{Ru}(\text{acac})_3]^-$, and nearly two orders of magnitude higher than that of $[\text{Ru}(\text{dbm})_3]^-$. This discovery is reflected in the $\Delta E_{1/2}$, the changes in the chemical shifts in the ^1H NMR spectrum, and the change in the UV-vis spectrum when Na^+ is added. Table 3.10 presents the $\log(K_{1\text{Na}})$, of each $[\text{Ru}(\text{diket})_3]^-$ to Na^+ in CH_3CN . The $\log(K_{1\text{Na}})$ of the $[\text{Ru}(\text{dbm})_3]^-$ and $[\text{Ru}(\text{acac})_3]^-$ hosts we measured are in agreement with the measurements found in Endo's work.³⁴

Table 3.10. Measurements of $\log(K_1)$ of each host to Na^+ in CH_3CN .

Reduced Host	$\log(K_{1\text{Na}})$
$[\text{Ru}(\text{acac})_3]^-$	3.8
$[\text{Ru}(\text{dbm})_3]^-$	2.6
$[\text{Ru}(\text{d1nm})_3]^-$	ca. 2.0
$[\text{Ru}(\text{dbm-2OMe})_3]^-$	ca. 4.5

Through this research, we have discovered that the $\text{Ru}(\text{dbm-2OMe})_3$ host has stronger interaction with the Na^+ guest because of the inductive and chelating effects from the methoxy groups. Nevertheless, we aimed to synthesize the $\text{Ru}(\text{dbm-4OMe})_3$ complex (Figure 3.22) to determine the importance of the inductive effect in cation binding. In the $\text{Ru}(\text{dbm-4OMe})_3$ host, the methoxy groups are far from the O diketonate atoms, eliminating the chelating effect. However, we had difficulty in synthesizing this complex and we were not able to study how the methoxyphenyl substituent can inductively increase guest binding.

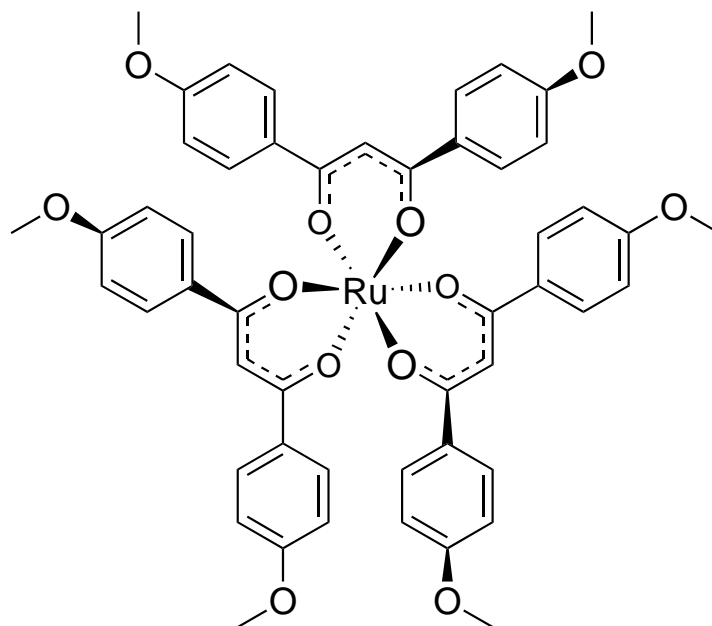


Figure 3.22. Chemical diagram of Ru(dbm-4OMe)₃.

The application of controlling host-guest interactions has tremendous potential in providing advances in fields such as medicinal chemistry and water purification. Studying this technique using a simpler system is essential for learning about how one can tune the binding constant of host-guest systems. This research demonstrates that a simple host-guest system can easily be manipulated using redox control. The large $\Delta E_{1/2}$ that is observed with the addition of Na⁺ ions is due to the reduced host's sensitivity to the cation and the Na⁺ ion(s) is readily released upon oxidation. This is shown in the changes seen in the Ru^{II} host's spectra when Na⁺ is added and not observed when added to the Ru^{III} host. This is further proven in the crystallography data of the Na₂[Ru(dbm-2OMe)₃] host-guest system. Our work has also resolved that exploiting the substituents of the diketonate ligand can improve the binding affinity of the host to the alkali ion guests. We also confirmed that chelating effects of the O atoms in the structure can greatly enhance the sensitivity of the host to the guests. These techniques are vital in being utilized in constructing exceptional hosts that have good affinity for the desired guest.

3.3. Experimental

3.3.1. General

All solvents and reagents were procured from Pressure Chemicals, Aldrich, Strem Chemicals, Alfa Aesar, TCI, Eastman Organic Chemicals, and BDH Chemicals without further purification. All Electrospray mass spectrometry (ESI-MS) data were done using an Agilent 6230 instrument. All ^1H NMR data were executed with Bruker AVIII 400 MHz spectrometer in CDCl_3 or CD_3CN . The assignment of the signals was based on the data of $\text{Ru}(\text{dbm})_3$.⁸¹

CV experiments were accomplished using an EC Epsilon EclipseTM potentiostat/galvanostat with Ag/AgCl reference electrode, glassy carbon working electrode, and Pt wire counter electrode. These electrochemical data was achieved by using 1 mM Ru(III) β -diketonate host in a 0.1 M tetrabutylammonium hexafluorophosphate (TBAPF_6) CH_3CN solutions. The scan rate for all experiments is 0.1 Vs^{-1} . Na^+ and K^+ sources are from NaClO_4 and $\text{KOS}_2(\text{CF}_2)_3\text{CF}_3$, respectively.

Crystallography data was attained using a Bruker Kappa Apex-II DUO diffractometer, with $\text{MoK}\alpha$ radiation. Spectroelectrochemistry of the Ru hosts were carried out on an Avantes spectrometer with an Ag/Ag⁺ reference electrode and a Pt honeycomb working electrode from Pine Research Instrumentation under nitrogen gas. $\text{Ru}(\text{acac})_3$ was obtained from STREM Chemicals, Inc. without further purification. The other Ru complexes were composed using techniques from Munery et al.⁸¹ and Endo et al.⁸³

3.3.2. Synthesis of $\text{Ru}(\text{dbm})_3$

A 125 mL mixture of ethanol and water (4:1) was purged with N_2 . Afterwards, $\text{RuCl}_3 \cdot x\text{H}_2\text{O}$ (1.0 g, 4.1 mmol as Ru) was added and refluxed for 4 - 5 hr until the solution turns blue. Dibenzoylmethane (dbm) (3.3 g, 14.7 mmol) was added in excess and the reaction was refluxed

for 1.5 hr until the mixture turned green. Then, the solution was cooled and the first portion of KHCO_3 (0.78 g, 7.8 mmol) was introduced to the solution and refluxed for 1 hr. The second portion of KHCO_3 (0.75 g, 7.5 mmol) was added and refluxed for 2 hr. Then the solution turned orange. Black precipitate was filtered and washed with cold ethanol and pentane to remove excess ligand. Silica column chromatography was executed using toluene as the eluent. The resulting black solid was collected through evaporation with a yield of 30 - 40%. Crystals were obtained through slow evaporation of DMF. ESI-MS (Figure 3.23): $m/z = 772.1394$ (calcd: 772.1406). The ^1H NMR data was in agreement with what was found in literature.⁸¹

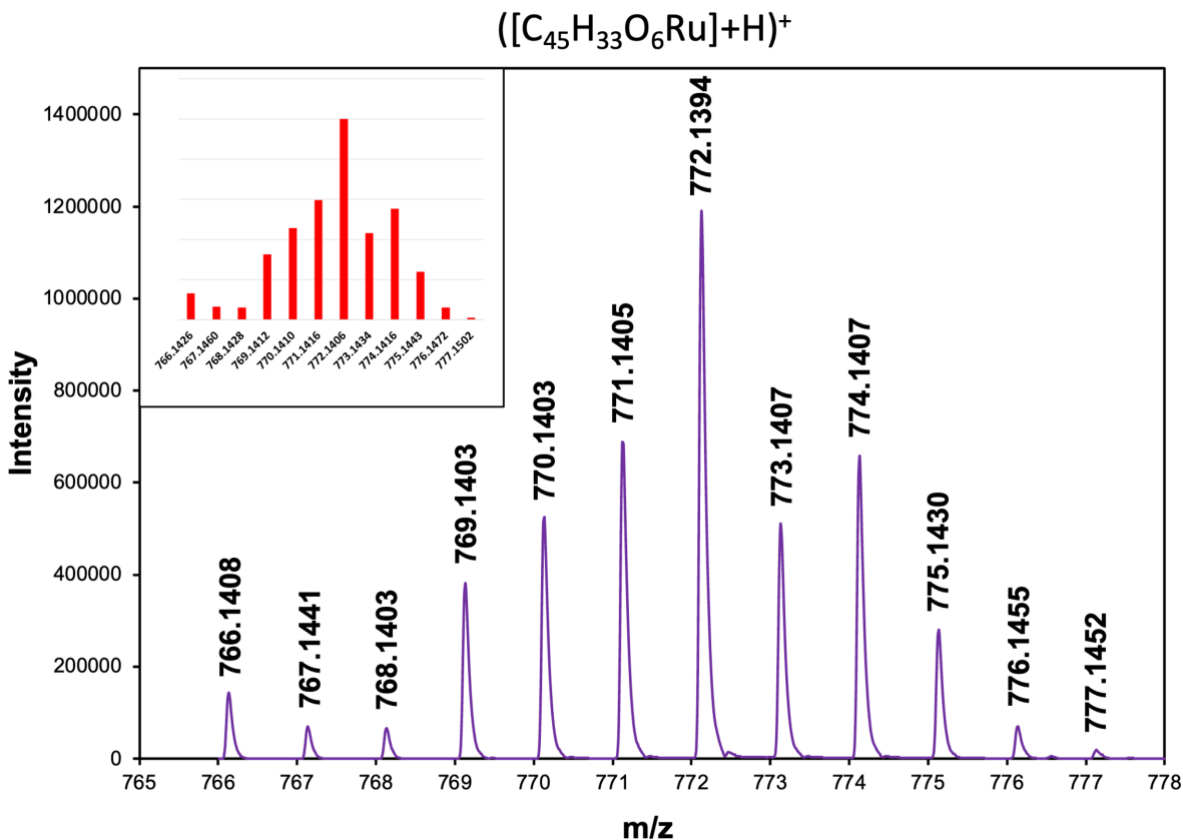


Figure 3.23. ESI mass spectra of $[\text{Ru}(\text{dbm})_3] + \text{H}^+$, m/z 772.1394 (calcd: 772.1406). Inset display calculated relative intensities.

3.3.3. Synthesis of Ru(d2nm)₃

This complex was composed by dissolving RuCl₃·xH₂O (0.25 g, 1.2 mmol as Ru) in a degassed 55 mL 1-propanol/water (4:1) solution and refluxed for 4 – 5 hr until the color turned blue-green. Excess 1,3-di(2-naphthyl)propane-1,3-dione (d2nm) (1.4 g, 4.3 mmol) was introduced quickly and the reaction was refluxed for 2 hr. KHCO₃ (0.23 g, 2.3 mmol) was added and refluxed for another hour and the solution turned light green. The mixture was then cooled to room temperature. Another portion of KHCO₃ (0.22 g, 2.2 mmol) was added and the mixture was refluxed for 2 hr and the solution turned light brown. The black precipitate was filtered and in a separate flask, the solid was washed with DMF to collect the crude product. Silica column chromatography with benzene was performed to separate the dark brown complex from the excess yellow d2nm ligand. The complex was collected and dried using evaporation (yield: < 1%). ESI-MS (Figure 3.24): $m/z = 1072.2345$ (calcd: 1072.2307).

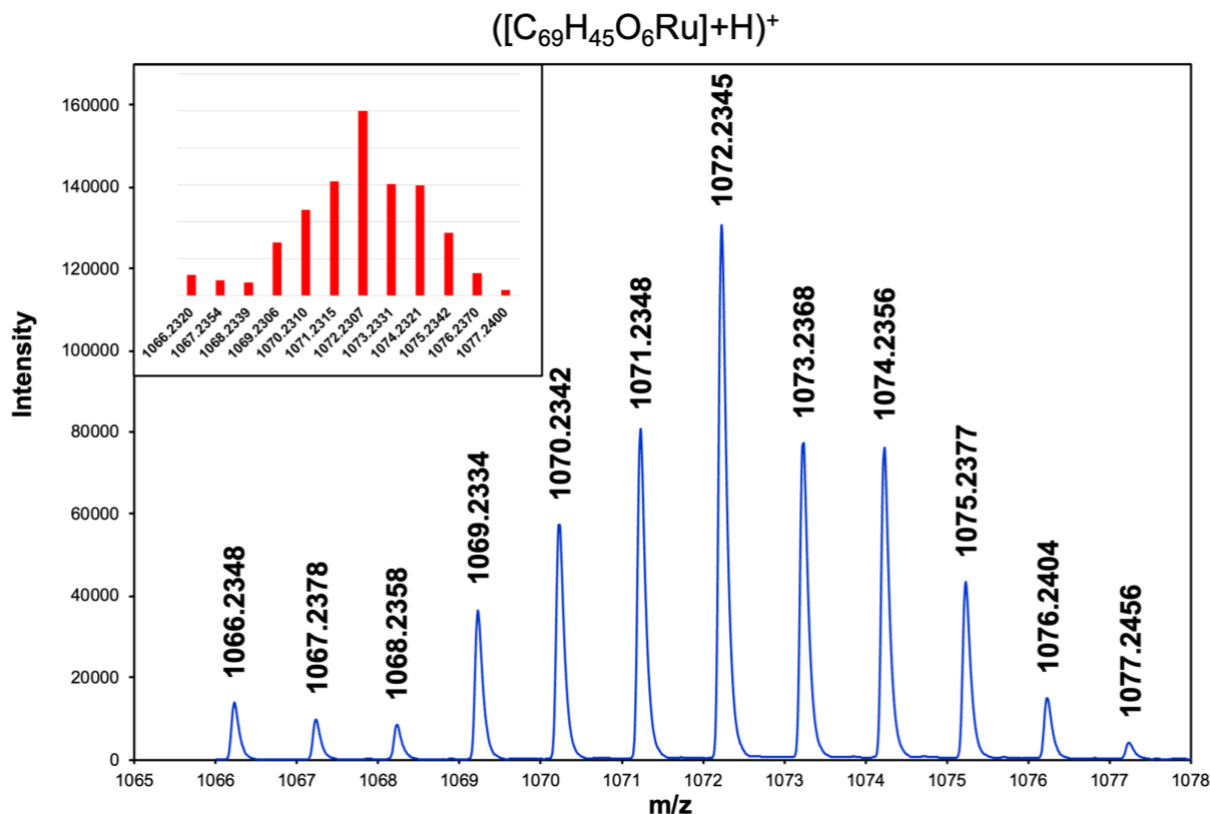


Figure 3.24. ESI mass spectra of $[Ru(d2nm)_3] + H^+$, m/z 1072.2345 (calcd: 1072.2307). Inset display calculated relative intensities.

3.3.4. Synthesis of $Ru(d1nm)_3$

The 1,3-di(1-naphthyl)propane-1,3-dione (d1nm) ligand was synthesized according to literature.⁸⁴ The $Ru(d1nm)_3$ was prepared using the ruthenium blue method with a slight variation.^{81,83} A 4:1 mixture of ethanol and water was degassed with N_2 . Then $RuCl_3 \cdot xH_2O$ (0.25 g, 1.2 mmol) was introduced to the solution and refluxed for 4 – 5 hr until the color turned deep blue. A little amount of black precipitate was observed on the flask, which is likely ruthenium metal or oxides. An excess amount of the ligand (1.4 g, 4.3 mmol) was added and refluxed for 2 hr and cooled to room temperature. The first portion of $KHCO_3$ (0.23 g, 2.3 mmol) was added and refluxed for an hour. The rest of the $KHCO_3$ (0.22 g, 2.2 mmol) was added and the reaction mixture turned orange. Gas was seen after each addition of $KHCO_3$. Then solution was cooled, filtered,

and washed with ethanol. In a separate flask, the collected solid was washed with DMF and the product was obtained in the filtrate. Column chromatography with silica was executed with DCM to collect the complex. Dark brown solid was received through evaporation (yield 4 – 5%). ESI-MS (Figure 3.25): $m/z = 1072.2364$ (calcd: 1072.2307), $^1\text{H NMR}$ (CDCl_3): 7.53 – 7.69 (m, 6H), 6.51 (d, 2H), 8.41 (d, 2H), 8.63 (d, 2H), 9.07 (d, 2H), –31.01 (s, 1H) ppm.

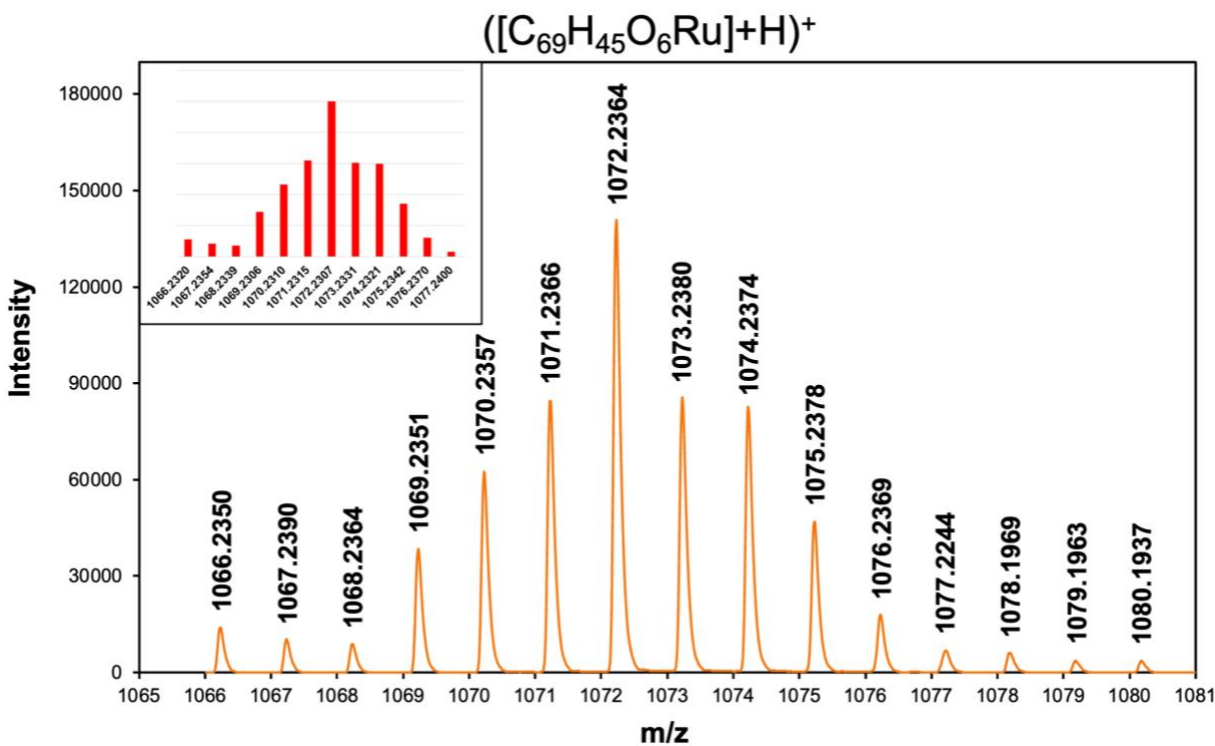


Figure 3.25. ESI mass spectra of $[\text{Ru}(\text{d1nm})_3] + \text{H}^+$, m/z 1072.2364 (calcd: 1072.2307). Inset display calculated relative intensities.

3.3.5. Synthesis of $\text{Ru}(\text{dbm-2OMe})_3$

The 1,3-bis(σ -methoxyphenyl)propane-1,3-dione (dbm-2OMe) compound was synthesized using the procedure from Dubrovina and co-workers.⁸⁴ The $\text{Ru}(\text{dbm-2OMe})_3$ was composed following the ruthenium blue synthesis with a slight modification.^{81,83} The ethanol/water mixture (4:1) was purged with nitrogen and $\text{RuCl}_3 \cdot x\text{H}_2\text{O}$ (0.65 g, 3.1 mmol) was quickly added and refluxed for 4 – 5 hr until the color turned blue. Black solid formed on the side

of the flask. After, the ligand was added and the solution was refluxed for 1.5 hr, then the now green mixture was cooled. KHCO_3 (0.59 g, 5.9 mmol) was added and refluxed for one hour and the solution turned orange. A second portion of KHCO_3 (0.57 g, 5.7 mmol) was introduced to the mixture and the reaction was refluxed for another 2 hr. The solution was cooled to room temperature and filtered. To separate the product from black ruthenium oxide, the solid was filtered with DMF into a new flask and the product was collected in the filtrate. The complex was purified using silica column chromatography with DCM/methanol (7:3). Dark red-brown precipitate was obtained from evaporation (yield 28 – 43%). Crystals were grown using air evaporation in CH_3CN . ESI-MS (Figure 3.26): $m/z = 952.2057$ $[\text{M}+\text{H}]^+$ (calcd 952.2042), 974.1878 $[\text{M}+\text{Na}]^+$ (calcd 974.1852), ^1H NMR (CDCl_3): 3.53 (s, 3H), 8.86 (s, 6H), 12.35 (s, 6H), 4.20 – 4.29 (m, 6H), 7.53 – 7.74 (dd, 6H), –36.85 (s, 3H) ppm.

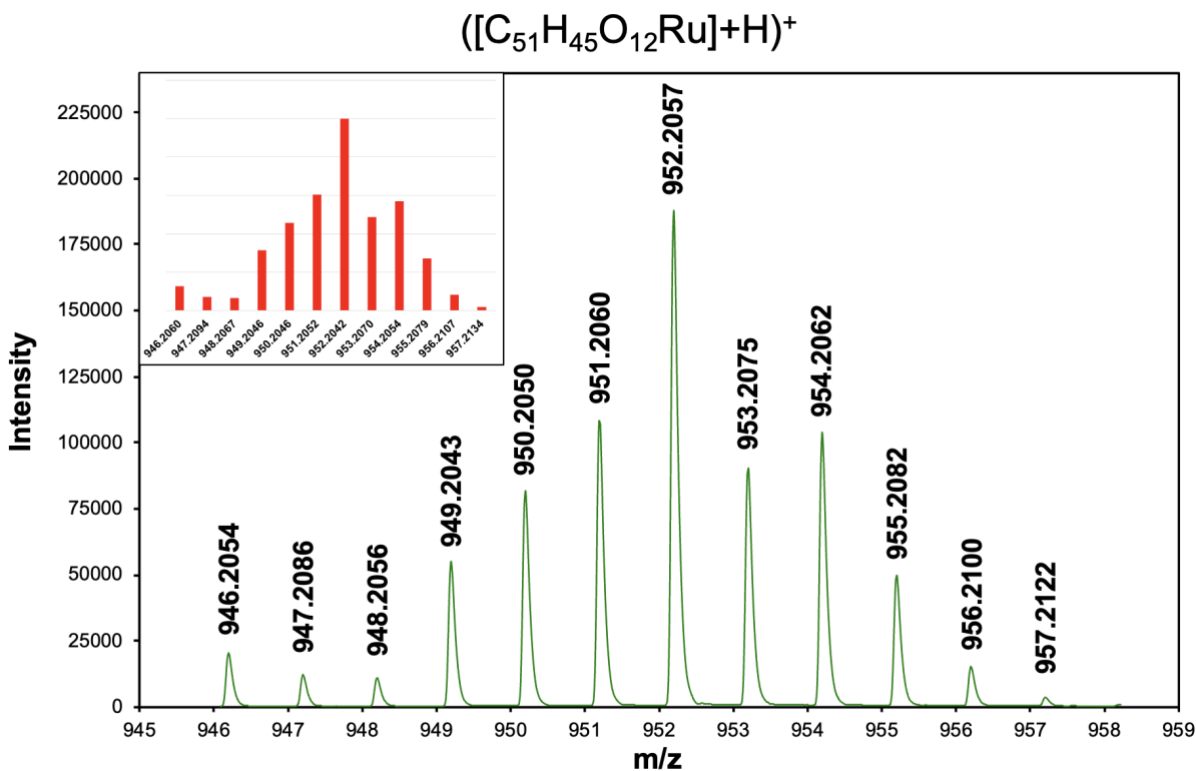


Figure 3.26. ESI mass spectra of $[\text{Ru}(\text{dbm}-2\text{OMe})_3] + \text{H}^+$, m/z 952.2057 (calcd: 952.2042). Inset display calculated relative intensities.

Chapter 4. Inducing Guest Binding with Cationic Ruthenium Hosts

4.1. Introduction

As mentioned in Chapter 3, redox chemistry has been used to increase the affinity of hosts to guests. This technique allows for the opportunity to produce inexpensive and quantitative evaluation of molecular recognition in real-life applications.⁸⁵ Like what was performed with the cationic guests, cyclic voltammetry (CV) can be executed to promote anionic binding. With this technique, the anions are able to bind and release from the hosts at the interface of the electrodes. A negative shift in the host's redox potential, $E_{1/2}$, is observed due to the higher oxidation state of the host being stabilized by the guest anion.⁸⁶

Complementary to the cationic guest binding in Chapter 3, the behavior anion interaction can be compared to the pairing of proton and electron transfers and redox reactions. We decided to replace the proton transfer with anion guest binding as well. Our aim is to use oxidation to increase the binding affinity of the host complex with a guest ion or molecule using a redox stimulus. Figure 4.1 expresses this coupling reaction as a square scheme.

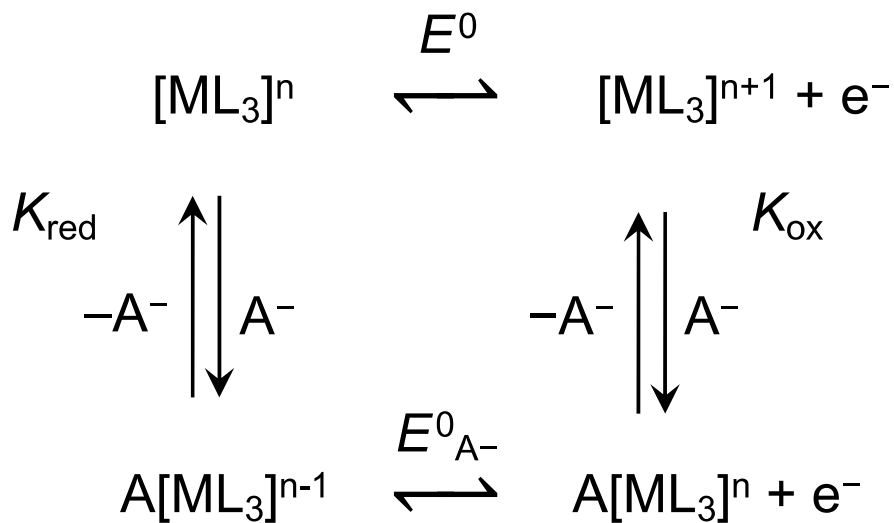


Figure 4.1. Square scheme of a cationic host's bind/release process with an monoanionic guest being manipulated by the host's redox properties.

The interaction of an anionic guest with the cationic host, $[\text{ML}_3]^n$, where n is the oxidation state of the host, is controlled by utilizing the electrodes to oxidize or reduce the host complex. This is executed to allow for the oxidized host, $[\text{ML}_3]^{n+1}$, to have greater sensitivity to the guest, A^- , than $[\text{ML}_3]^n$. The anion would associate much easier to the oxidized host than that of the starting host. This means that the binding constant, K_{ox} , of $[\text{ML}_3]^{n+1}$ to A^- is greater than that of $[\text{ML}_3]^n$ to A^- , K_{red} . Complementary to the behavior of cations to a reduced host, the $\text{M}^{\text{II/III}}$ redox potential of the host shifts due to stabilization of the oxidized host that has more affinity for the guest. This causes the removal of electrons to become easier to accomplish. In turn, this provokes the redox potential to shift in the negative direction. This suggests that the standard potential of $[\text{ML}_3]^n$, E^0 , is greater than the redox potential of $\text{A}[\text{ML}_3]^n$, $E^0_{\text{A}^-}$. Afterwards, the $\text{A}[\text{ML}_3]^n$ host-guest system is reduced to a less positive oxidation state and A^- is released.

Because anion guests are known to associate with hosts through hydrogen binding and electrostatic interactions,⁸⁵ we elected to explore hosts that are redox-active and can hydrogen bond with anion guests. For example, the Yamatera Group developed a crystal structure where they discovered that chloride ions are interacting with a $[\text{Co}(\text{hexaen})]^{3+}$ host through a second coordination sphere.³⁹ The host has ethylenediamine (en) ligands that are able to interact with Cl^- through its NH_2 hydrogen bond donors. The en ligand's acidity permits the NH_2 groups to achieve $\text{NH}\cdots\text{A}^-$ binding (Figure 4.2).

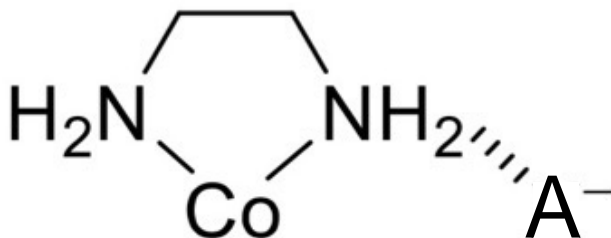


Figure 4.2. Second sphere interaction of ethylenediamine ligand of $\text{Co}(\text{en})_3$ complex with an anion, A^- .

This system can also enhance anion binding using electrostatic affects. Our group decided to look into the $[\text{Co}(\text{en})_3]^{2+/3+}$ system. The cobalt host has the capacity to be in the 2+ and 3+ state, which means that the host-guest association can be controlled by changing the oxidation state. Even though the $[\text{Co}(\text{en})_3]^{2+/3+}$ hosts are both cationic, the chloride ion would have greater sensitivity for the 3+ state than the 2+. Previously, our group has studied the redox properties of $[\text{Co}(\text{en})_3]^{2+/3+}$ to indicate if it can undergo redox-control. Unfortunately, the voltammogram of $[\text{Co}(\text{en})_3]^{2+/3+}$ was found to be irreversible due to ligand dissociation.⁴⁰

Instead, we decided to study this host system using a metal center that is more reliable in redox chemistry. We elected to study the $\text{Ru}(\text{en})_3$ framework because of ruthenium's known stability in redox chemistry. Another facet that is promising about the $\text{Ru}(\text{en})_3$ host is that it can be synthesized in the 2+ and 3+ form. The $[\text{Ru}(\text{en})_3]^{3+/2+}$ redox potential is also known to be approximately -0.4 vs. $\text{Fc}^{+/0}$.^{43, 87} This makes the host attractive for chloride guest binding. If $E_{1/2}$ for a host is too positive, then oxidation of the host might also promote oxidation of Cl^- guest to Cl_2 gas.⁴⁴ However, $[\text{Ru}(\text{en})_3]^{2+}$ is subject to oxidation in air much more than the 3+ framework. Air can oxidize the ethylenediamine ligand into an imine as shown in Figure 4.3. Oxidation of en into imine can decrease the affinity of the anion guest due to a loss of hydrogen.

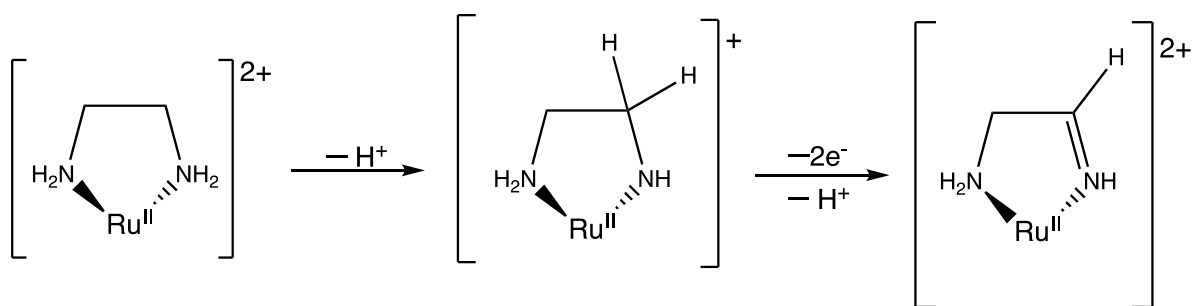


Figure 4.3. Oxidation reaction of ethylenediamine ligand of Ru-en framework to imine.

Even though the imine ligand might still bind to anions with its remaining hydrogens, these reactions would complicate studying the $[\text{Ru}(\text{en})_3]^{3+/2+}$ system. Thus, we looked for host systems that can incorporate ethylenediamine, maintain air stability, and has practical synthesis.

In Chapter 2, we briefly discussed how bpy is popularly used as an N-donor ligand. For example, one stable octahedral ruthenium framework is the $[\text{Ru}(\text{bpy})_3]^{2+}$ complex,⁸⁸ but its H atoms are unlikely to bind strongly to anions. Instead, a mixture of bpy and en ligands provides a good redox potential and the capability of anion binding to NH groups. Curtis et al. demonstrated the redox behaviors of ruthenium(III) ethylenediamine structures.⁴³ We focused on $[\text{Ru}(\text{bpy})(\text{en})_2](\text{PF}_6)_2$ (Figure 4.4).

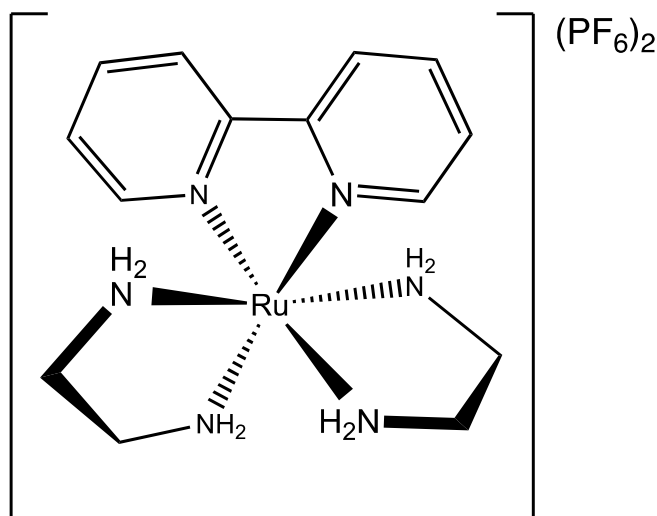


Figure 4.4. Chemical diagram of $[\text{Ru}(\text{bpy})(\text{en})_2](\text{PF}_6)_2$.

This en-bpy structure has two ethylenediamine ligands that can induce hydrogen bonding with anions, but instead of a third en ligand, this host has a bpy ligand in its place. The bpy ligand aids in enhancing the host's stability by preventing it from being oxidized by air. This host also has a much more feasible synthesis to execute than $\text{Ru}(\text{en})_3$. Although this host has one less en ligand, it still has a promising aspect of binding to two chloride ions with its two en ligands, particularly where the two en NH_2 groups come together. Another encouraging facet of this

complex is that its redox properties have been studied. The $E_{1/2}$ of en-bpy complex was discovered to be 0.226 V (vs $\text{Fc}^{0/+}$) in CH_3CN , according to the Curtis Group.⁴³

More complicated techniques were developed to attract anions, such as assembling hosts that have binding sites.⁴⁶ Previously, the Crabtree Group showed that diamides bind greatly to acetates and halides through $\text{NH}\cdots\text{A}^-$ interactions.^{47,48} To associate with the anion, the diamide distorts into an abnormal *syn-syn* conformation, which forms a binding pocket out of the two hydrogen bonding NH substituents. This study emphasizes how the arrangement of the ligand is important for binding guests.^{47, 89} If the architecture of the ligand does not form a good binding site, the guest will have difficulty binding to the host.⁴⁹

The synthesis of octahedral complexes may produce two types of isomers: facial (*fac*, C_3 symmetry) and meridional (*mer*, C_{2v} symmetry). Asymmetric chelating tris metal frameworks can have these *fac* and *mer* conformations (Figure 4.5).

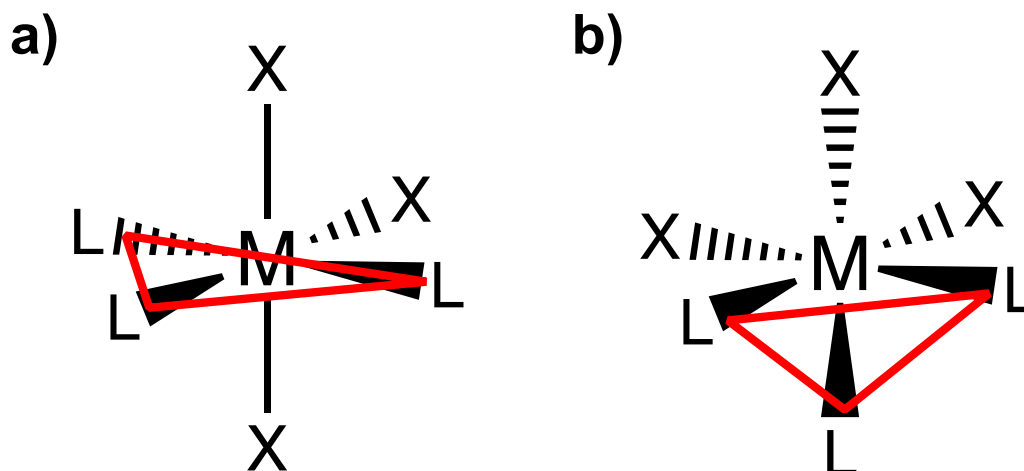


Figure 4.5. Illustration of a) *mer* and b) *fac* isomers of octahedral metal complex. Red marking displays how the *fac* isomer brings all three L groups together, which could allow them to interact more strongly to the guest than the *mer* isomer.

The *fac* isomer is able to bind much better to guests than the *mer* cage due to its lack of steric hindrance. What also makes the *fac* isomer the better host is that this configuration creates a binding pocket on one face of the structure.⁵⁰ For anionic binding, the hydrogen donor site is

induced on one face of the structure. The *mer* isomer, however, does not have the binding pocket formed due to the ligands being on the same plane. This displays the importance of separating the *mer* and *fac* isomers.

Ward et al. have prepared a series of mononuclear ruthenium(II) tris(pyrazoyl-pyridine) complexes.⁵¹ They discovered that the *fac* isomers of these structures have a hydrogen donor pocket. This recognition site interacts with the guest, leading to changes in the protons' NMR signals. Host-guest interaction can be examined using NMR and the change in chemical shifts signifies guest binding.^{90, 91} This occurrence does not happen with the *mer* isomers due to it not having the hydrogen recognition site (Figure 4.6).

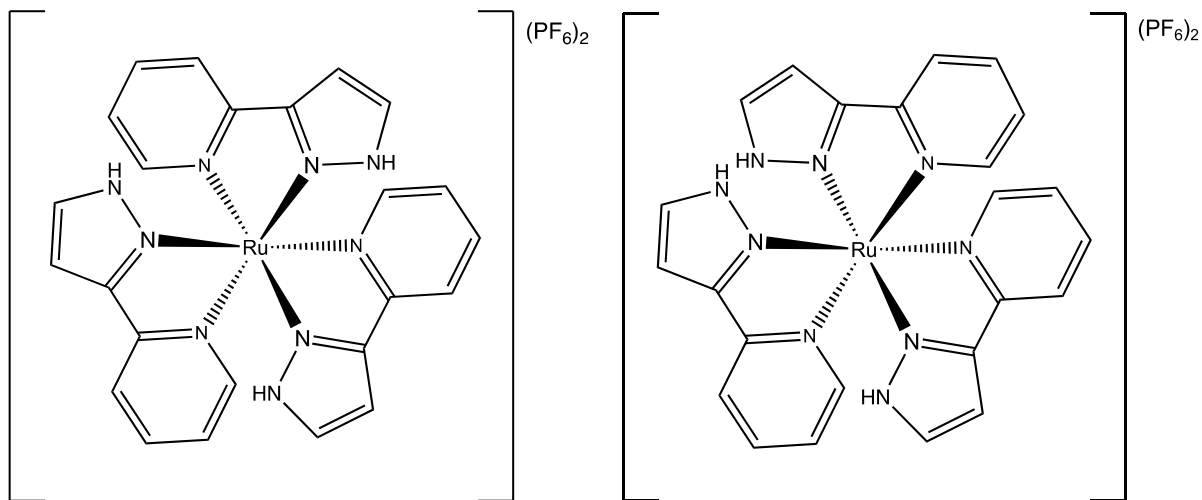


Figure 4.6. Chemical diagram of *fac*- $[Ru(pypz)_3](PF_6)_2$ (left) and *mer*- $[Ru(pypz)_3](PF_6)_2$ (right).

One of the pyrazolyl-pyridine hosts they synthesized is *fac*- $[Ru(pypz)_3](PF_6)_2$. This host has NH groups that makes a hydrogen bond donor site that can be using for guest binding. The *fac* configuration creates the donor site by have the NH groups point in the same direction, which induces guest binding. In the literature, they measured the host-guest interaction between the *fac*- $[Ru(pypz)_3](PF_6)_2$ host and isoquinoline-N-oxide guest. They observed that the guest association

is between the electron-rich O atom of the guest and the hydrogen bonding in the recognition site.⁵¹ We aim to use oxidation of the 2+ metal center to 3+ to increase guest binding. We have selected $-\text{SO}_3(\text{CF}_2)_3\text{CF}_3$, TPPO, and HF_2^- as guests, which have potential in displaying good guest association with this host through ionic or hydrogen bonding.

4.2. Results and Discussion

4.2.1. $[\text{Ru}(\text{bpy})(\text{en})_2](\text{PF}_6)_2$ Host with Cl^- ion Guest

We looked into performing redox-controlled host-guest interaction with the $[\text{Ru}(\text{bpy})(\text{en})_2](\text{PF}_6)_2$ host due to its good redox properties and the potential for hydrogen bonding with anionic guests. We also wanted to see if oxidizing the complex to Ru^{III} leads to an increase in the number of anions bound. Using cyclic voltammetry, we determined the redox properties of $[\text{Ru}(\text{bpy})(\text{en})_2](\text{PF}_6)_2$ with and without added chloride ions. First, we studied the electrochemistry of the host in CH_3CN to compare the $E_{1/2}$ with the literature value. Then, we added Cl^- using benzyltriethylammonium chloride (BTAC). Figure 4.7 shows the voltammograms of this analysis. The electrochemical parameters are quantitatively shown in Table 4.1.

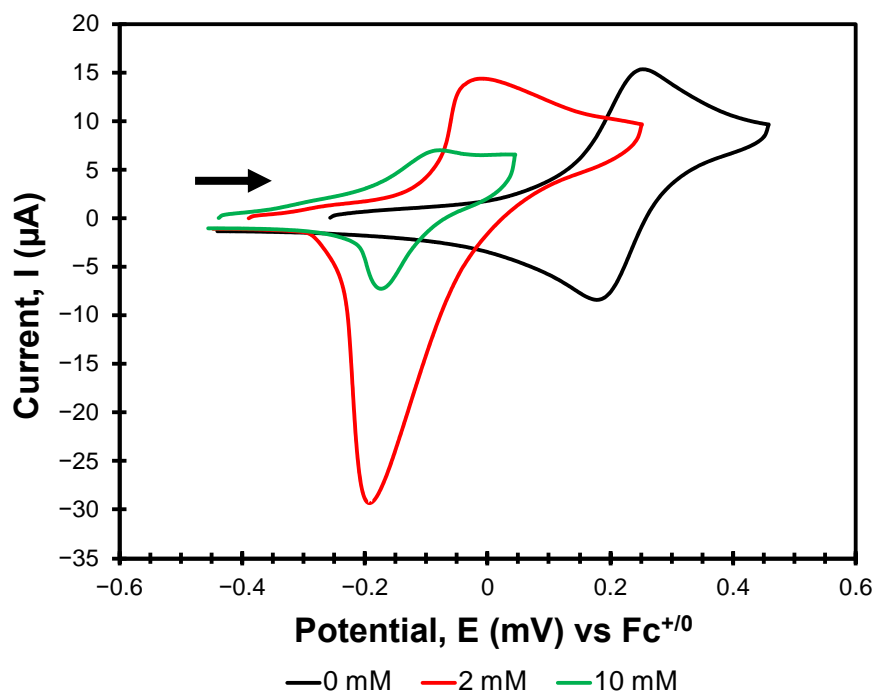


Figure 4.7. CV of $[\text{Ru}(\text{bpy})(\text{en})_2](\text{PF}_6)_2$ with the addition of BTAC (CH_3CN , 0.1 M TBAPF_6 , 0.1 Vs^{-1}). The data were measured using an Ag/AgCl reference electrode, glassy carbon working electrode, but plotted vs. $\text{Fc}^{+/0}$ reference redox couple, which has $E_{1/2} = 0.445 \text{ V}$ vs. Ag/AgCl under these conditions.

Table 4.1. Electrochemical parameters in volts (V vs. $\text{Fc}^{+/0}$) of $[\text{Ru}(\text{bpy})(\text{en})_2](\text{PF}_6)_2$ with added BTAC.

[BTAC]	E_{pa}	E_{pc}	ΔE_{p}	$E_{1/2}$
0 mM	0.253	0.177	0.076	0.215
2 mM	-0.010	-0.192	0.182	-0.101
10 mM	-0.079	-0.175	0.096	-0.127

The black voltammogram of the host, without any BTAC added, displays the redox potential of the complex. The $E_{1/2}$ of this framework is at 0.215 V, which is near the recorded potential from the Curtis Group.⁴³ Then 2 mM of Cl^- guest was added (1:2 host/guest ratio) and immediately, distortion in the voltammogram of the host was observed. The green trace represents 10 mM BTAC added and the voltammogram remains altered. We believe that the cause of the

obscure voltammogram is due to deprotonation of the en ligands. This could likely be from the large amount of chloride increasing the pH.

To inhibit H⁺ loss from the Ru complex, in subsequent CV experiments, the electrolyte solution had 5% of 0.1 M HNO₃ added (Figure 4.8).

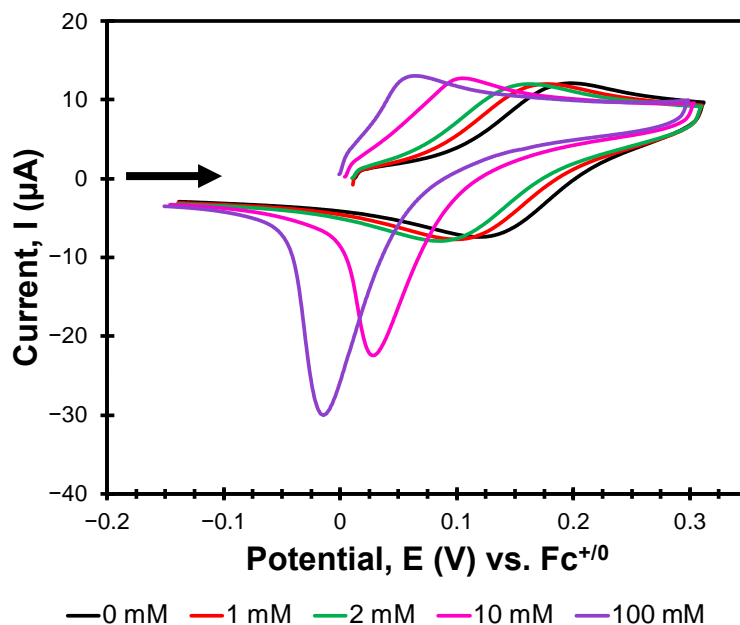


Figure 4.8. CV of [Ru(bpy)(en)₂](PF₆)₂ with the addition of BTAC (CH₃CN with 5% 0.1 M HNO₃, 0.1 M TBAPF₆, 0.1 Vs⁻¹). The data were measured using an Ag/AgCl reference electrode, glassy carbon working electrode, but plotted vs. Fc⁺⁰ reference redox couple, which has E_{1/2} = 0.388 V vs. Ag/AgCl under these conditions.

Table 4.2. Electrochemical parameters in volts (V vs. Fc⁺⁰) of [Ru(bpy)(en)₂](PF₆)₂ with added BTAC in acidic solution.

[BTAC]	E _{pa}	E _{pc}	ΔE _p	E _{1/2}
0 mM	0.198	0.118	0.080	0.158
1 mM	0.177	0.101	0.076	0.139
2 mM	0.161	0.084	0.077	0.123
10 mM	0.104	0.028	0.076	0.066
100 mM	0.063	-0.014	0.077	0.025

The voltammogram for the complex (black trace) retains its reversibility in the solution with HNO₃(aq) added. After the 1 and 2 mM BTAC concentrations were added, small negative

shifts in the voltammogram could only be observed. This indicates some anion guest binding. However, when more chloride ions are added, the voltammogram is distorted. This signals that studying the host-guest interaction using redox for this system may not be suitable with a higher concentration of guest. Nernstian calculations were performed to determine how many more cations bind to the 3+ state than the 2+ using the $E_{1/2}$ for the 1 mM and 2 mM traces (Figure 4.9).

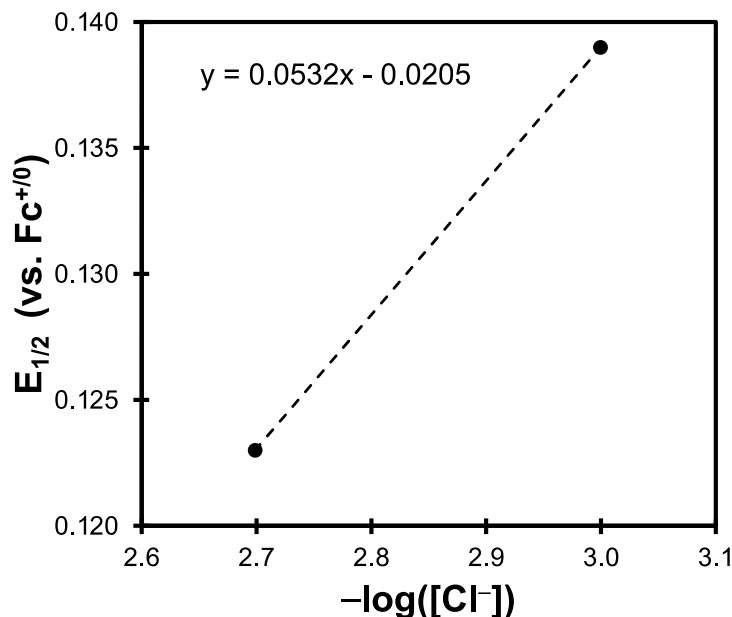


Figure 4.9. $E_{1/2}$ (vs. $\text{Fc}^{+/0}$) vs. $-\log([\text{Cl}^-])$ of 1 mM $[\text{Ru}(\text{bpy})(\text{en})_2](\text{PF}_6)_2$.

Likewise in Chapter 3, the number of more bound Cl^- ions to the oxidized state were ascertained between the 1 mM and 2 mM redox potentials. In this one-electron transfer reaction, $E_{1/2}$ should shift by -0.0592 V for each factor of 10 increase in $[\text{Cl}^-]$ if there is one more chloride ion binding to the oxidized host. This should appear as a slope of 0.0592 V in Figure 4.8, because its x axis is $-\log([\text{Cl}^-])$.

Between the first two concentrations of added guest, the slope was found to be -0.0532 V. This finding shows that the oxidized host can bind to one more Cl^- than the starting 2+ host. It is reasonable that the 2+ complex can bind to Cl^- as well. We decided to perform crystallography on the 2+ state to see if it can interact with Cl^- ions. Thus, we make a solution of 1:100 host/guest

ratio of $[\text{Ru}(\text{bpy})(\text{en})_2](\text{PF}_6)_2$ and BTAC in CH_3CN in 5% 0.1 M HNO_3 . The crystal was grown in a closed vial in the solution (Figure 4.10).

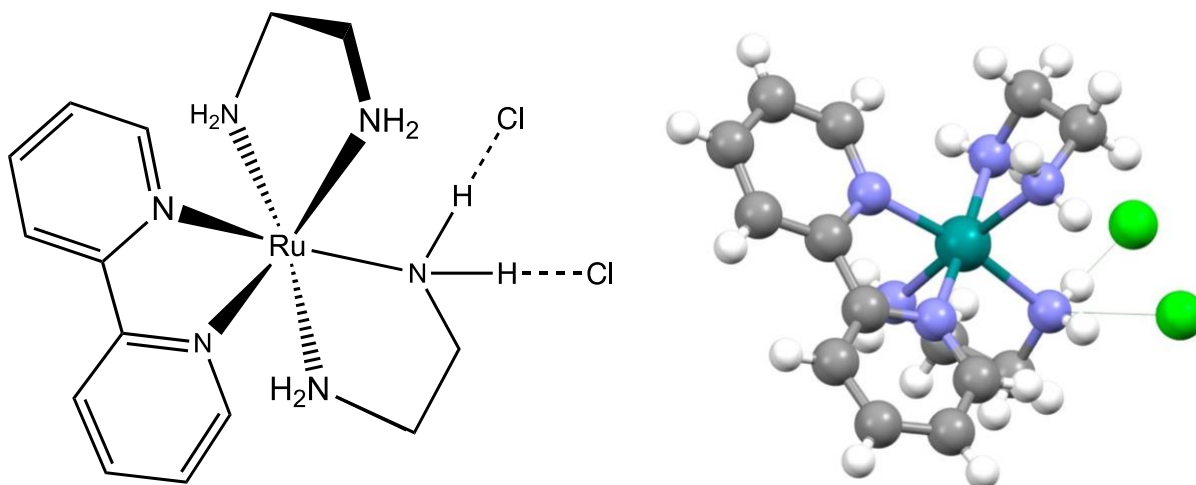


Figure 4.10. Chemical diagram and X-ray crystal structure of $[\text{Ru}(\text{bpy})(\text{en})_2](\text{PF}_6)_2$. Cl^- guest ions (lime green) associate with the N–H groups in the en ligands.

The crystal structure shows that the NH groups in $[\text{Ru}(\text{bpy})(\text{en})_2]^{2+}$ can associate with chloride ions. This interaction is in the solid state, and may not be very strong in solution. However, it is likely that association with Cl^- would be stronger if the complex is oxidized. This is consistent with the decrease in $E_{1/2}$ for $[\text{Ru}(\text{bpy})(\text{en})_2]^{3+/2+}$ that we observe when Cl^- is added. The Ru– N_{bpy} bond distances were 2.0337(9) and 2.0210(9) and the Ru– N_{en} has 2.1385(9), 2.1296(9), 2.145(1), and 2.1204(9). This is comparable to measurements found in the literature of $\text{Ru}(\text{en})_3$ and $\text{Ru}(\text{bpy})_3$ structures.⁹²⁻⁹⁴

4.2.2. *fac*- $[\text{Ru}(\text{pypz})_3](\text{PF}_6)_2$ Host with Guest Ions and Molecules

As with the previous host in this chapter, we aim to achieve better guest binding with *fac*- $[\text{Ru}(\text{pypz})_3](\text{PF}_6)_2$ by oxidizing the host. In order to execute controlled host-guest chemistry using redox, we had to investigate whether this complex has good redox properties. We first scanned the complex alone and discovered that it has a reversible voltammogram with a ΔE_p of 0.072 V and a $E_{1/2}$ of 0.788 V. Although this framework has good redox behavior, its $E_{1/2}$ is too positive for

studying Cl^- binding (because oxidation of Cl^- would probably compete with oxidation of Ru(II)). Instead, we decided to use other guests to analyze its capabilities in controlled guest association. First, we chose to utilize $^-\text{SO}_3(\text{CF}_2)_3\text{CF}_3$ as a guest (Figure 4.11). It is a weak base, but its three O atoms may be well matched for the *fac*-NH groups in $[\text{Ru}(\text{pypz})_3]^{2+}$.

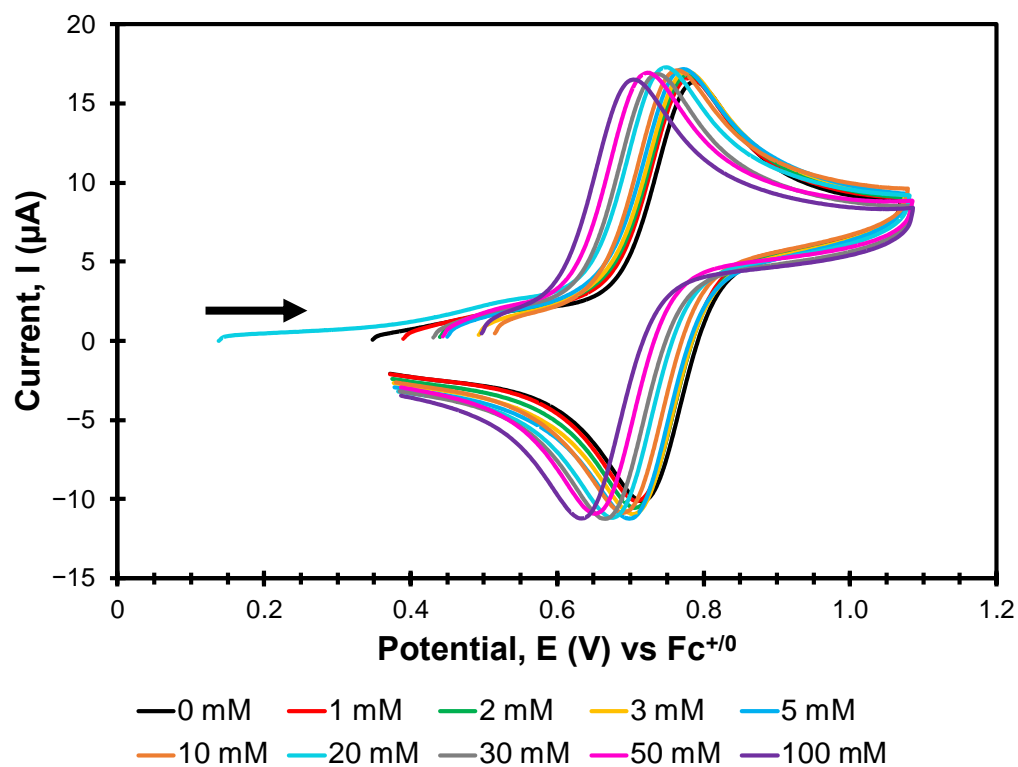


Figure 4.11. CV of *fac*- $[\text{Ru}(\text{pypz})_3](\text{PF}_6)_2$ with $\text{KOSO}_2(\text{CF}_2)_3\text{CF}_3$ added (CH_3CN , 0.1 M TBAPF_6 , 0.1 V s^{-1}).

Table 4.3. Electrochemical parameters in volts (V vs. $\text{Fc}^{+/0}$) of 1 mM fac-[Ru(pypz)₃](PF₆)₂ in CH₃CN with added KOSO₂(CF₂)₃CF₃, 0.1 V s⁻¹.

[$-\text{SO}_3(\text{CF}_2)_3\text{CF}_3$]	E_{pa}	E_{pc}	ΔE_p	$E_{1/2}$
0 mM	0.788	0.716	0.072	0.752
1 mM	0.782	0.708	0.074	0.745
2 mM	0.779	0.706	0.073	0.743
3 mM	0.776	0.705	0.071	0.741
5 mM	0.775	0.699	0.076	0.737
10 mM	0.763	0.690	0.073	0.727
20 mM	0.749	0.674	0.075	0.712
30 mM	0.738	0.664	0.074	0.701
50 mM	0.723	0.652	0.071	0.688
100 mM	0.705	0.633	0.072	0.669

A gradual negative change in the redox potential is discerned as more guest is added, as expected if the guest binds preferentially to Ru^{III}. Throughout the experiment, the Ru^{II}/Ru^{III} redox process remains reversible, with $\Delta E_p < 0.080$ V. A plot of $E_{1/2}$ vs. $-\log([\text{O}_3\text{S}(\text{CF}_2)_3\text{CF}_3])$ (Figure 4.12) is clearly curved at low concentrations, where there is a limited supply of guest and the fraction of guest bound is probably small. At high concentrations (10 - 100 mM), the plot is nearly linear, with a slope as expected for one more guest bound in Ru^{III} than in Ru^{II}.

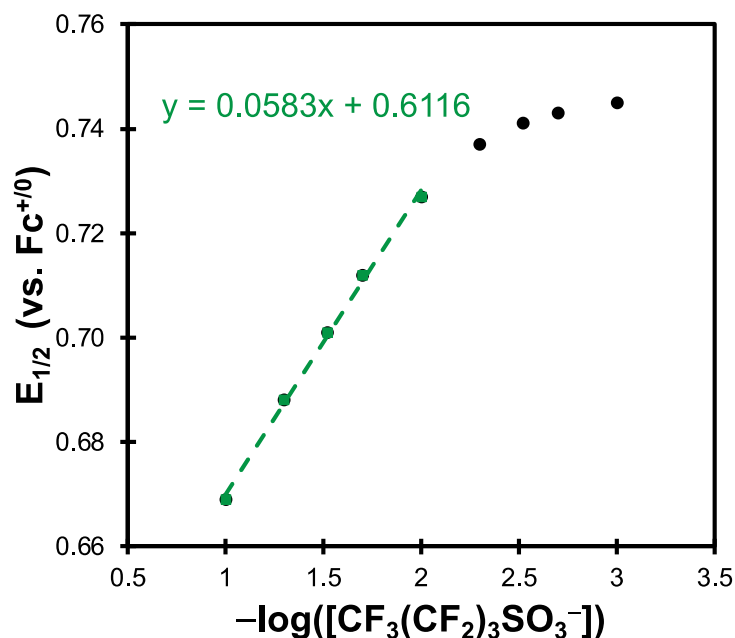


Figure 4.12. $E_{1/2}$ (vs. $\text{Fc}^{+/0}$) vs. $-\log([\text{SO}_3(\text{CF}_2)_3\text{CF}_3^-])$ of 1 mM *fac*- $[\text{Ru}(\text{pypz})_3](\text{PF}_6)_2$. All concentrations (black). Slope for 10 – 100 mM concentrations (green).

The Ward Group succeeded in binding isoquinoline-N-oxide to the *fac*- $[\text{Ru}(\text{pypz})_3](\text{PF}_6)_2$ host.⁵¹ They showed that this neutral guest can bind weakly to the Ru^{II} host. To follow up on this result, we were interested in whether a neutral guest would exhibit enhanced binding to the Ru^{III} complex. We first attempted to do this by studying the electrochemistry of the host with added pyridine-N-oxide (Appendix B9). However, the electrochemistry with this guest was poor. We next tested triphenylphosphine oxide (TPPO). We expected that its electron-rich O atom would bind to the hydrogen donor site. In this, the guest acts as a hydrogen bond acceptor.⁵¹ The results are shown in Figure 4.13 and Table 4.4.

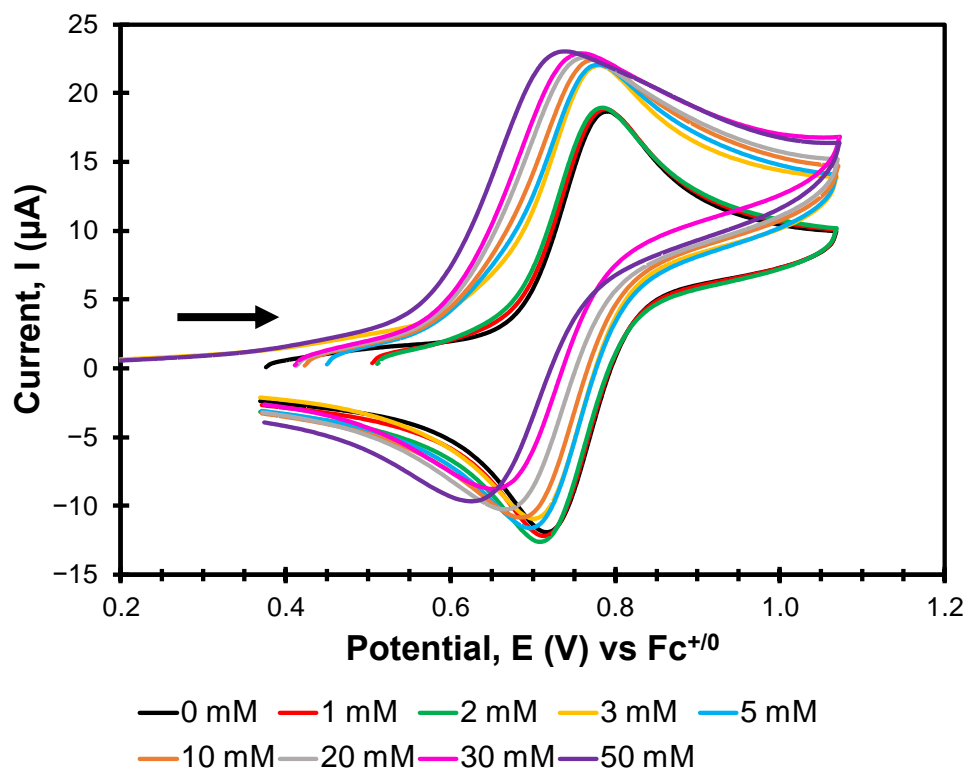


Figure 4.13. CV of *fac*-[Ru(pypz)₃](PF₆)₂ with TPPO added (CH₃CN, 0.1 M TBAPF₆, 0.1 V s⁻¹).

Table 4.4. Electrochemical parameters in volts (V vs. Fc⁺⁰) of 1 mM *fac*-[Ru(pypz)₃](PF₆)₂ in CH₃CN with added TPPO, 0.1 V s⁻¹.

[TPPO]	E _{pa}	E _{pc}	ΔE _p	E _{1/2}
0 mM	0.794	0.716	0.078	0.755
1 mM	0.789	0.713	0.076	0.751
2 mM	0.784	0.709	0.075	0.747
3 mM	0.781	0.701	0.080	0.741
5 mM	0.779	0.698	0.081	0.739
10 mM	0.772	0.686	0.086	0.729
20 mM	0.763	0.667	0.096	0.715
30 mM	0.755	0.655	0.100	0.705
50 mM	0.739	0.626	0.113	0.683

The host-guest interaction of this system is reminiscent of what was discovered with the KOSO₂(CF₂)₃CF₃ guest. In this study, there is a steady negative shift in the redox potential as more TPPO is added. When higher concentrations of guest than 50 mM are added, the solubility of the TPPO becomes difficult. At 50 mM, the ΔE_{1/2} is -72 mV. This overall change can be compared to the -O₃S(CF₂)₃CF₃ guest at 50 mM (-64 mV). This host-guest system also displays an obvious

better TPPO guest affinity for the oxidized state than the starting 2+ host. The Nernstian measurements that were performed likewise for the $^{-}\text{O}_3\text{S}(\text{CF}_2)_3\text{CF}_3$ guest (Figure 4.14).

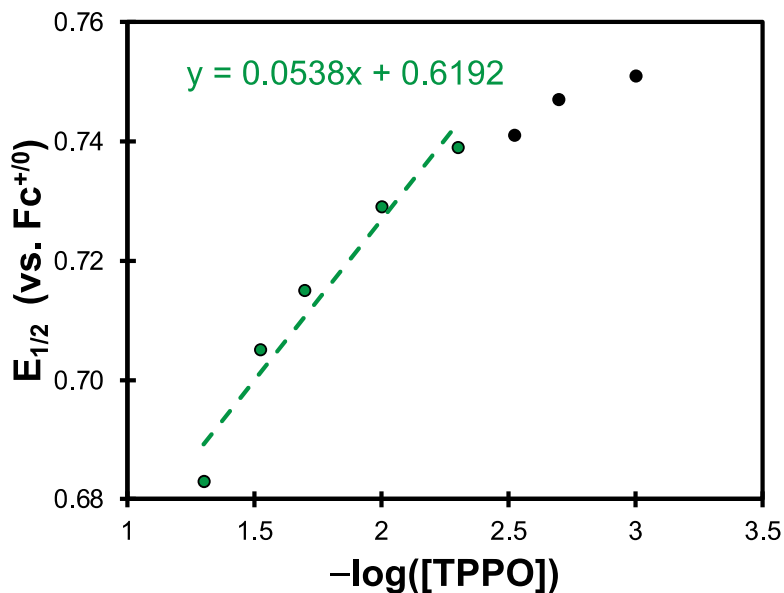


Figure 4.14. $E_{1/2}$ (vs. $\text{Fc}^{+/0}$) vs. $-\log([\text{TPPO}])$ of 1 mM *fac*- $[\text{Ru}(\text{pypz})_3](\text{PF}_6)_2$. All concentrations (black). Slope for 5 – 50 mM concentrations (green).

Lastly, we utilized another guest for controlled binding with the *fac*- $[\text{Ru}(\text{pypz})_3](\text{PF}_6)_2$. We decided to look into other anions. We first looked into fluoride guests through tetrabutylammonium fluoride (TBAF), however, TBAF is very hygroscopic. The other option is utilizing NBu_4HF_2 . This is a more promising guest due to it not being as hygroscopic as TBAF. We studied the electrochemistry of *fac*- $[\text{Ru}(\text{pypz})_3](\text{PF}_6)_2$ with NBu_4HF_2 (Figure 4.15).

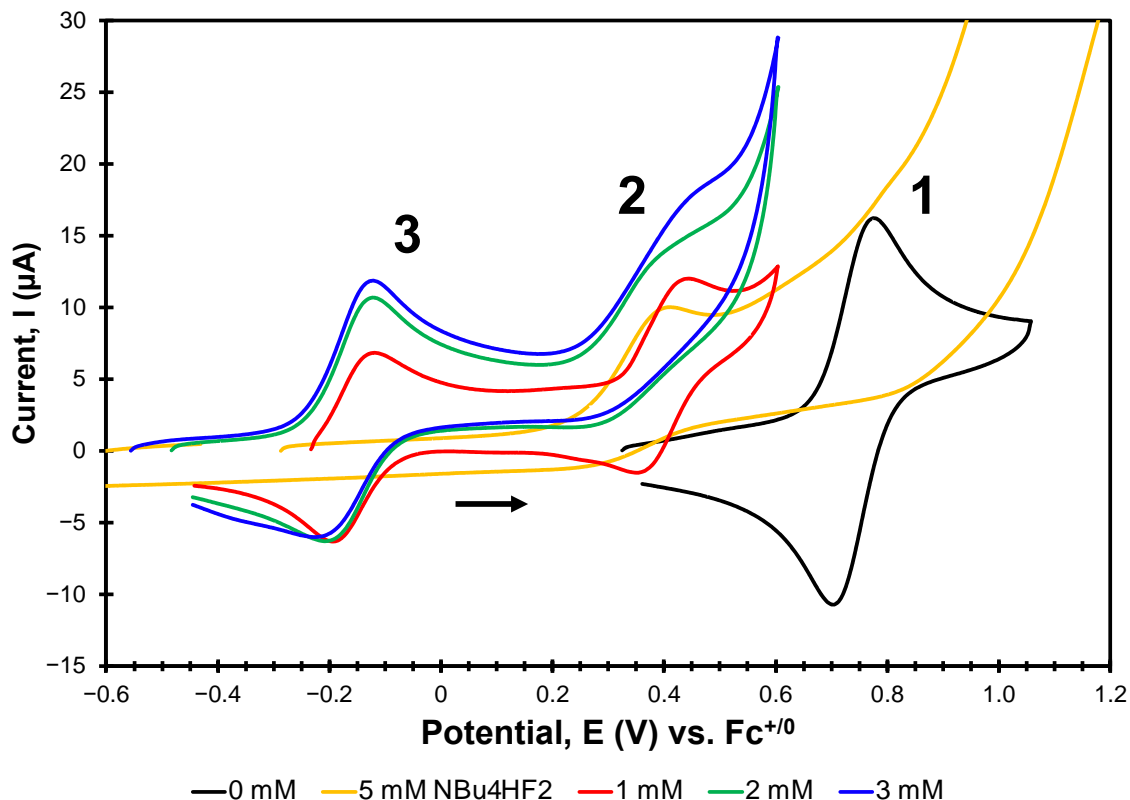


Figure 4.15. CV of *fac*-[Ru(pypz)₃](PF₆)₂ with the addition of NBu₄HF₂ (CH₃CN, 0.1 M TBAPF₆, 0.1 V s⁻¹).

Table 4.5. Electrochemical parameters in volts (V vs. Fc⁺⁰) of 1 mM *fac*-[Ru(pypz)₃](PF₆)₂ in CH₃CN with added NBu₄HF₂, 0.1 V s⁻¹.

[NBu ₄ HF ₂]	E _{pa1}	E _{pc1}	E _{pa3}	E _{pc3}	ΔE _{p3}	E ³ _{1/2}
0 mM	0.791	0.714	----	----	----	----
1 mM	----	----	-0.118	-0.192	0.074	-0.155
2 mM	----	----	-0.122	-0.209	0.087	-0.166
3 mM	----	----	-0.125	-0.231	0.106	-0.178

The voltammogram of the complex is identical to what is shown in the other experiments and is labeled as **1** in the figure. The yellow trace represents the electrochemistry of 5 mM of NBu₄HF₂ guest alone. The activity symbolized by **2** on the voltammograms is from the electrochemical properties of NBu₄HF₂ and not related to the host-guest interaction. Starting with 1 mM (1:1 host/guest ratio), there was an immediate color change from the yellow host solution to bright orange. When scanning the analyte for this concentration, there is a large negative shift

in the redox potential of the host. The negative $\Delta E_{1/2}$ is over 0.9 V and this new voltammogram is represented by **3**. This voltammogram produced is from a possible host-guest system where the NBu_4HF_2 remains attached to the host. This is further evidenced by the lack of change in the $E_{\text{pa}2}$ and the broadening of $E_{\text{pc}2}$ as more guest is added. The instant color change that is observed when NBu_4HF_2 is first added also shows this as well. This indicates that the same number of guest is binding to Ru^{II} and Ru^{III} . To analyze the sensitivity this guest has with the 2+ complex, UV-vis studies were accomplished (Figure 4.16). The quantitative results of this experimentation are listed in Table 4.6.

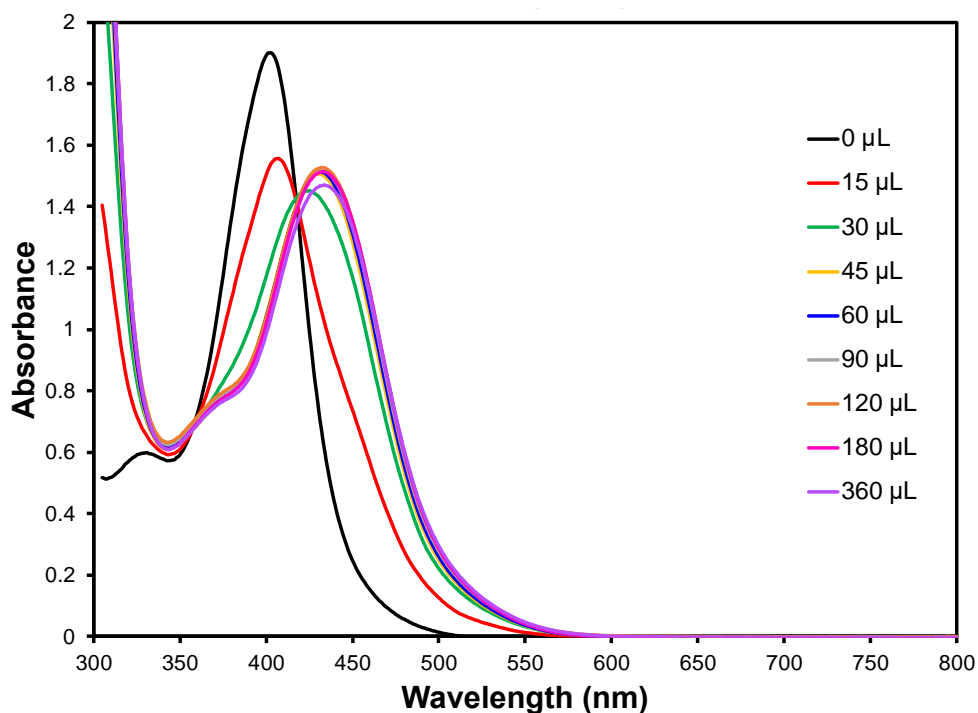


Figure 4.16. UV-Vis spectra of 0.125 mM of $\text{fac-}[\text{Ru}(\text{pypz})_3](\text{PF}_6)_2$ in CH_3CN and additions of small 1 mM solutions of NBu_4HF_2 .

Table 4.6. UV-vis data of the λ_{\max} (nm) for each addition of guest solution (μL).

Guest added	Host : Guest	λ_{\max}
0	----	402
15	33 : 1	407
30	17 : 1	425
45	11 : 1	430
60	8 : 1	431
90	6 : 1	432
120	4 : 1	432
180	3 : 1	433
360	1.5 : 1	434

The λ_{\max} of yellow host appears at 402 nm. This is in agreement with similar hosts that were studied by the Ward Group.⁵¹ To slowly introduce the guest to the host, small microliter 1 mM NBu_4HF_2 solutions were added to the analyte. The UV-vis spectrum was recorded after each addition of guest solution. Small solutions were added so that the host-guest behavior can be slowly examined since a host/guest ratio higher than 1:1 displays no change in the $E_{1/2}$. A gradual decrease in absorbance of the host's 402 nm λ_{\max} is observed and a new λ_{\max} appears at 407 nm. Between the 15 and 30 μL guest concentrations, an obvious color change occurs from yellow to gold. After more additions of NBu_4HF_2 solution, the λ_{\max} stops at 434 nm, even when excess guest is added, a difference of the 32 nm. However, another possibility is that HF_2^- is only deprotonating the complex, creating a $\text{Ru}^{\text{II}}\text{-HF}_2$ adduct, likely *fac, fac*- $[\text{Ru}(\text{pypz})_3\text{Ru}(\text{pypz}^-)_3](\text{HF}_2)$.

Overall, this host is promising for analyzing host-guest chemistry. Its binding pocket is strong enough to even attract bigger anions such as $^-\text{O}_3\text{S}(\text{CF}_2)_3\text{CF}_3$. However, as seen by the bifluoride guest, the recognition site can be capable of being too sensitive for controlled host-guest interaction. Nevertheless, this structure has potential to be further studied in this application because of its exceptional reversibility. One method can be to modify a pyrazole ligand with an amide group to promote greater anion binding. Work from Liu et al. has shown that having too

many hydrogen donors in the recognition site can cause guest binding to be so strong that the anion cannot be released.¹¹ To prevent the guest binding from being too strong, only one of the pyrazole ligands can be modified with the amide group (Figure 4.17).

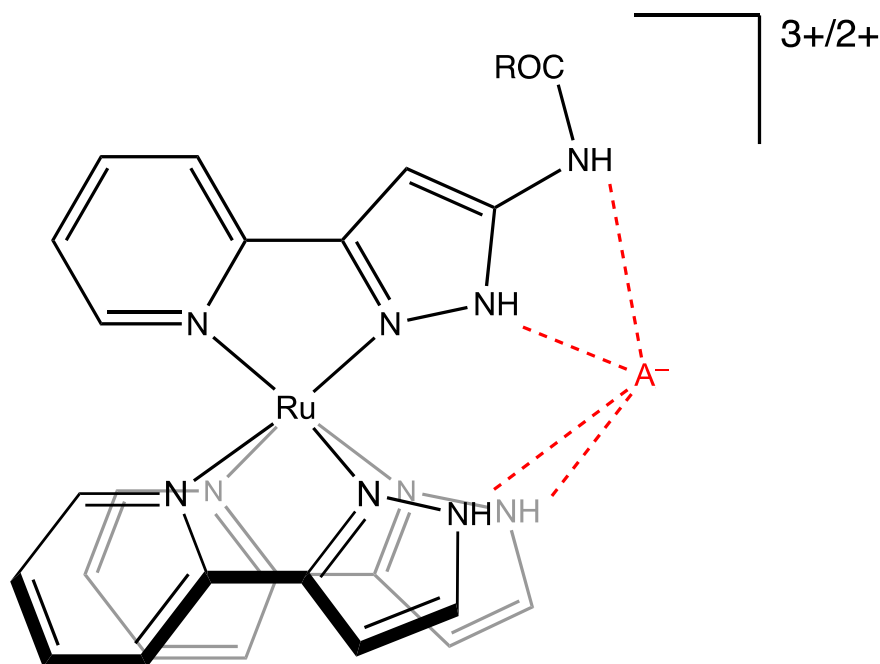


Figure 4.17. Chemical diagram of the *fac*-[Ru(pypz)₃]^{3+/2+} structure associating with A⁻, where one of the pyrazole ligands are modified with an amide group.

4.3. Experimental

4.3.1. General

Commercially available reagents were purchased from Pressure Chemicals, Alfa Aesar, BeanTown Chemicals, Sigma-Aldrich, and J.T. Baker and were used without further purification. Trifluoroacetic acid and ethylenediamine were purified by distillation before use. Electrospray ionization mass spectra (ESI-MS) were measured by using an Agilent 6230 instrument. UV/vis spectrometry was performed with an Aviv 14DS spectrometer. ¹H NMR experiments were executed with Bruker AVIII 400 MHz spectrometer in CD₃CN. Crystallography was implemented using a Bruker Kappa Apex-II DUO diffractometer, with MoK α radiation.

Cyclic voltammetry of the metal host complexes was determined using an EC Epsilon Eclipse potentiostat/galvanostat with glassy carbon working electrode, Pt wire counter electrode, and Ag/AgCl reference electrode. Cyclic voltammetry was done using 1 mM Ru hosts in a 0.1 M tetrabutylammonium, hexafluorophosphate (TBAPF₆) acetonitrile electrolyte solution, at a scan rate of 0.1 V s⁻¹, unless stated otherwise.

4.3.2. Synthesis of [Ru(bpy)(en)₂](PF₆)₂

This compound was prepared using the method from Curtis and co-workers.⁴³ RuCl₃·xH₂O (0.25 g, 1.2 mmol) was dissolved in 40 mL of an ethanol/water (1:5) solution. 2,2'-bipyridine (0.19 g, 1.2 mmol) was slowly added throughout a 1-hr period to the 40 – 50 °C reaction mixture. The solution was refluxed for 4 hours and cooled to room temperature. A dark-red brown solution is observed. The reaction was placed in the fridge overnight in a salt-ice bath. Ethylenediamine (0.6 mL, 12.1 mmol) was added while stirring and refluxed for 6 hr, then cooled. 2.5 equivalents of NH₄PF₆ were added while stirring to get the PF₆ salt. EtOH was removed from the solution using rotovap. Dark red solid precipitate was observed after filtration. Then the solid was dissolved in a small amount of acetone, then reprecipitated out using diethyl ether (crude: yield 46%).

Afterwards, the product was further purified in alumina column chromatography. The neutral alumina was treated with HCl of a 10% slurry (w/v in water). Two bands that are red and pink were observed in the column. The red band was collected first using a 3:1 toluene/acetonitrile eluent and it represents the [Ru(bpy)₂(en)](PF₆)₂ complex. Then a 2% MeOH aqueous solution was added and the pink band was collected as [Ru(bpy)(en)₂](PF₆)₂ (yield 15% of crude). UV-vis is in agreement with the aforementioned literature. Dark red crystals of [Ru(bpy)(en)₂]Cl₂ was grown using a solution of [Ru(bpy)(en)₂](PF₆)₂ with BTAC in acetonitrile solution with 5% 0.1 M

HNO₃ added in a sealed vial. ESI-MS (Figure 4.18): m/z [Ru(bpy)₂(en)]²⁺ 189.0559 (calcd: 189.0549). ESI-MS (Figure 4.19): m/z [Ru(bpy)(en)₂]²⁺ 189.0559 (calcd: 189.0549).

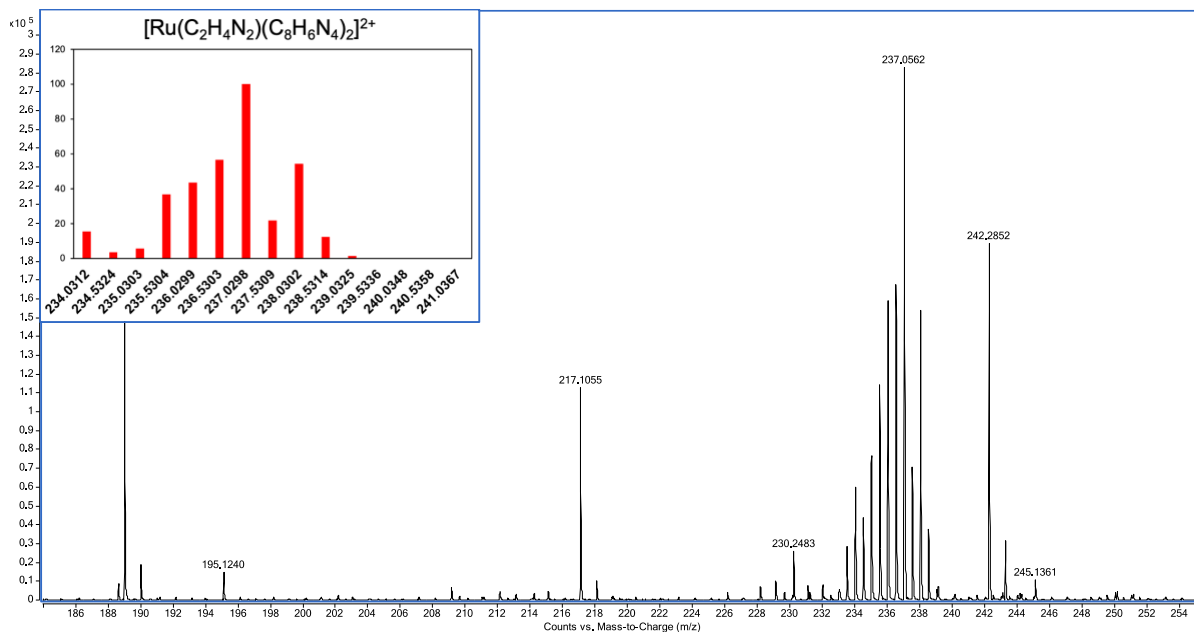


Figure 4.18. ESI mass spectra of [Ru(bpy)₂(en)]²⁺, m/z 237.0562 (calcd: 237.0296). Inset display calculated relative intensities.

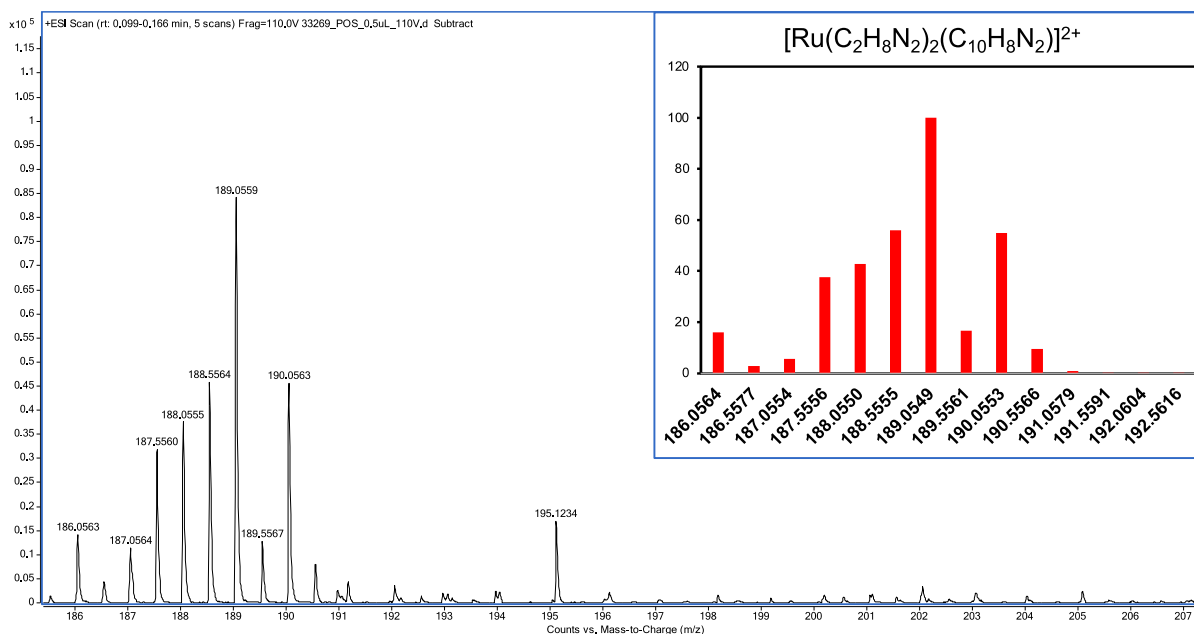


Figure 4.19. ESI mass spectra of [Ru(bpy)(en)₂]²⁺, m/z 189.0559 (calcd: 189.0549). Inset display calculated relative intensities.

4.3.3. Synthesis of *fac*-[Ru(*pypz*)₃](PF₆)₂

fac-[Ru(*pypz*)₃](PF₆)₂ was prepared using the procedure from literature.⁵¹ Yellow solid was achieved in this synthesis and ¹H NMR analysis is in agreement with Ward (yield 15% of *fac* isomer).

Chapter 5. Facilitating Anion Guest Binding with Ruthenium Hosts

5.1. Introduction

Anionic sensing is essential for many environmental and mechanical applications, however, it continues to be more difficult to examine because of how its easily manipulated by water, pH, and its intricate geometry.^{86, 95, 96} Anionic binding is usually performed by hydrogen-bonding and electrostatic interactions.⁸⁵ Vasdev and co-workers noticed that a ferrocene-containing palladium triangular cage, $[\text{Pd}_3(\text{L}_{4\text{EFc}})_6]^{6+}$, have good binding to *p*-toluenesulfonate (OTs) due to electrostatic interactions and hydrogen bonding between 3-pyridyl arms and sulfonate O atoms.^{97, 98} Using ^1H NMR studies, they also concluded that this host has better binding affinity to OTs than the $[\text{Pd}_2(\text{L}_{3\text{EFc}})_4]^{4+}$ counterpart due to it having a more positive charge.⁹⁷

Researchers have had much success in increasing the sensitivity of hosts to anionic guests by producing hosts that have anionic receptors attached to it. Previously, Li and co-workers have also implemented a study on the anion sensing of a tetrathiafulvalene (TTF) compound with F^- and noticed a negative redox potential shift with each addition of fluoride.⁹⁹ An increase in the host's absorption band is also induced as more fluoride guest is added. They were able to accomplish this due to the hosts having boron-based receptors that have good affinity for fluoride guests.

In Chapter 2, I discussed performing redox chemistry of Cu-xpt to allow direct coordination of Cl^- guest to the copper(II) center, which could then be released by reduction to copper(I). However, this system was not suitable for studying redox control via electrochemistry, because the host's voltammogram became increasingly irreversible as more Cl^- was added. Because of this, we searched for a system that can execute anionic guest binding through a second coordination sphere. We decided to manipulate the oxidation state of the host complex to increase

the host's affinity for the guest through electrostatic interactions. In this chapter, we will discuss other potential hosts for redox-controlled guest binding.

Taking advantage of the versatility of the en-bpy host system, a way to advance this is by substituting the en ligands with diphenylethylenediamine (dpen). The phenyl attachments can be used to place groups in the ortho position to increase the affinity of anions to the host. Amide groups can be placed on the phenyl rings to induce more hydrogen bonding with the guest. This can be accomplished by having the anion interact with the NH₂ and amide groups (Figure 5.1).

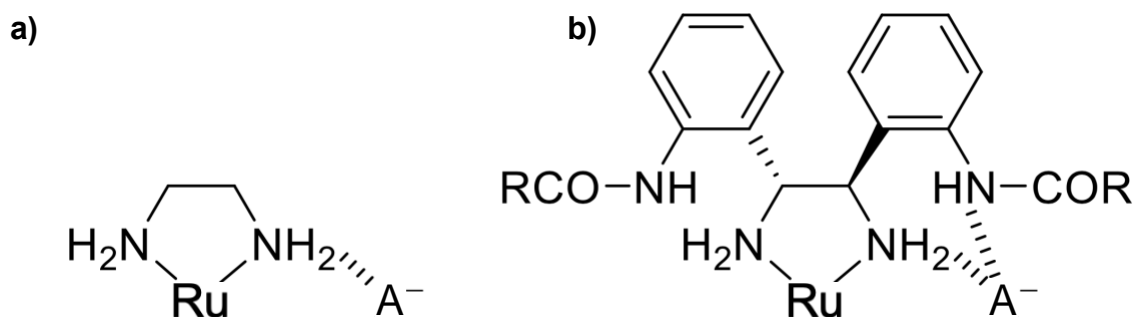


Figure 5.1. Diagram of hydrogen bonding between the anionic guest, A⁻, and the aminyl ruthenium hosts. a) Association between A⁻ and ethylenediamine, b) Amide-substituted (*R,R*)-1,2-diphenylethylenediamine ligand interacting with A⁻.

According to literature, the [Ru(bpy)(dpen)₂](PF₆)₂ complex has not been synthesized. In order to expand this host system, the [Ru(bpy)(dpen)₂](PF₆)₂ host's redox properties need to be examined. This must be accomplished so that the benefits of the substituted dpen structures can be observed by comparing the experimental results with [Ru(bpy)(dpen)₂](PF₆)₂.

Another way to attract anions using hydrogen bond donors is through OH \cdots A⁻ interactions. For example, in the crystal structure of ruthenium(II) dimethylgloxime (dmgH₂) dichloride, [Ru(dmgh₂)₃]Cl₂, (Figure 5.2) the oxime OH groups interact with chloride ions (Figure 5.3).⁴⁵

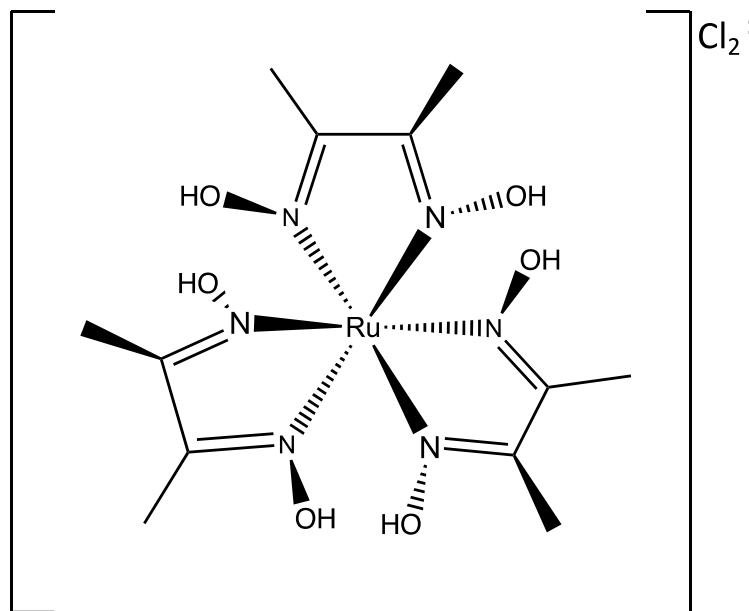


Figure 5.2. Chemical diagram of [Ru(dmgh₂)₃]Cl₂.

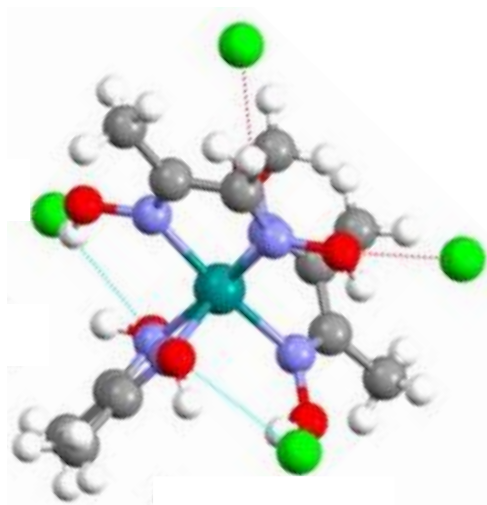


Figure 5.3. Crystallography of the interaction of Cl⁻ guest ions (green) with the O...H bonds of the [Ru(dmgh₂)₃]²⁺ host viewed down the c-axis.⁴⁵

We studied this complex as a host because of the stabilization, potential electrostatic effects from oxidation, and the near proximity of the OH groups can promote better anion interaction. The weak intermolecular H bonding between the OH groups and Cl⁻ stabilizes the structure. The greater positive charge on the complex through oxidation is also capable of attracting anion guests.

Another advantage of studying this framework as a host is that the OH groups are close to the metal center and can get the anions to bind to the host using a second coordination sphere.

5.2. Results and Discussion

5.2.1. [Ru(bpy)(dpen)₂](PF₆)₂ Host

As mentioned, the [Ru(bpy)(dpen)₂](PF₆)₂ complex was synthesized in order to be able to enhance the tunability of the [Ru(bpy)(en)₂](PF₆)₂ system. This structure has potential for substituents to be attached to the phenyl rings to increase guest sensitivity that the en host cannot accomplish. The electrochemistry was executed using cyclic voltammetry (CV), as in the previous chapters. In the first study, the [Ru(bpy)(dpen)₂](PF₆)₂ complex was separated using a column as what was described in the [Ru(bpy)(en)₂](PF₆)₂ synthesis.⁴³ However, isolating the pure compound has been challenging using this method.

Because we had difficulty in separating the host using column chromatography, we decided to execute thin-layer chromatography (TLC), but with the crude [Ru(bpy)(dpen)₂]Cl₂ instead. This form of chromatography is known to create better separation between the two bands.¹⁰⁰ This time, a small pink band appeared, which is reminiscent of what was discovered to be [Ru(bpy)(en)₂](PF₆)₂ in its chromatography. Afterwards, the host was converted to a PF₆ salt. Mass spectrometry and ¹H NMR have displayed that it is the correct host complex. Figure 5.5 and Table 5.1 shows the electrochemical properties of [Ru(bpy)(dpen)₂](PF₆)₂. This analysis was determined using CV in an acidic solution. Due to a small amount of product available, the CV was measured with a minimal amount of host present.

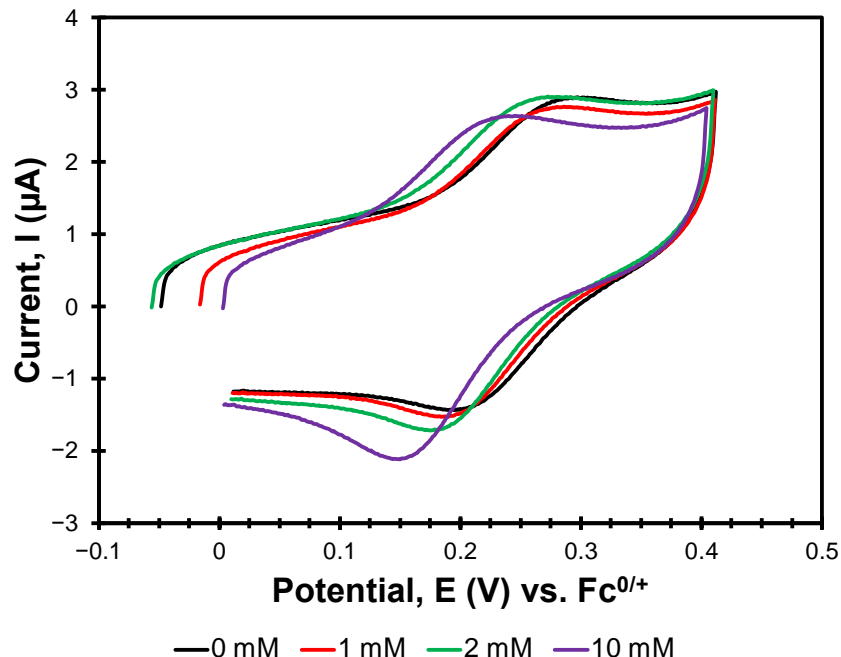


Figure 5.5. CV of $[\text{Ru}(\text{bpy})(\text{dpen})_2](\text{PF}_6)_2$ with the addition of BTAC (CH_3CN with 5% 0.1 M HNO_3 , 0.1 M TBAPF_6 , 0.1 V s^{-1}). The data were measured using an Ag/AgCl reference electrode, glassy carbon working electrode, but plotted vs. $\text{Fc}^{+/0}$ reference redox couple, which has $E_{1/2} = 0.388 \text{ V}$ vs. Ag/AgCl under these conditions.

Table 5.1. Electrochemical parameters in volts (V vs. $\text{Fc}^{+/0}$) of 0.3 mM $[\text{Ru}(\text{bpy})(\text{dpen})_2](\text{PF}_6)_2$ in CH_3CN with 5% 0.1 M HNO_3 with added BTAC, 0.1 V s^{-1} .

[BTAC]	E_{pa}	E_{pc}	ΔE_{p}	$E_{1/2}$
0 mM	0.297	0.195	0.102	0.246
1 mM	0.286	0.184	0.102	0.235
2 mM	0.273	0.175	0.098	0.224
10 mM	0.240	0.150	0.090	0.195

A small voltammogram is displayed, representing the $[\text{Ru}(\text{bpy})(\text{dpen})_2](\text{PF}_6)_2$ complex. Its redox potential (0.246 V vs. $\text{Fc}^{+/0}$) is near that of the $[\text{Ru}(\text{bpy})(\text{en})_2](\text{PF}_6)_2$ host mentioned in Chapter 4 (0.215 V vs. $\text{Fc}^{+/0}$). This makes it a reasonable $E_{1/2}$ of the host. We elected to study how the Cl^- guest is able to bind with the host throughout redox. In comparison to $[\text{Ru}(\text{bpy})(\text{en})_2](\text{PF}_6)_2$, the $\Delta E_{1/2}$ of this host is smaller. This may be due to the NH_2 groups in dpen being more electron-rich than those in en, due to the phenyl substituents. At the addition of 100 mM BTAC, the electrochemical solution turns turbid. However, it behaves well with added guest up to higher guest

concentrations than $[\text{Ru}(\text{bpy})(\text{en})_2](\text{PF}_6)_2$ (see Chapter 4). This suggests that modified dpen ligands could be useful in future host-guest studies (see Figure 5.1(b)).

As mentioned in the previous chapters, the number of more bound cations in the oxidized state was determined using Nernstian calculations (Figure 5.6). This figure shows that with a slope of -0.0415 , some of the new $[\text{Ru}(\text{bpy})(\text{dpen})_2](\text{PF}_6)_2$ host can bind to one more Cl^- ion when oxidized to Ru^{3+} .

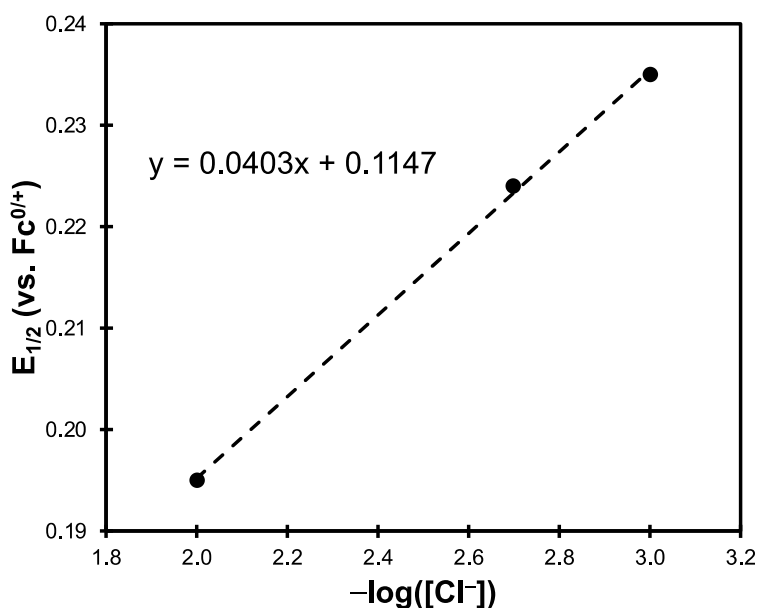


Figure 5.6. $E_{1/2}$ (vs. $\text{Fc}^{0/+}$) vs. $-\log([\text{Cl}^-])$ of 1 mM $[\text{Ru}(\text{bpy})(\text{dpen})_2]\text{Cl}_2$.

5.2.2. $[\text{Ru}(\text{dmgH}_2)_3](\text{PF}_6)_2$ Host

The redox properties of this host are unknown. In order to see how the electrostatic effects can increase the affinity of the chloride guest, we intend to oxidize the ruthenium(II) center to III. We tried to accomplish this using CV, but this complex appears to be unable to perform oxidation in our potential window. Instead, reduction of Ru^{II} to Ru^{I} is detected (Figure 5.7).

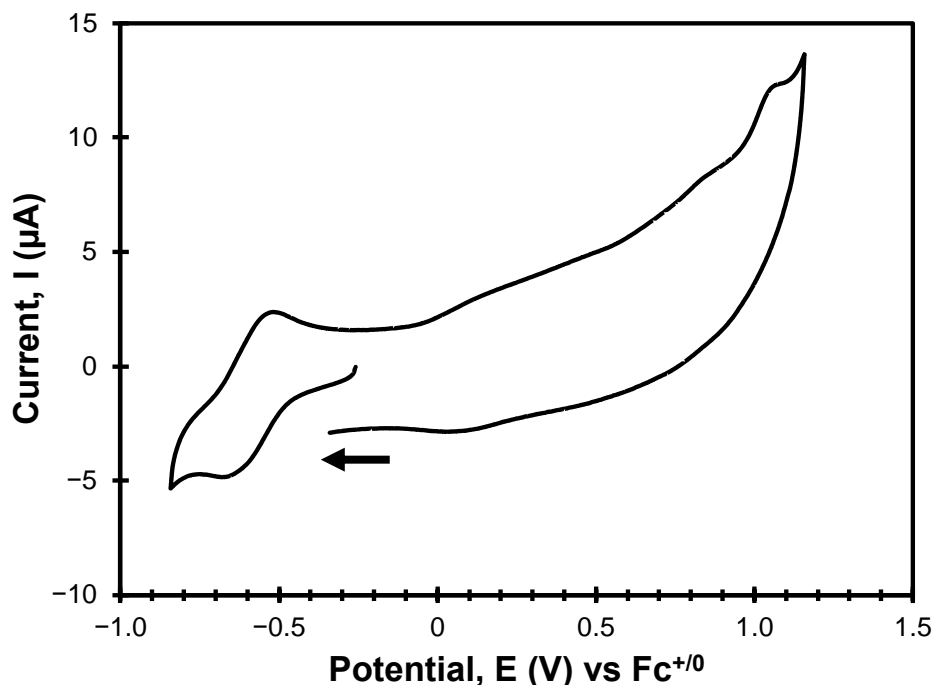


Figure 5.7. CV of $[\text{Ru}(\text{dmgH}_2)_3](\text{PF}_6)_2$ (CH_3CN , 0.1 M TBAPF_6 , 0.1 V s^{-1}). The data were measured using an Ag/AgCl reference electrode, glassy carbon working electrode, but plotted vs. $\text{Fc}^{+/0}$ reference redox couple, which has $E_{1/2} = 0.445 \text{ V vs. Ag}/\text{AgCl}$ under these conditions.

Although the host-guest interaction cannot be analyzed by comparing the binding affinity between 2+ and 3+ states, we can still monitor how well the 2+ starting material associates with Cl^- in correlation to the 1+ form. Figure 5.8 displays the chloride guest association of the 2+ host in comparison to the 1+ complex. Table 5.2 shows how much host's redox potential changes due to chloride guest association.

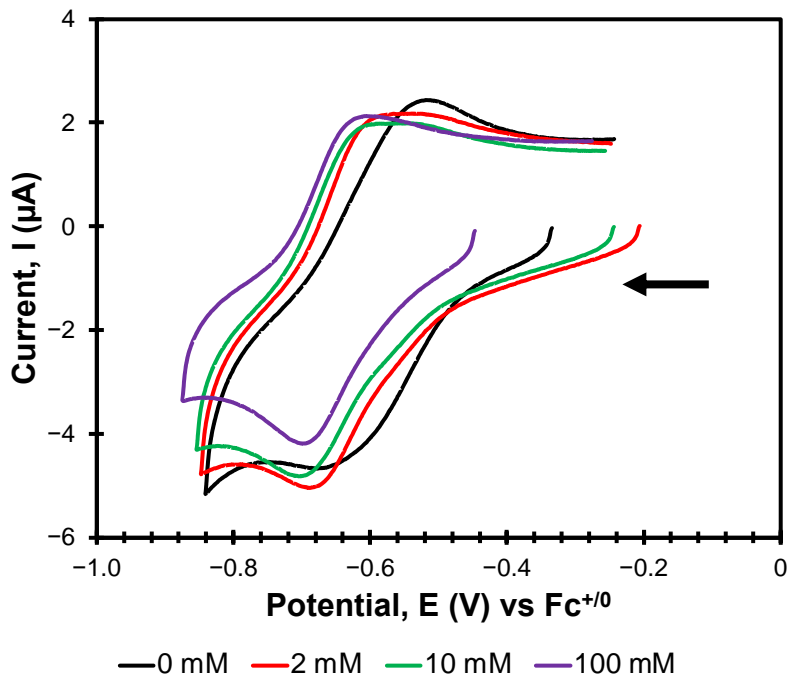


Figure 5.8. CV of $[\text{Ru}(\text{dmgH}_2)_3](\text{PF}_6)_2$ with BTAC added (CH_3CN , 0.1 M TBAPF_6 , 0.1 V s^{-1}).

Table 5.2. Electrochemical parameters in volts (V vs. $\text{Fc}^{+/0}$) of $1 \text{ mM } [\text{Ru}(\text{dmgH}_2)_3](\text{PF}_6)_2$ in CH_3CN with added BTAC, 0.1 V s^{-1} .

[BTAC]	E_{pa}	E_{pc}	ΔE_{p}	$E_{1/2}$
0 mM	-0.510	-0.675	0.165	-0.593
2 mM	-0.537	-0.693	0.156	-0.615
10 mM	-0.582	-0.703	0.121	-0.643
100 mM	-0.609	-0.701	0.092	-0.655

This structure displays quasi-reversible behavior at a redox potential of -0.593 V (black trace). The anodic peak back to the $2+$ state is more pronounced than the cathodic peak, which appears to be broadened out. The $E_{1/2}$ of the host begins to shift more negatively as Cl^- is added, signaling that more guest is binding in the $2+$ state than $1+$. What is also noticed is that the voltammogram of the host becomes more reversible as BTAC is added. This is likely because the complex is more stabilized when interacting with chloride. After the addition of $100 \text{ mM } \text{Cl}^-$ (purple trace), the voltammogram is reversible. The $\Delta E_{1/2}$ is -62 mV , suggesting that the chloride is able to be released in the $1+$ state and bind back to the host when oxidized to $2+$.

Afterwards, Nernstian measurements were done to determine the number of more bound anions in the 2+ than the 1+ structure (Figure 5.9). Due to the lack in the reversibility in the host's redox potential, the E_{pa} was measured to determine the number of bound anions.

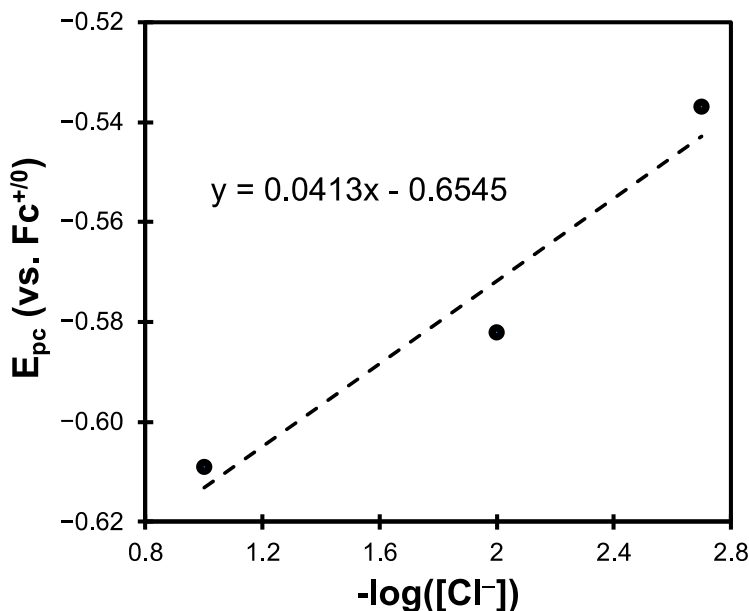


Figure 5.9. $E_{1/2}$ (vs. $Fc^{+/0}$) vs. $-\log([Cl^-])$ of 1 mM $[Ru(dmgh_2)_3](PF_6)_2$.

The slope of the E_{pa} for each $-\log([Cl^-])$ unit for the overall experiment displays a slope of -0.0413 , which means that most of the host in the starting state is able to bind to one more guest than the reduced state. The slope suggests that some of the host is able to bind and release Cl^- for this system. This figure shows that with a slope of -0.0415 , some of the new $[Ru(dmgh_2)_2](PF_6)_2$ host can bind to one more Cl^- ion when oxidized to Ru^{3+} .

Chapters 4 and 5 display that we can utilize redox to manipulate the host-guest binding between supramolecular complexes and anions. This is displayed in the negative shift of $E_{1/2}$ of the host and the Nernstian calculations.

5.3. Experimental

5.3.1. General

Commercially available reagents were purchased from Pressure Chemicals, Combi-Blocks, Alfa Aesar, BeanTown Chemicals, Sigma-Aldrich, VWR Chemicals, AmBeed, and J.T. Baker were used without further purification. Dimethylgloxime (dmgH₂) was purified using the method from Merritt and co-workers.¹⁰¹ Electrospray ionization mass spectra (ESI-MS) were measured using the Agilent 6230 instrument. UV/vis spectrometry was implemented with an Aviv 14DS spectrometer. ¹H NMR experiments were performed with a Bruker AVIII 400 MHz spectrometer in CD₃CN. [Ru(dmgH₂)₃](PF₆)₂ was characterized by ¹H NMR analysis, where the downfield shifts of the ligands from complexation were in comparison to Ni, Zn, and Pd dimethylgloxime complexes.¹⁰²

Cyclic voltammetry of the ruthenium complexes was studied using an EC Epsilon Eclipse potentiostat/galvanostat with Pt wire counter electrode, glassy carbon working electrode, and Ag/AgCl reference electrode. Most cyclic voltammetry experiments were done using 1 mM Ru hosts in a 0.1 M tetrabutylammonium hexafluorophosphate (TBAPF₆) acetonitrile electrolyte solution with 5% 0.1 M HNO₃ added. The [Ru(dmgH₂)₃](PF₆)₂ experiment was executed without the acidic solution. All scans were performed at 0.1 V s⁻¹, unless stated otherwise. Additions of Cl⁻ or TBAHSO₄ were accomplished throughout the experimentations.

5.3.2. Synthesis of [Ru(bpy)(dpen)₂](PF₆)₂

[Ru(bpy)(dpen)₂](PF₆)₂ was synthesized using the same procedure for [Ru(bpy)(en)₂](PF₆)₂, using a Ru:dpen mole ratio of 1:10, like that of Ru:en.¹⁰¹ The NH₄PF₆ step in the literature procedure was not done. Instead of the column chromatography mentioned in the literature, alumina thin-layered chromatography with 2% MeOH was performed and the complex

was collected as a pink band. The product was extracted from the alumina using an acidic aqueous solution. Then, the complex was extracted as a PF₆ salt using KPF₆ (aq) solution and DCM (yield 19 – 31%). ESI-MS crude (Figure 5.10): m/z [(Ru(bpy)(dpen)₂) + 2H]²⁺ 341.1178 (calcd: 341.1179) ESI-MS purified complex (Figure 5.11): m/z [(Ru(bpy)(dpen)₂) – 2H]²⁺ 339.1043 (calcd: 339.1020). ¹H NMR (CD₃CN): 2.24 (s, 4H), 3.18 (m, 9H), 4.21 (m, 3H), 4.34 (s, 3H), 7.06 (d, 3H), 7.32 (m, 6H), 7.52 (m, 6H), 7.62 (m, 3H), 7.73 (m, 3H).

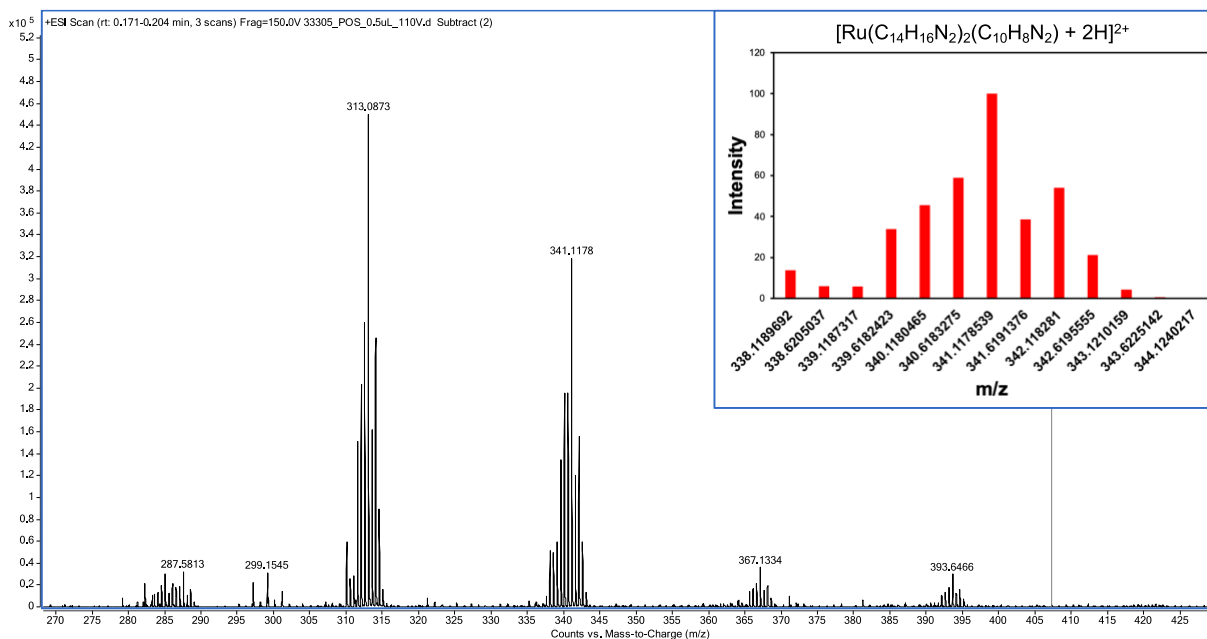


Figure 5.10. ESI mass spectra of [(Ru(bpy)(dpen)₂)]²⁺, m/z 341.1178 (calcd: 341.1178). Inset display calculated relative intensities.

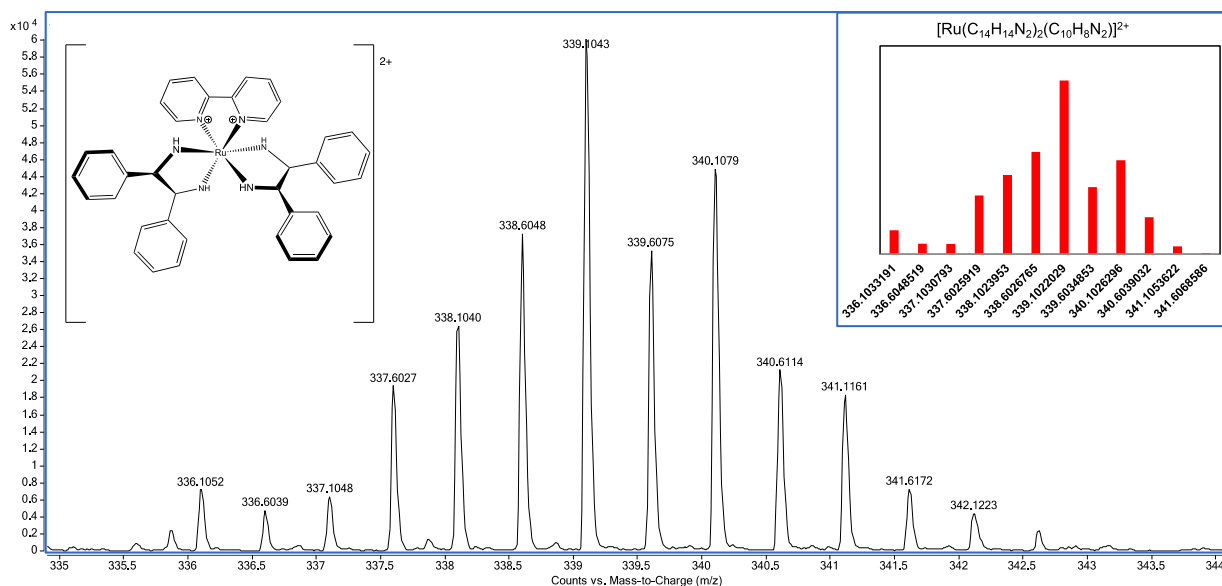


Figure 5.11. ESI mass spectra of $[(Ru(bpy)(dppe))_2]^{2+}$, m/z 339.1043 (calcd: 339.1020). Inset display calculated relative intensities.

5.3.3. Synthesis of $[Ru(dmgh_2)_3](PF_6)_2$

The literature procedure for this complex involved a simple reflux of $Ru^{II}(dmsO)_4Cl_2$ with $dmgh_2$ in methanol under an inert environment.⁴⁵ However, this reaction did not produce the host complex and instead yielded unknown orange material. $[Ru(dmgh_2)_3](PF_6)_2$ was synthesized using a modified ruthenium blue technique. A mixture of ethanol and water (4:1) was degassed with N_2 . Then, $RuCl_3 \cdot xH_2O$ (0.5 g, 2.4 mmol) was added immediately and refluxed for 4 – 5 hr until the solution turned blue. While still being refluxed, Dimethylglyoxime, $dmgh_2$ (0.9 g, 7.7 mmol) was added in excess and refluxed for 2 hr. The normal next step for the Ru blue method is to add $KHCO_3$, but that was not done because the $dmgh_2$ ligand does not need to be deprotonated to coordinate. Afterwards, the reaction mixture was allowed to cool to room temperature and filtered. Black solid was collected in the filter. The precipitate was washed with DMF into a separate flask, the product was collected in the filtrate. Silica column chromatography was executed using methanol as the eluent. Dark brown solid was received through evaporation. The product was dissolved in the smallest amount of acetone, then a red solid was precipitated out with

diethyl ether. The precipitate was washed with KPF_6 and extracted using DCM (yield 7%). ESI-MS (Figure 5.12): m/z $[\text{Ru}(\text{dmgH}_2)_3]^{2+}$ 449.0709 (calcd: 449.0726), ^1H NMR (400 MHz, CD_3CN , ppm): 2.29 (s, 18H), 3.63 (s, 6H).

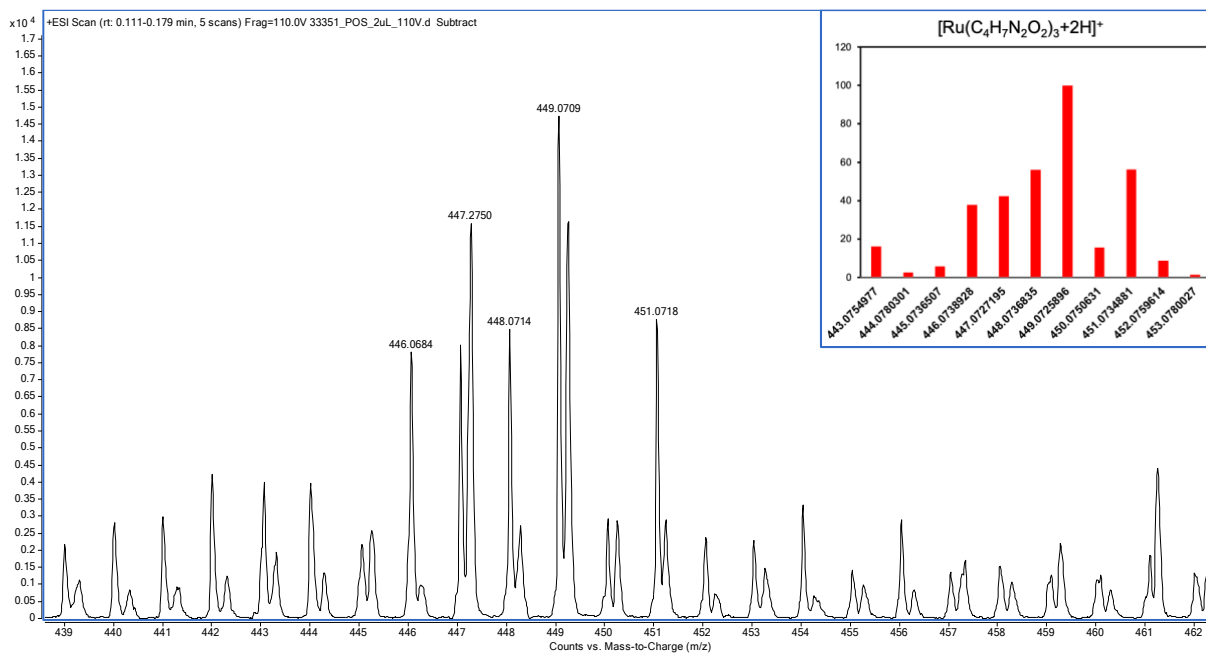


Figure 5.12. ESI mass spectra of $[\text{Ru}(\text{dmgH}_2)_3]^{2+}$, m/z 449.0709 (calcd: 449.0726). Inset displays calculated m/z values and relative intensities.

Chapter 6. Conclusions

The integral target of this dissertation is to propose tunable host-guest chemistry using redox reactions. This is demonstrated in Chapters 2 – 5 of various host-guest systems that were able to bind and release guest ions or molecules using redox. However, in Chapters 2 and 5, the importance of the host's redox properties is displayed as well. The host systems discussed in Chapters 3 – 5 have promising aspects that can be utilized in future applications.

In Chapter 3, the ruthenium β -diketonates are able to bind to alkali ions through reduction of the host. This guest binding was observed with the positive change in $E_{1/2}$ and UV-vis data. This was visibly seen in the crystal structure of the reduced $[\text{Ru}(\text{dbm}-2\text{OMe})_3]^-$ interacting with two Na^+ ions. Our work ultimately displays how modifying the substituents of the host can increase the binding constant with its guest.

Other techniques that can be executed with this host system is attaching other activating groups on the phenyl rings, such as amines and hydroxy groups. These substituents can inductively increase the affinity of the host to cations. Another method of constructing new hosts for cationic binding is through the use of 2'-methoxyethoxy substituents to the ring.¹⁰³ This introduces one more O atom for each cation to bind than the 2'-methoxy host, which can be effective in interacting with guests at low concentrations.

Chapters 4 and 5 demonstrated that the approach used in Chapter 3 can be implemented with anionic guests. The $[\text{Ru}(\text{bpy})(\text{en})_2](\text{PF}_6)_2$ and $[\text{Ru}(\text{pypz})_3](\text{PF}_6)_2$ hosts exhibit good redox properties and that advantage aided in accomplishing controlled host-guest chemistry using redox. The TPPO experiments show that this procedure can be studied with neutral guest molecules. $[\text{Ru}(\text{bpy})(\text{dpen})_2](\text{PF}_6)_2$ also shows encouraging results in its ability to remain stable in the

presence of high guest concentration. This finding was not exhibited in the analysis with the $[\text{Ru}(\text{bpy})(\text{en})_2](\text{PF}_6)_2$ host.

Likewise with the Ru β -diketonates, these hosts can be used as host systems to create frameworks that have greater sensitivity to a particular guest. The $[\text{Ru}(\text{pypz})_3](\text{PF}_6)_2$ host can be functionalized by attaching substituents on the pyrazole to increase hydrogen binding to guests. $[\text{Ru}(\text{bpy})(\text{en})_2](\text{PF}_6)_2$ can be improved by using the dpen structure. The stability of $\text{Ru}(\text{bpy})(\text{dpen})_2(\text{PF}_6)_2$ prompts the conception that this host can be tuned by composing new structures that can associate with guests. This host has phenyl groups that can be modified with amide or OH groups to enhance anion binding.

The host-guest systems we have selected are simple to observe and can be evaluated in real-time measurements. Tuning the ligands of these structures is a promising method in advancing the association of the host and guest. In the future, scientists can construct new supramolecular complexes that have great affinity for guests and utilize redox chemistry to manipulate their interactions.

Appendix A. X-ray Crystallography and Structure Refinement

Table A1. Crystallographic Data and Structure Refinement Parameters for Ru complexes in Chapter 3.

Empirical formula	C ₄₅ H ₃₃ O ₆ Ru	C ₅₁ H ₄₅ O ₁₂ Ru
Formula Weight	770.78	950.94
Temperature	150 K	90.0(5) K
Wavelength	0.71073 Å	0.71073 Å
Crystal system	Monoclinic	Triclinic
Space Group	<i>P</i> 2 ₁ / <i>c</i>	<i>P</i> -1
Unit cell dimensions	a = 16.9929(6) Å b = 9.7251(4) Å c = 21.4202(9) Å α = β = 90.000° γ = 92.597(2)	a = 12.1893(13) Å b = 18.4266(17) Å c = 19.728(2) Å α = 102.479(4)° β = 91.980(4)° γ = 90.146(4)°
Volume	3536.2(2)	4323.6(8)
Z	4	4
F(000)	1580	1964
Theta	2.30 to 33.10	2.26 to 21.27
Index Ranges	-26 ≤ h ≤ 26, -14 ≤ k ≤ 14, -32 ≤ l ≤ 32	-16 ≤ h ≤ 16, -24 ≤ k ≤ 24, -26 ≤ l ≤ 26
Reflections	13494	21733
Independent Reflections	9784	11175
Completeness to theta	0.999	0.988
Refinement method	SHELXL 2018/3 (Sheldrick, 2015)	SHELXL-2017/1 (Sheldrick, 2017)
Data/restraints/parameters	9784/0/469	11175/0/1165
Goof	1.059	1.045
Final R [I > 2σ(I)]	R1 = 0.0308, wR2 = 0.0781	R1 = 0.0871, wR2 = 0.1611
All R	R1 = 0.0464, wR2 = 0.0894	R1 = 0.1906, wR2 = 0.1957
Largest diff. peak and hole	0.699 and -0.965 e/Å ³	1.888 and -1.358 e/Å ³

Table A2. Crystallographic Data and Structure Refinement Parameters for Ru(dbm-2OMe)₃ and 2 Na⁺ host-guest system in Chapter 3.

Empirical formula	C ₅₁ H ₄₅ ClNa ₂ O ₁₆ Ru, C ₂ H ₃ N
Formula Weight	1137.42
Temperature	100.0(5) K
Wavelength	1.54184 Å
Crystal system	Orthorhombic
Space Group	<i>Pbca</i>
Unit cell dimensions	a = 19.0031(13) Å b = 19.3358(11) Å c = 27.208(2) Å α = β = γ = 90.000°
Volume	9997.4(12)
Z	8
F(000)	4672
Theta	3.249 to 59.009
Index Ranges	-21 ≤ h ≤ 21, -21 ≤ k ≤ 21, -30 ≤ l ≤ 26
Reflections	7175
Independent Reflections	3360
Completeness to theta	0.997
Refinement method	SHELXL-2018/1
Data/restraints/parameters	7175/0/675
GooF	0.985
Final R [I > 2σ(I)]	R1 = 0.0724, wR2 = 0.1558
All R	R1 = 0.1759, wR2 = 0.2108
Largest diff. peak and hole	0.684 and -0.651 e/Å ³

Table A3. Crystallographic Data and Structure Refinement Parameters for Ru complex in Chapter 4.

Empirical formula	C ₁₄ H ₂₆ Cl ₂ N ₆ ORu
Formula Weight	466.38
Temperature	100.0(5) K
Wavelength	0.71073 Å
Crystal system	Monoclinic
Space Group	<i>P n</i>
Unit cell dimensions	a = 8.4870(10) Å b = 8.1191(10) Å c = 14.1496(17) Å α = 90° β = 94.421(2)° γ = 90°
Volume	972.1(2)
Z	2
F(000)	476
Theta	2.51 to 38.56
Index Ranges	-14<=h<=12, -14<=k<=14, -24<=l<=24
Reflections	32727
Independent Reflections	9237
Completeness to theta	0.995
Refinement method	SHELXL-2017/1 (Sheldrick, 2017)
Data/restraints/parameters	9886/3/247
GooF	1.068
Final R [I>2sigma(I)]	R1 = 0.0126, wR2 = 0.0305
All R	R1 = 0.0129, wR2 = 0.0306
Largest diff. peak and hole	0.564 and -0.378 e/Å ³

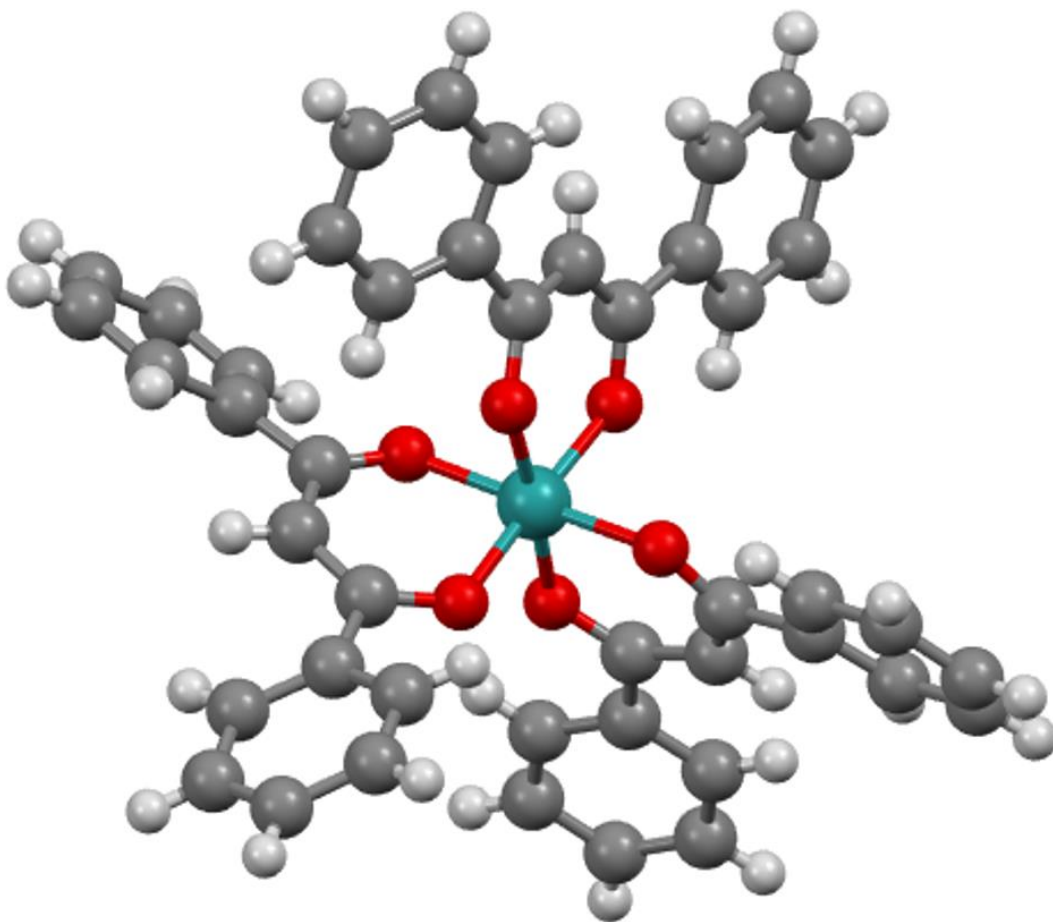


Figure A1. New Ru(dbm)₃ X-ray structure that is isomorphous with Mn, Co, and Cr analogues.

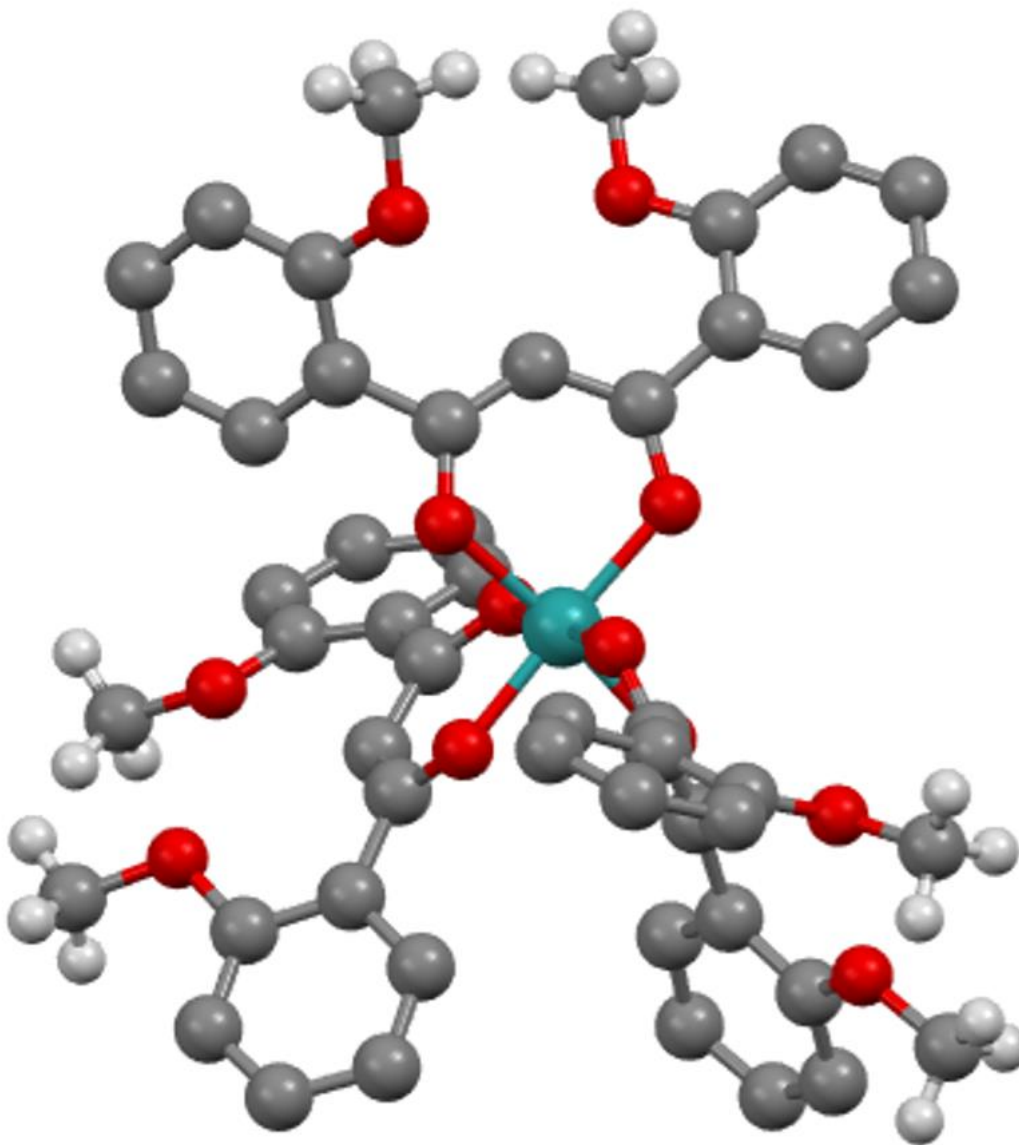


Figure A2. Ru(dbm-2OMe)₃ X-ray structure.

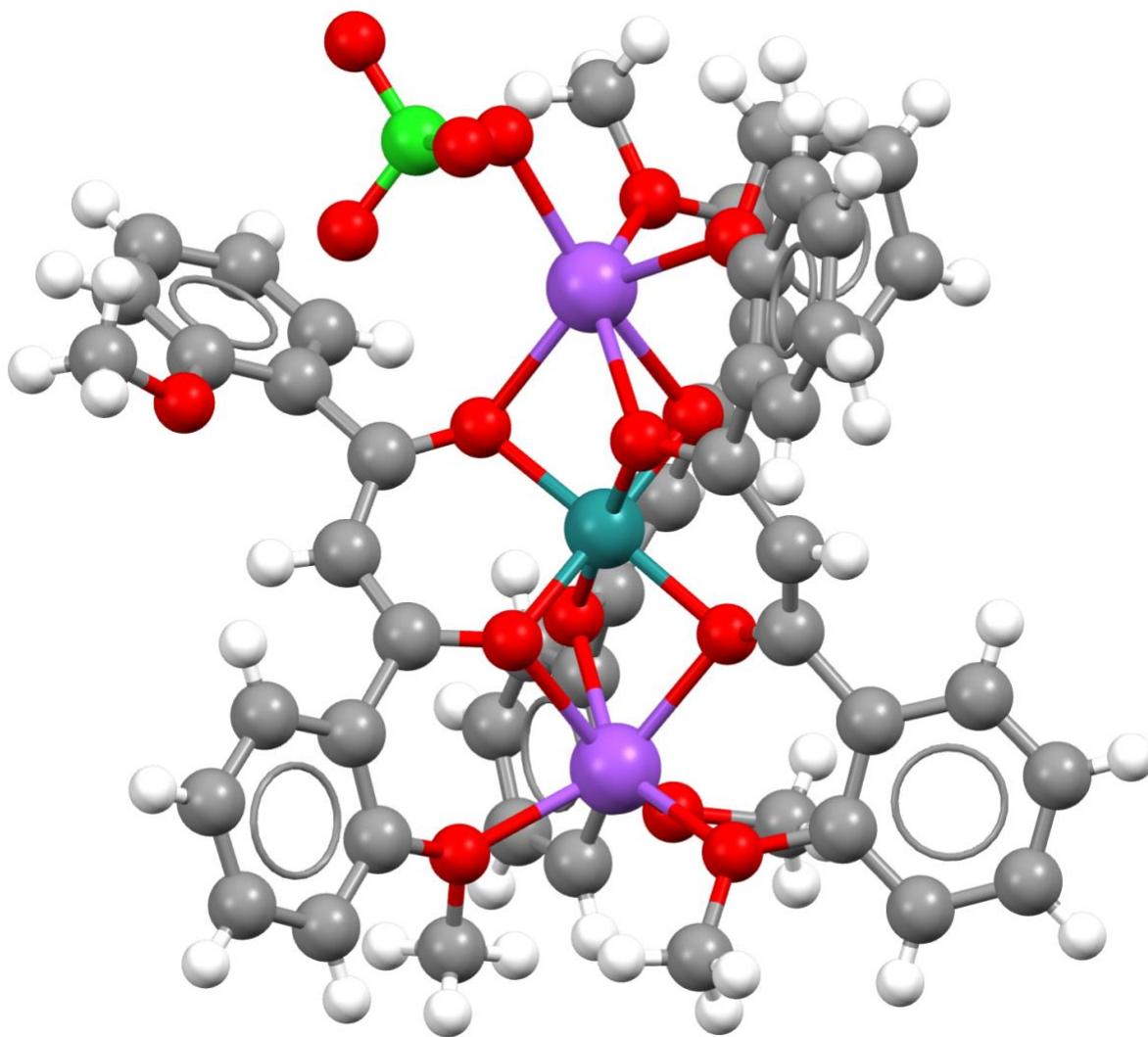


Figure A3. X-ray structure depicting $\text{Na}_2[\text{Ru}(\text{dbm}-2\text{OMe})_3]\text{ClO}_4$ host-guest system. CH_3CN solvent molecule was omitted for clarity.

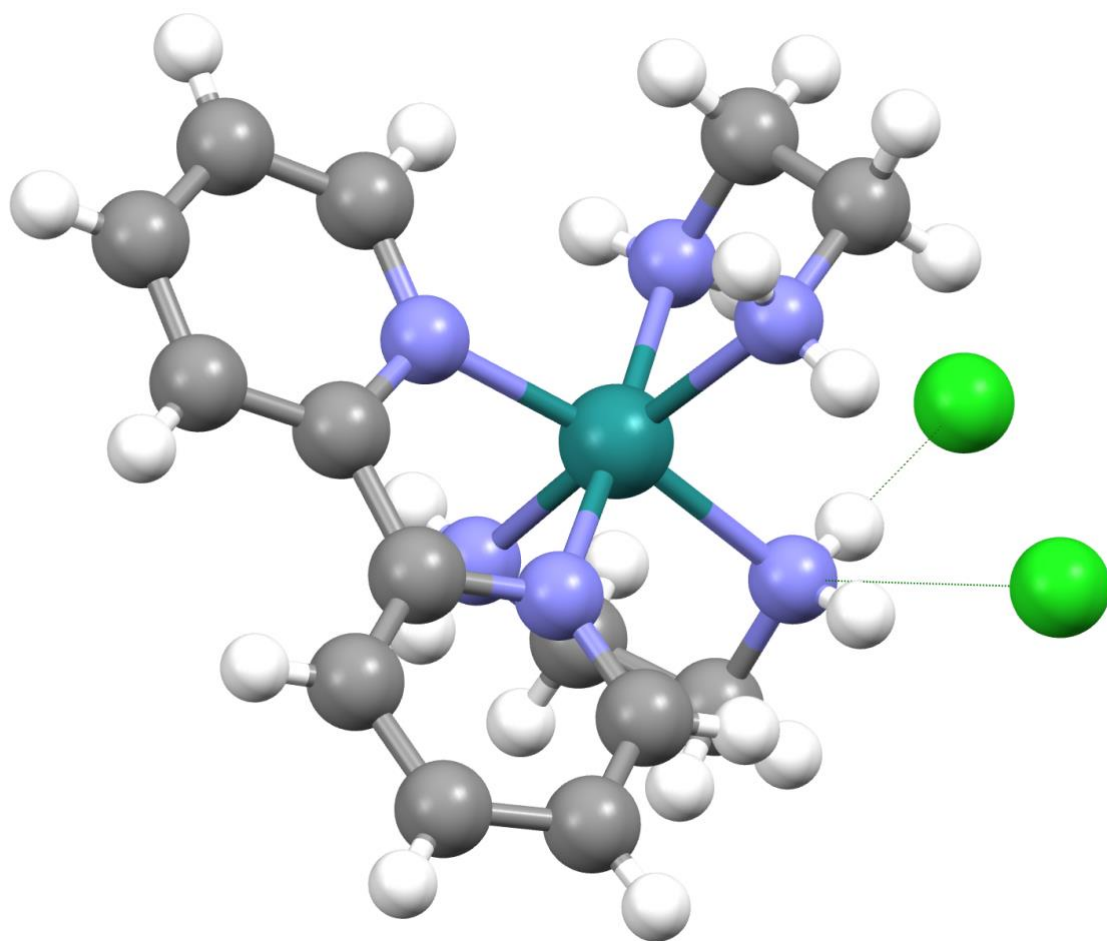


Figure A4. X-ray structure of $[\text{Ru}(\text{bpy})(\text{en})_2](\text{PF}_6)_2$ interacting with Cl^- ions through hydrogen bonding.

Appendix B. Electrochemical and ^1H NMR Analysis of Metal-Organic Hosts with Guests

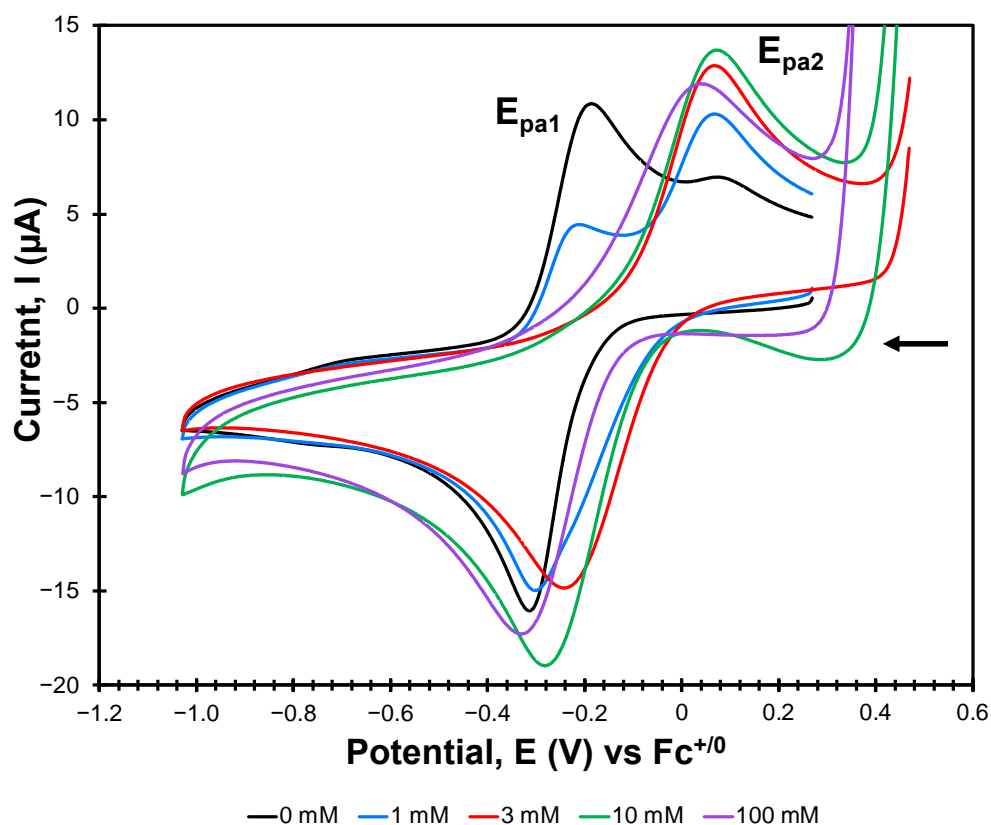


Figure B1. CV of $[\text{Cu}_2(m\text{-xpt})_2\text{Cl}_2](\text{PF}_6)_2$ with the addition of BTAC (DMF, 0.1 M TBAPF₆, 0.1 Vs⁻¹). The data were measured using an Ag/AgCl reference electrode, glassy carbon working electrode, but plotted vs. Fc⁺⁰ reference redox couple, which has $E_{1/2} = 0.541$ V vs. Ag/AgCl under these conditions.

Table B1. Electrochemical parameters in volts (V vs. Fc⁺⁰) of $[\text{Cu}_2(m\text{-xpt})_2\text{Cl}_2](\text{PF}_6)_2$ with added BTAC.

[BTAC]	E_{pa1}	E_{pa2}	E_{pc}	ΔE_p	$E_{1/2}$
0 mM	-0.187	--	-0.314	0.127	-0.251
1 mM	-0.210	0.066	-0.301	0.091	-0.256
3 mM	--	0.069	-0.240	0.309	-0.155
10 mM	--	0.071	-0.281	0.352	-0.176
100 mM	--	0.043	-0.332	0.375	-0.188

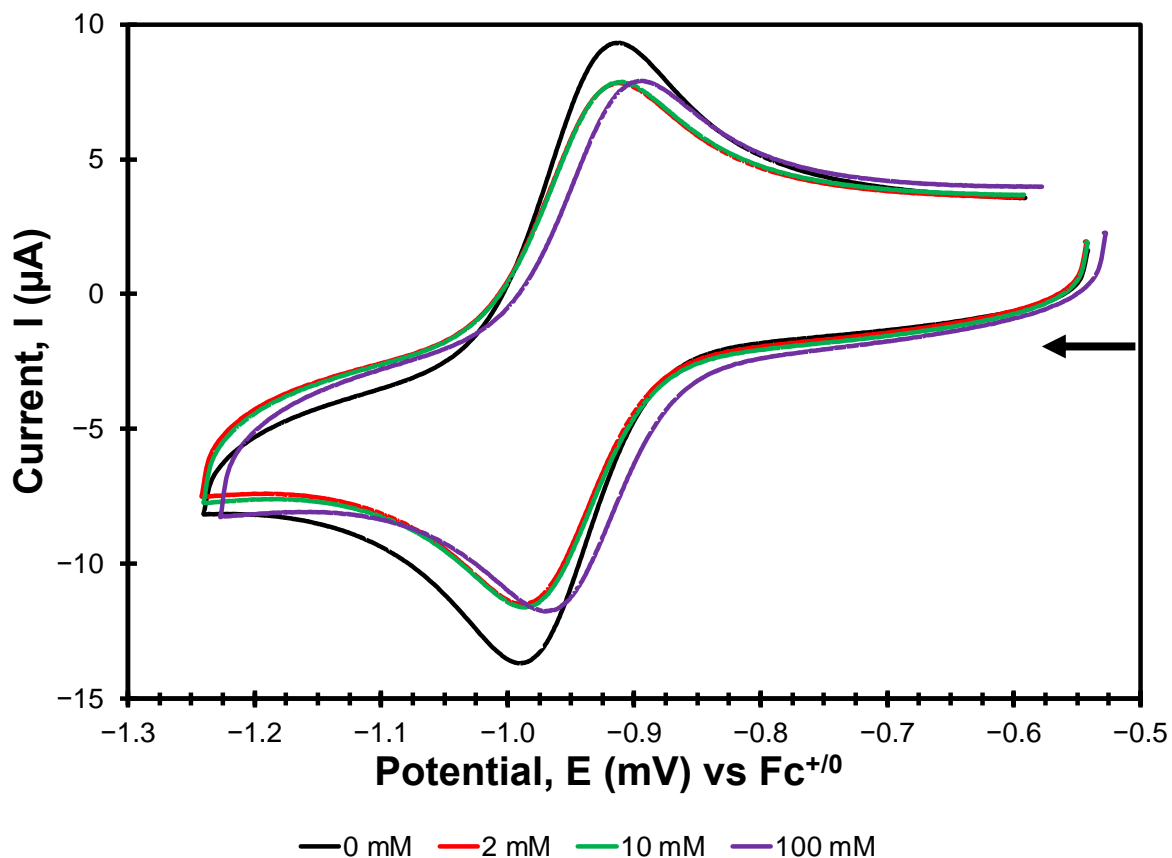


Figure B2. CV of Ru(dbm)₃ with the addition of NaClO₄ (DMF, 0.1 M TBAPF₆, 0.1 V s⁻¹).

Table B2. Electrochemical parameters in volts (V vs. Fc⁺⁰) of Ru(dbm)₃ with added NaClO₄.

[Na ⁺]	E _{pa}	E _{pc}	ΔE _p	E _{1/2}
0 mM	-0.914	-0.989	0.075	-0.952
2 mM	-0.913	-0.987	0.074	-0.950
10 mM	-0.913	-0.985	0.072	-0.949
100 mM	-0.894	-0.975	0.081	-0.935

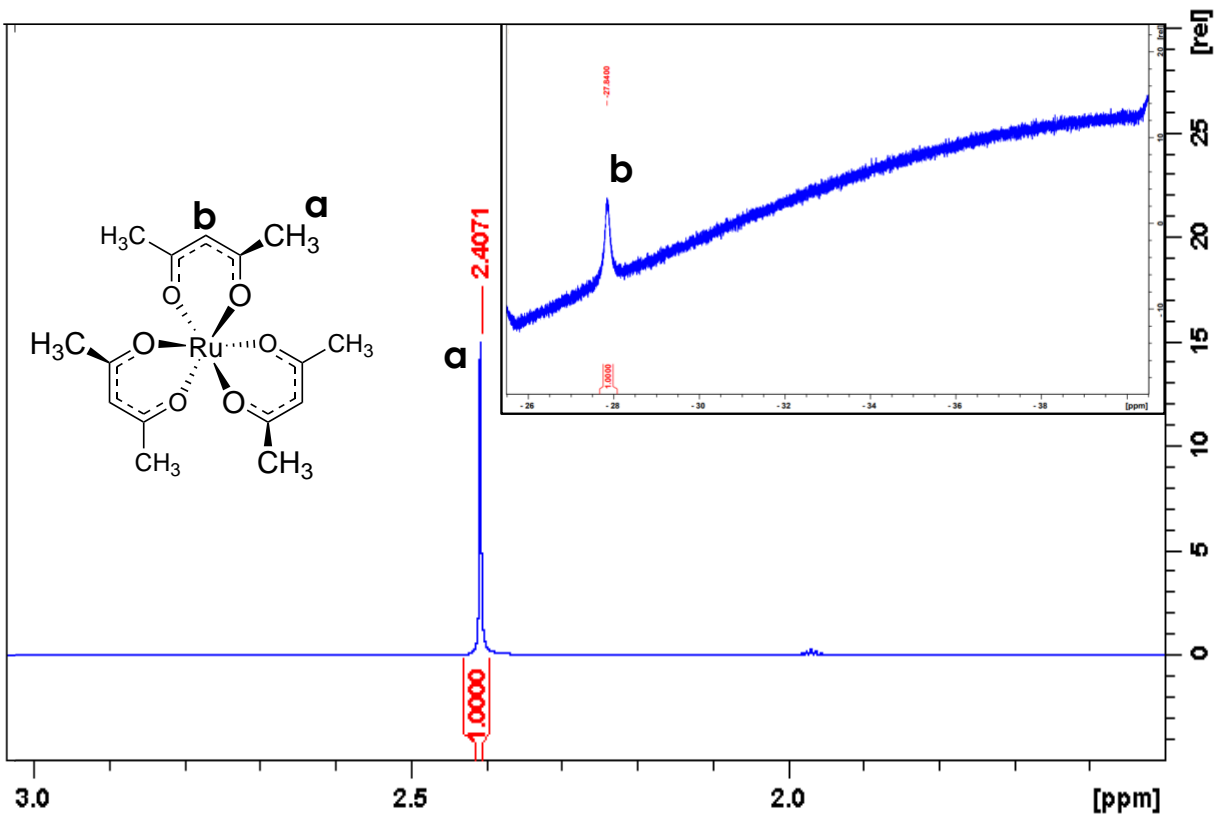


Figure B3. ^1H NMR spectrum of $\text{Ru}^{\text{III}}(\text{acac})_3$ with 100 mM NaClO_4 in CD_3CN .

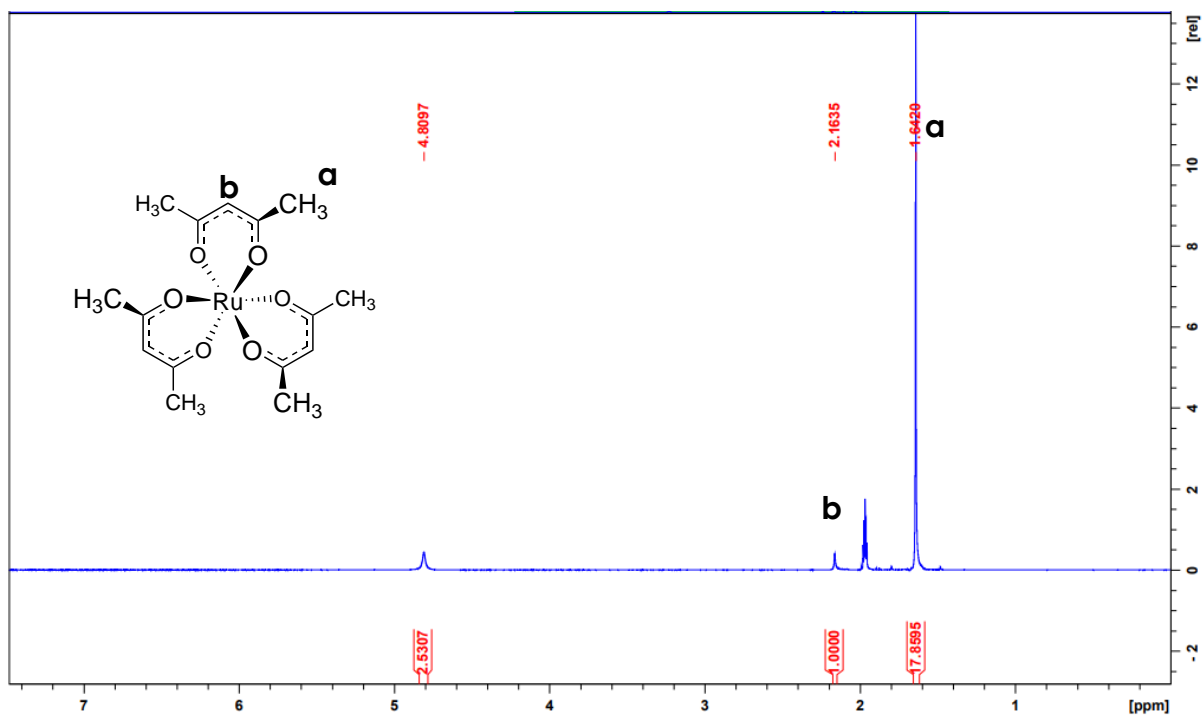


Figure B4. ^1H NMR spectrum of $\text{Ru}^{\text{II}}(\text{acac})_3$ in CD_3CN .

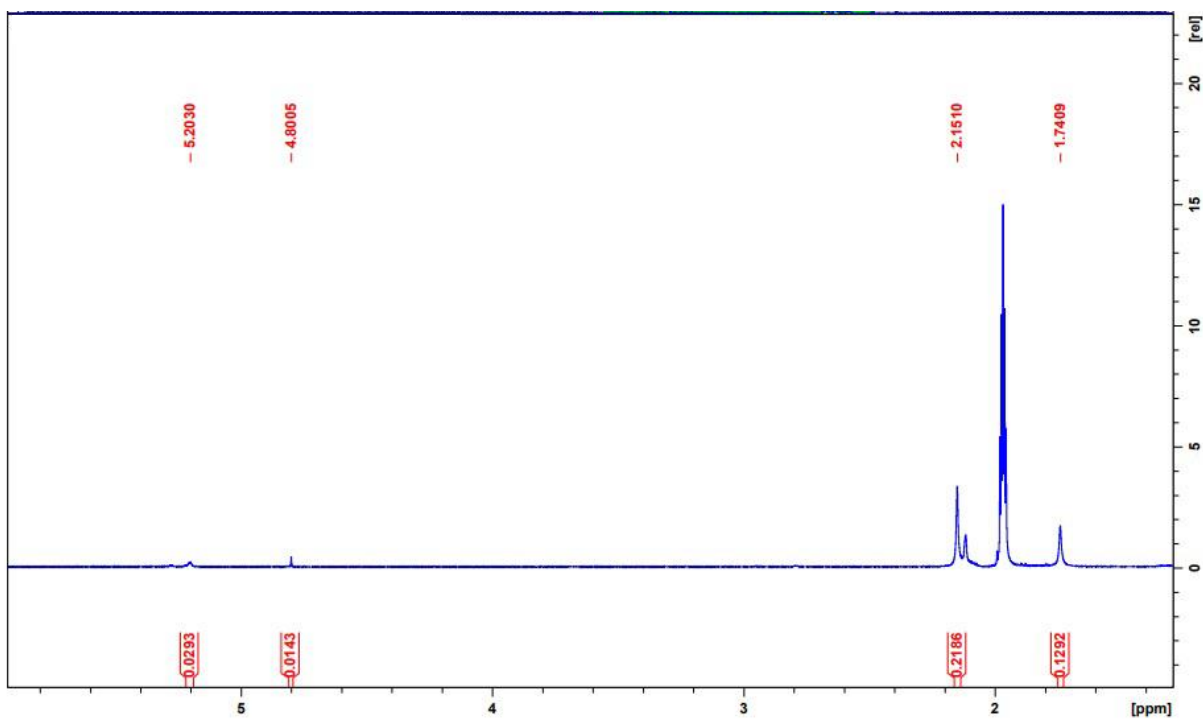


Figure B5. ^1H NMR spectrum of $\text{Ru}^{\text{II}}(\text{acac})_3$ with NaClO_4 in CD_3CN .

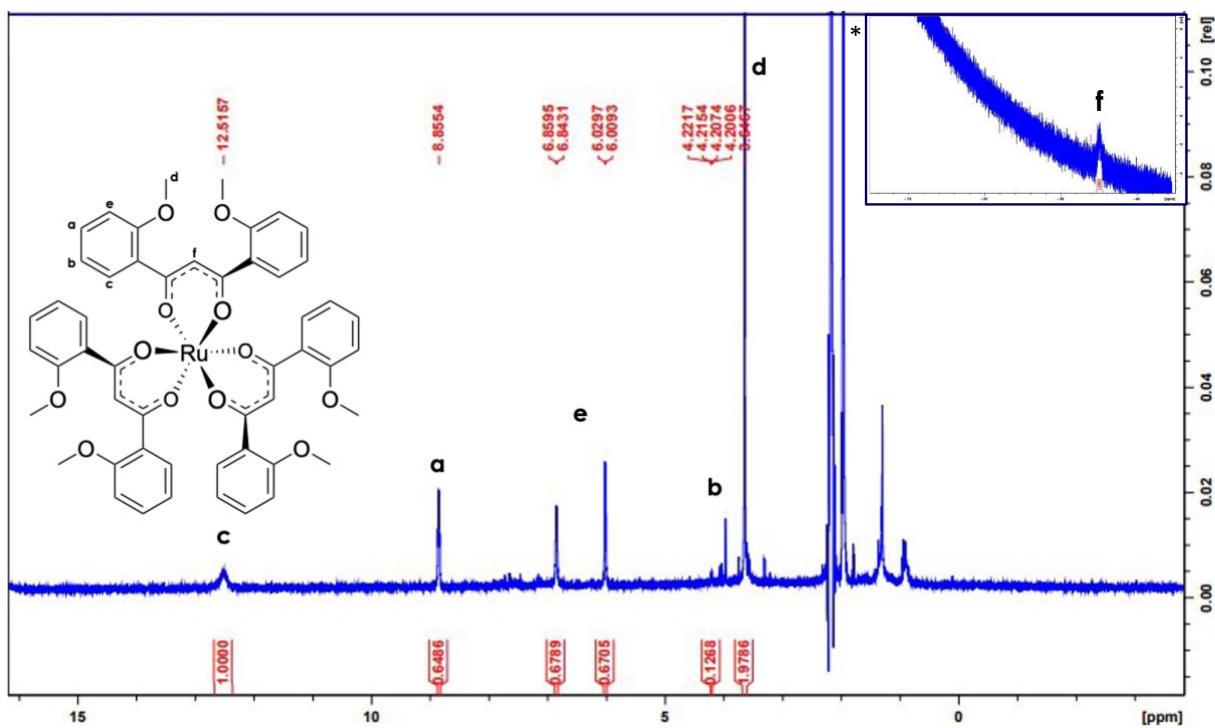


Figure B6. ^1H NMR spectrum of $\text{Ru}^{\text{III}}(\text{dbm-2OMe})_3$ with 100 mM NaClO_4 in CD_3CN .

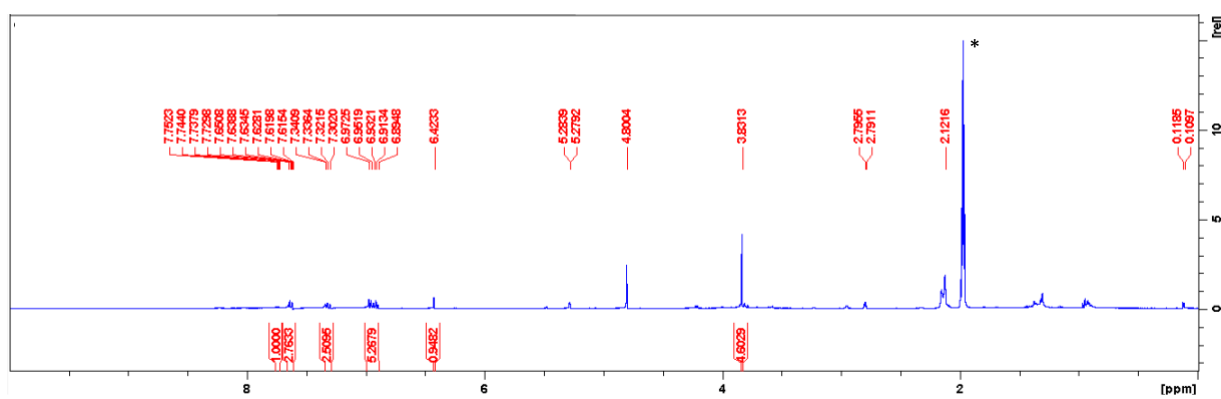


Figure B7. ^1H NMR spectrum of $\text{Ru}^{\text{II}}(\text{dbm-2OMe})_3$ in CD_3CN .

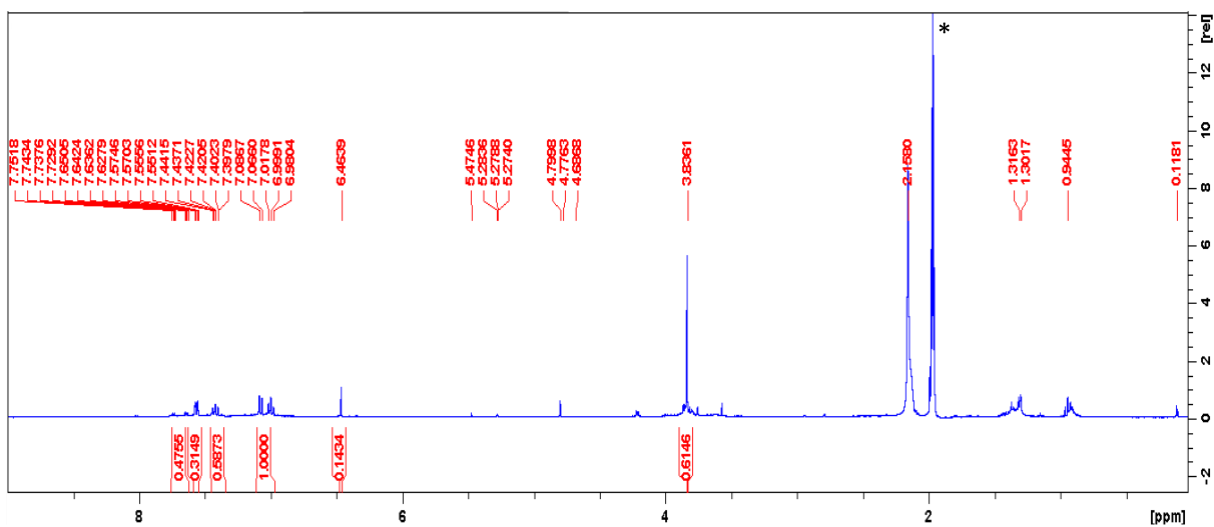


Figure B8. ¹H NMR spectrum of Ru^{II}(dbm-2OMe)₃ with added Na⁺ in CD₃CN.

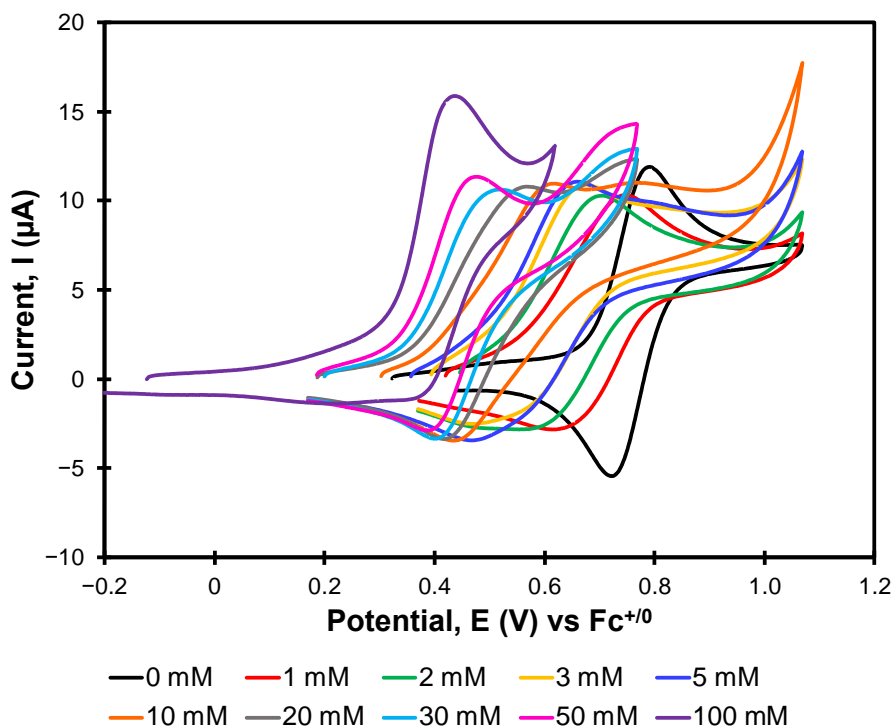


Figure B9. CV of *fac*-[Ru(pypz)₃](PF₆)₂ with the addition of pyridine N-oxide (CH₃CN, 0.1 M TBAPF₆, 0.1 Vs⁻¹). The data were measured using an Ag/AgCl reference electrode, glassy carbon working electrode, but plotted vs. Fc⁺⁰ reference redox couple, which has E_{1/2} = 0.445 V vs. Ag/AgCl under these conditions.

Table B3. Electrochemical parameters in volts (V vs. Fc⁺⁰) of *fac*-[Ru(pypz)₃](PF₆)₂ with added pyridine N-oxide.

[pyridine N-oxide]	E _{pa}	E _{pc}	ΔE _p	E _{1/2}
0 mM	0.790	0.721	0.069	0.756
1 mM	0.745	0.615	0.130	0.680
2 mM	0.706	0.555	0.151	0.631
3 mM	0.676	0.466	0.210	0.571
5 mM	0.661	0.469	0.192	0.565
10 mM	0.616	0.437	0.179	0.527
20 mM	0.567	0.416	0.151	0.492
30 mM	0.521	0.400	0.121	0.461
50 mM	0.475	0.387	0.088	0.431
100 mM	0.436	0.223	0.213	0.330

Appendix C. Permission

Permission for Figures 1.3 printed from *Chemical Communications* 2011, 47 (32), 9149- 9151.



This is a License Agreement between Jasmine Sanford ("User") and Copyright Clearance Center, Inc. ("CCC") on behalf of the Rights holder identified in the order details below. The license consists of the order details, the Marketplace Permissions General Terms and Conditions below, and any Rights holder Terms and Conditions which are included below.

All payments must be made in full to CCC in accordance with the Marketplace Permissions General Terms and Conditions below.

Order Date	20-Sep-2023	Type of Use	Republish in a thesis/dissertation
Order License ID	1398766-1	Publisher	ROYAL SOCIETY OF CHEMISTRY
ISSN	1364-548X	Portion	Image/photo/illustration

LICENSED CONTENT

Publication Title	Chemical communications	Rights holder	Royal Society of Chemistry
Article Title	A single tripodal ligand stabilizing three different oxidation states (II, III, and IV) of manganese.	Publication Type	e-Journal
Author/Editor	Royal Society of Chemistry (Great Britain)	Start Page	9149
Date	01/01/1996	End Page	9151
Language	English	Issue	32
Country	United Kingdom of Great Britain and Northern Ireland	Volume	47

Continued Permission for Figures 1.3 printed from *Chemical Communications* 2011, 47 (32), 9149-9151.

REQUEST DETAILS

Portion Type	Image/photo/illustration	Distribution	United States
Number of Images / Photos / Illustrations	1	Translation	Original language of publication
Format (select all that apply)	Electronic	Copies for the Disabled?	No
Who Will Republish the Content?	Academic institution	Minor Editing Privileges?	No
Duration of Use	Life of current edition	Incidental Promotional Use?	No
Lifetime Unit Quantity	Up to 499	Currency	USD
Rights Requested	Main product		

NEW WORK DETAILS

Title	Controlling Guest Binding to Transition Metal Hosts Via Redox Stimuli	Institution Name	Louisiana State University
		Expected Presentation Date	2023-10-23
Instructor Name	Jasmine Sanford		

9/29/23, 3:11 PM marketplace.copyright.com/rs-ui-web/mp/license/af4b895a-0f2b-49ef-81c3-1677a42783d6/e32aeb65-527e-4fc2-a243-7b6d466e5bf3

ADDITIONAL DETAILS

Order Reference Number	1	The Requesting Person/Organization to Appear on the License	Jasmine Sanford
------------------------	---	---	-----------------

REQUESTED CONTENT DETAILS

Title, Description or Numeric Reference of the Portion(s)	Figure 4	Title of the Article/Chapter the Portion Is From	A single tripodal ligand stabilizing three different oxidation states (II, III, and IV) of manganese.
Editor of Portion(s)	Sunatsuki, Yukinari; Kishima, Yukana; Kobayashi, Tamami; Yamaguchi, Tomoka; Suzuki, Takayoshi; Kojima, Masaaki; Krzystek, J.; Sundberg, Markku R.	Author of Portion(s)	Sunatsuki, Yukinari; Kishima, Yukana; Kobayashi, Tamami; Yamaguchi, Tomoka; Suzuki, Takayoshi; Kojima, Masaaki; Krzystek, J.; Sundberg, Markku R.
Volume / Edition	47	Issue, if Republishing an Article From a Serial	32
Page or Page Range of Portion	9149-9151	Publication Date of Portion	2011-08-27

References

- (1) Wu, C. D.; Lin, W. Heterogeneous Asymmetric Catalysis with Homochiral Metal–Organic Frameworks: Network-Structure-Dependent Catalytic Activity. *Angewandte Chemie International Edition* **2007**, *46* (7), 1075–1078.
- (2) Lee, J.; Farha, O. K.; Roberts, J.; Scheidt, K. A.; Nguyen, S. T.; Hupp, J. T. Metal–Organic Framework Materials as Catalysts. *Chemical Society Reviews* **2009**, *38* (5), 1450–1459.
- (3) Wei, Y.; Kumagai, M.; Takashima, Y.; Asou, M.; Namba, T.; Suzuki, K.; Maekawa, A.; Ohe, S. The Application of an Advanced Ion Exchange Process to Reprocessing Spent Nuclear Fuels, (I) Separation Behavior of Fission Products from Uranium. *Journal of Nuclear Science and Technology* **1998**, *35* (5), 357–364.
- (4) Taylor-Pashow, K. M. L.; Rocca, J. D.; Xie, Z.; Tran, S.; Lin, W. Postsynthetic Modifications of Iron-Carboxylate Nanoscale Metal–Organic Frameworks for Imaging and Drug Delivery. *Journal of the American Chemical Society* **2009**, *131*, 14261–14263.
- (5) Horcajada, P.; Chalati, T.; Serre, C.; Gillet, B.; Sebrie, C.; Baati, T.; Eubank, J. F.; Heurtaux, D.; Clayette, P.; Kreuz, C. Porous Metal–Organic-Framework Nanoscale Carriers as a Potential Platform for Drug Delivery and Imaging. *Nature Materials* **2010**, *9* (2), 172–178.
- (6) Sen, R.; Saha, D.; Koner, S.; Brandão, P.; Lin, Z. Single Crystal to Single Crystal (SC-to-SC) Transformation from a Nonporous to Porous Metal–Organic Framework and Its Application Potential in Gas Adsorption and Suzuki Coupling Reaction through Postmodification. *Chemistry– A European Journal* **2015**, *21* (15), 5962–5971.
- (7) Li, J.-R.; Kuppler, R. J.; Zhou, H.-C. Selective Gas Adsorption and Separation in Metal–Organic Frameworks. *Chemical Society Reviews* **2009**, *38* (5), 1477–1504.
- (8) Bellussi, G.; Carati, A.; Rizzo, C.; Millini, R. New Trends in the Synthesis of Crystalline Microporous Materials. *Catalysis Science & Technology* **2013**, *3*, 833–857.
- (9) Wang, Q.-Q.; Day, V. W.; Bowman-James, K. Chemistry and Structure of a Host–Guest Relationship: The Power of NMR and X-Ray Diffraction in Tandem. *Journal of the American Chemical Society* **2013**, *135* (1), 392–399.
- (10) Darawsheh, M. D.; Barrios, L. A.; Roubeau, O.; Teat, S. J.; Aromí, G. Guest-Tuned Spin Crossover in Flexible Supramolecular Assemblies Templated by a Halide (Cl^- , Br^- or I^-). *Chemical Communications* **2017**, *53* (3), 569–572.
- (11) Liu, Y.; Zhao, W.; Chen, C.-H.; Flood, A. H. Chloride Capture Using a C–H Hydrogen-Bonding Cage. *Science* **2019**, *365* (6449), 159–161.
- (12) Pokharel, U. R.; Fronczek, F. R.; Maverick, A. W. Cyclic Pyridyltriazole–Cu(II) Dimers as Supramolecular Hosts. *Dalton Transactions* **2013**, *42* (39), 14064.

- (13) Chan, A. K.-W.; Lam, W. H.; Tanaka, Y.; Wong, K. M.-C.; Yam, V. W.-W. Multiaddressable Molecular Rectangles with Reversible Host–Guest Interactions: Modulation of pH-Controlled Guest Release and Capture. *Proceedings of the National Academy of Sciences* **2015**, *112* (3), 690–695.
- (14) Wang, R.; Sun, Y.; Zhang, F.; Song, M.; Tian, D.; Li, H. Temperature-Sensitive Artificial Channels through Pillar[5]Arene- Based Host–Guest Interactions. *Angewandte Chemie International Edition* **2017**, *56*, 5294–5298.
- (15) Yang, H.; Yuan, B.; Zhang, X. Supramolecular Chemistry at Interfaces: Host–Guest Interactions for Fabricating Multifunctional Bionterfaces. *Accounts of Chemical Research* **2014**, *47*, 2106–2115.
- (16) Lee, S-F.; Zhu, X-M.; Wang, Y-X. J.; Xuan, S-H.; You, Q.; Chan, W-H.; Wong, C-H.; Wang, F.; Yu, J. C.; Cheng, C. H. K.; Leung, K. C-F. Ultrasound, pH, and Magnetically Responsive Crown-Ether-Coated Core/Shell Nanoparticles as Drug Encapsulation and Release Systems. *ACS Applied Materials and Interfaces* **2013**, *5*, 1566–1574.
- (17) Conn, D. 2.4 Protection from Light Damage. *Northeast Document Conservation Center* **2012**.
- (18) Szalóki, G.; Croué, V.; Carré, V.; Aubriet, F.; Alévêque, O.; Levillain, E.; Allain, M.; Aragó, J.; Ortí, E.; Goeb, S.; Sallé, M. Controlling the Host-Guest Interaction Mode through a Redox Stimulus. *Angewandte Chemie International Edition* **2017**, *56* (51), 16272–16276.
- (19) Sunatsuki, Y.; Kishima, Y.; Kobayashi, T.; Yamaguchi, T.; Suzuki, T.; Kojima, M.; Krzystek, J.; Sundberg, M. R. A Single Tripodal Ligand Stabilizing Three Different Oxidation States (II, III, and IV) of Manganese. *Chemical Communications* **2011**, *47* (32), 9149–9151.
- (20) Stang, P. J.; Cao, D. H.; Saito, S.; Arif, A. M. Self-Assembly of Cationic, Tetranuclear, Pt(II) and Pd(II) Macrocyclic Squares. X-Ray Crystal Structure of $[\text{Pt}^{2+}(\text{Dppp})(4,4\text{-Bipyridyl})_2\text{-OSO}_2\text{CF}_3]_4$. *Journal of the American Chemical Society* **1995**, *117*, 6273–6283.
- (21) Fujita, M.; Yazaki, J.; Ogura, K. Preparation of a Macrocyclic Polynuclear Complex, $[(\text{En})\text{Pd}(4,4\text{-Bpy})]_4(\text{NO}_3)_8$,¹ Which Recognizes an Organic Molecule in Aqueous Media. *Journal of the American Chemical Society* **1990**, *112*, 5645–5647.
- (22) Fujita, M. Metal-Directed Self-Assembly of Two- and Three-Dimensional Synthetic Receptors. *Chemical Society Reviews* **1998**, *27*, 417–425.
- (23) Maverick, A. W.; Klavetter, F. E. Cofacial Binuclear Copper Complexes of a Bis(β -Diketone) Ligand. *Inorganic Chemistry* **1984**, *23*, 4129–4130.
- (24) Maverick, A. W.; Buckingham, S. C.; Yao, Q.; Bradbury, J. R.; Stanley, G. G. Intramolecular Coordination of Bidentate Lewis Bases to a Cofacial Binuclear Copper(II) Complex. *Journal of the American Chemical Society* **1986**, *108*, 7430–7431.

- (25) Pariya, C.; Fronczek F. R.; Maverick, A. W. Bis(o-Phenylenebis(Acetylacetonato))Dicopper(II): A Strained Copper(II) Dimer Exhibiting a Wide Range of Colors in the Solid State. *Inorganic Chemistry* **2011**, *50*, 2748–2753.
- (26) Pariya, C.; Sparrow, C. R.; Back, C.-K.; Sandí, G.; Fronczek, F. R.; Maverick, A. W. Copper β -Diketonate Molecular Squares and Their Host–Guest Reactions. *Angewandte Chemie* **2007**, *119* (33), 6421–6424.
- (27) Davidson, G. J.; Baer, A. J.; Côté, A. P.; Taylor, N. J.; Hanan, G. S.; Tanaka, Y.; Watanabe, M. Solution and Solid-State Characterization of a Dicopper Receptor for Large Substrates. *Canadian Journal of Chemistry* **2002**, *80* (5), 496–498.
- (28) Crowley, J. D.; Bandeen, P. H. A multicomponent CuAAC “click” approach to a library of hybrid polydentate 2-pyridyl-1,2,3-triazole ligands: new building blocks for the generation of metallosupramolecular architectures. *Dalton Transactions* **2010**, *39* (2), 612–623.
- (29) Sharma, R. (unpublished work).
- (30) Pokharel, U. R.; Fronczek, F. R.; Maverick, A. W. RETRACTED ARTICLE: Reduction of Carbon Dioxide to Oxalate by a Binuclear Copper Complex. *Nature Communications* **2014**, *5* (1), 5883.
- (31) Cherutoi, J. K.; Sandifer, J. D.; Pokharel, U. R.; Fronczek, F. R.; Pakhomova, S.; Maverick, A. W. Externally and Internally Functionalized Copper(II) β -Diketonate Molecular Squares. *Inorganic Chemistry* **2015**, *54* (16), 7791–7802.
- (32) Murray, R. W.; Hiller, L. Kenneth. Supporting Electrolyte Effects in Nonaqueous Electrochemistry. Coordinative Relaxation Reactions of Reduced Metal Acetylacetonates in Acetonitrile. *Analytical Chemistry* **1967**, *39* (11), 1221–1229.
- (33) Gritzner, G. Solvent Effects on Redox Potentials: Studies in N-Methylformamide. *Journal of Electroanalytical Chemistry and Interfacial Electrochemistry* **1983**, *144* (1–2), 259–277.
- (34) Endo, Akira. Electrochemical Reduction of Some Tris(β -Diketonato)Ruthenium(III) Complexes in Acetonitrile and Interaction of the Reduced Anions with Lithium and Sodium Ions. *Bulletin of the Chemical Society of Japan*. **1983**, *56* (9), 2733–2738.
- (35) Steinbach, J. F.; Burns, J. H. Chloroform-Bearing Chelates. *Journal of the American Chemical Society* **1958**, *80* (8), 1839–1841.
- (36) Weinberg, D. R.; Gagliardi, C. J.; Hull, J. F.; Murphy, C. F.; Kent, C. A.; Westlake, B. C.; Paul, A.; Ess, D. H.; McCafferty, D. G.; Meyer, T. J. Proton-Coupled Electron Transfer. *Chemical Reviews* **2012**, *112* (7), 4016–4093.

- (37) Lexa, D.; Rentien, P. Methods for Investigating the Mechanistic and Kinetic Role of Ligand Exchange Reactions in Coordination Electrochemistry: Cyclic Voltammetry of Chloroiron(III)Tetraphenylporphyrin in Dimethylformamide. *The Journal of Electroanalytical Chemistry* **1985**, *191* (2), 253–279.
- (38) Patterson, G. S.; Holm, R. H. Effects of Chelate Ring Substituents on the Polarographic Redox Potentials of Tris(β -Diketonato)Ruthenium(II,III) Complexes. *Inorganic Chemistry* **1972**, *11* (9), 2285–2288.
- (39) Yoshikawa, Y.; Toriumi, K.; Ito, T.; Yamatera, H. Isomerism of the Metal Complexes Containing Multidentate Ligands. IX. Structure of the meso Isomer of $[\text{Co}(\text{Hexaen})]^{3+}$ (Hexaen=1,4,7,10,13,16-Hexaazacyclooctadecane). *Bulletin of the Chemical Society of Japan* **1982**, *55*, 1422–1424.
- (40) Shinohara, N.; Lilie, J.; Simic, M. G. Kinetics and Mechanism of Ligand Dissociation of Cobalt(II)-Polyamine Complexes in Aqueous Solution. *Inorganic Chemistry* **1977**, *16* (11), 2809–2813.
- (41) Takahashi, T.; Koiso, T. Conductometric Studies on the Ion-Pair Formations of $[\text{Cr}(\text{NH}_3)_6]^{3+}$, $[\text{Co}(\text{NH}_3)_6]^{3+}$, $[\text{Cr}(\text{en})_3]^{3+}$, and $[\text{Co}(\text{en})_3]^{3+}$ with Several Anions in Aqueous Solutions. *Bulletin of the Chemical Society of Japan* **1978**, *51* (5), 1307–1310.
- (42) Abbott, A. P.; El Ttaib, K.; Ryder, K. S.; Smith, E. L. Electrodeposition of Nickel Using Eutectic Based Ionic Liquids. *The International Journal of Surface Engineering and Coatings* **2008**, *86*, 234–240.
- (43) Yang, J.; Seneviratne, D.; Arbatin, G.; Andersson, A. M.; Curtis, J. C. Spectroscopic and Electrochemical Evidence for Significant Electronic Coupling in Mixed-Valence Hydrogen-Bonded Adducts of Ruthenium Cyano and Ethylenediamine Complexes. *J. Am. Chem. Soc.* **1997**, *119*, 5329–5336.
- (44) Du, J.; Chen, Z.; Chen, C.; Meyer, T. J. A Half-Reaction Alternative to Water Oxidation: Chloride Oxidation to Chlorine Catalyzed by Silver Ion. *Journal of the American Chemical Society* **2015**, *137*, 3193–3196.
- (45) Taqui Khan, M. M.; Venkatasubramanian, K.; Abdi, S. H. R.; Bhadbhadem, M. M.; Tyagi. Structure of Tris(Dimethylglyoxime)Ruthenium(II) Dichloride. *Acta Crystallographica Section C: Crystal Structure Communications* **1992**, *48* (8), 1402–1405.
- (46) Caballero, A.; Zapata, F.; Beer, P. D. Interlocked Host Molecules for Anion Recognition and Sensing. *Coordination Chemistry Reviews* **2013**, *257*, 2434–2455.
- (47) Kavallieratos, K.; de Gala, S. R.; Austin, D. J.; Crabtree, R. H. A Readily Available Non-Preorganized Neutral Acyclic Halide Receptor with an Unusual Nonplanar Binding Conformation. *Journal of the American Chemical Society* **1997**, *119*, 2325–2326.

- (48) Kavallieratos, K.; Bertao, C. M.; Crabtree, R. H. Hydrogen Bonding in Anion Recognition: A Family of Versatile, Nonpreorganized Neutral and Acyclic Receptors. *The Journal of Organic Chemistry* **1999**, *64*, 1675–1683.
- (49) Xue, W.; Wu, K.; Ouyang, N.; Brotin, T.; Nitschke, J. R. Allosterically Regulated Guest Binding Determines Framework Symmetry for an Fe^{II}₄L₄ Cage. *Angewandte Chemie International Edition* **2023**, *135* (18), e202301319.
- (50) Dabb, S. L.; Fletcher, N. C. Mer and Fac Isomerism in Tris Chelate Diimine Metal Complexes. *Dalton Transactions* **2015**, *44*, 4406–4422.
- (51) Metherell, A. J.; Cullen, W.; Stephenson, A.; Hunter, C. A.; Ward, M. D. Fac and Mer Isomers of Ru(II) tris(pyrazolyl-pyridine) Complexes as Models for the Vertices of Coordination Cages: Structural Characterisation and Hydrogen-Bonding Characteristics. *Dalton Transactions* **2014**, *43*, 71–84.
- (52) Wagner, H. E.; Di Martino-Fumo, P.; Boden, P.; Zimmer, M.; Klopper, W.; Breher, F.; Gerhards, M. Structural Characterization and Lifetimes of Triple-Stranded Helical Coinage Metal Complexes: Synthesis, Spectroscopy and Quantum Chemical Calculations. *Chemistry–A European Journal* **2020**, *26* (47), 10743–10751.
- (53) Cook, T. R.; Stang, P. J. Recent Developments in the Preparation and Chemistry of Metallacycles and Metallacages via Coordination. *Chemical Reviews* **2015**, *115* (15), 7001–7045.
- (54) Maverick, A. W.; Klavetter, F. E. Cofacial binuclear copper complexes of a bis(beta-diketone) ligand. *Inorganic Chemistry* **1984**, *23* (25), 4129–4130.
- (55) Pariya, C.; Sparrow, C. R.; Back, C. K.; Sandí, G.; Fronczek, F. R.; Maverick, A. W. Copper β- Diketonate Molecular Squares and Their Host–Guest Reactions. *Angewandte Chemie* **2007**, *119* (33), 6421–6424.
- (56) Pariya, C.; Fronczek, F. R.; Maverick, A. W. Bis(o-phenylenebis(acetylacetonato)) dicopper(II): A strained copper(II) dimer exhibiting a wide range of colors in the solid state. *Inorganic Chemistry* **2011**, *50* (7), 2748–2753.
- (57) Rancan, M.; Tessarolo, J.; Casarin, M.; Zanonato, P. L.; Quici, S.; Armelao, L. Double Level Selection in a Constitutional Dynamic Library of Coordination Driven Supramolecular Polygons. *Inorganic Chemistry* **2014**, *53*, 7276–7287.
- (58) Muley, A.; Karumban, K. S.; Kumbhakar, S.; Giri, B.; Maji, S. High Phenoxazinone Synthase Activity of Two Mononuclear Cis-Dichloro Cobalt(II) Complexes with a Rigid Pyridyl Scaffold. *New Journal of Chemistry* **2022**, *46*, 521–532.
- (59) Zhang, B.; Li, J.; Pang, M.; Wang, Y-S.; Liu, M-Z.; Zhao, H-M. Four Discrete Silver Iodobismuthates/Bromobismuthates with Metal Complexes: Syntheses, Structures, Photocurrent Responses, and Theoretical Studies. *Inorganic Chemistry* **2022**, *61*, 406–413.

- (60) Liu, Z.; Wu, Y.; Zhao, Y.; Cheng, M.; Liu, Qi. Inorganic–Organic Hybrids Assembled by Flexible Multidentate Linker: Design, Structure and Luminescence. *Transition Metal Chemistry* **2021**, *46*, 575–581.
- (61) Hancock, R. The Pyridyl Group in Ligand Design for Selective Metal Ion Complexation and Sensing. *Chemical Society Reviews* **2021**, *42*, 1500–1524.
- (62) Guo, K-K.; Jiang, X-Y.; Xu, M.; Li, F-Y.; Dong, S-M.; Zheng, Y.; Xu, L. An Unprecedented Polyoxometalate-Based 1D Double Chain Compound with Opposite Charges Enables Conductivity Improvement. *Chemical Communications* **2021**, *57*, 11398–11401.
- (63) Crowley, J. D.; McMorran, D. A. “Click-triazole” coordination chemistry: Exploiting 1,4-disubstituted-1,2,3-triazoles as ligands. *Click Triazoles* **2012**, 31-83.
- (64) Stuart I. Bailey; Ian M. Ritchie; Frank R. Hewgill. The Construction and Use of Potential-pH Diagrams in Organic Oxidation-Reduction Reactions. *Journal of the Chemical Society. Perkin Transactions 2* **1983**, *5*, 645–652.
- (65) Beverskog, B.; Puigdomenech, I. Revised Pourbaix Diagrams for Iron at 25-300°C. *Corrosion Science* **1996**, *38* (12), 2121–2135.
- (66) Sepehrpour, H.; Fu, W.; Sun, Y.; Stang, P. J. Biomedically Relevant Self-Assembled Metallacycles and Metallacages. *Journal of the American Chemical Society* **2019**, *141*, 14005–14020.
- (67) Inokuma Yasuhide; Tatsuhiko Arai; Makoto Fujita. Networked Molecular Cages as Crystalline Sponges for Fullerenes and Other Guests. *Nature Chemistry* **2010**, *2*, 780–783.
- (68) Jones, L.; Kilner, C. A.; Halcrow, M. A. A Cobalt Metallacrown Anion Host with Guest-Dependent Redox Activity. *Chemistry– A European Journal* **2009**, *15*, 4667–4675.
- (69) Ballester, P. Experimental Quantification of Anion- π Interactions in Solution Using Neutral Host-Guest Model Systems. *Accounts of Chemical Research* **2013**, *46*, 874–884.
- (70) Mattsson, J.; Govindaswamy, P.; Furrer, J.; Sei, Y.; Yamaguchi, K.; Suss-Fink, G.; Therrien, B. Encapsulation of Aromatic Molecules in Hexanuclear Arene Ruthenium Cages: A Strategy to Build Up Organometallic Carceplex Prisms with a Dangling Arm Standing Out. *Organometallics* **2008**, *27*, 4346–4356.
- (71) Mishra, A.; Jeong, Y. J.; Jo, J-H.; Kang, S. C.; Kim, H.; Chi, K-W. Coordination-Driven Self-Assembly and Anticancer Potency Studies of Arene–Ruthenium-Based Molecular Metalla-Rectangles. *Organometallics* **2014**, *33*, 1144–1151.
- (72) Singh, N.; Jang, S.; Jo, J-H.; Kim, D. H.; Park, D. W.; Kim, I.; Kim, H.; Kang, S. C.; Chi, K-W. Coordination-Driven Self-Assembly and Anticancer Potency Studies of Ruthenium–Cobalt-Based Heterometallic Rectangles. *Chemistry– A European Journal* **2016**, *22*, 16157–16164.

- (73) Plajer, A. J.; Rizzuto, F. J.; von Krbek, L. K. S.; Gisbert, Y.; Martínez-Agramunt, V.; Nitschke, J. R. Oxidation Triggers Guest Dissociation during Reorganization of an FeII₄L₆ Twisted Parallelogram. *Chemical Science* **2020**, *11* (38), 10399–10404.
- (74) Chantarojsiri, T.; Ziller, J. W.; Yang, J. Y. Incorporation of Redox-Inactive Cations Promotes Iron Catalyzed Aerobic C–H Oxidation at Mild Potentials. *Chemical Science* **2018**, *9*, 2567–2574.
- (75) Kang, K.; Fuller, J.; Reath, A.; Ziller, J. W.; Alexandrova, A. N.; Yang, J. Y. Installation of Internal Electric Fields by Non-Redox Active Cations in Transition Metal Complexes. *Chemical Science* **2019**, *10*, 10135–10142.
- (76) Ma, J. C.; Dougherty, D. A. The Cation– π Interaction. *Chemical Reviews* **1997**, *97*, 1303–1324.
- (77) Elschenbroich, C.; Wolf, M.; Schiemann, O.; Harms, K.; Burghaus, O.; Pebler, J. Head-on versus Side-on [5-5]Bitrovacenes Featuring Benzene and Naphthalene Units as Spacers: How π -Stacking Affects Exchange Coupling and Redox Splitting. *Organometallics* **2002**, *21*, 5810–5819.
- (78) Connelly, N. G.; Geiger, W. E. Chemical Redox Agents for Organometallic Chemistry. *Chemical Reviews* **1996**, *96*, 877–910.
- (79) Blackburn, P. T.; Mansoor, I. F.; Dutton, K. G.; Tyryshkin, A. M.; Lipke, M. C. Accessing Three Oxidation States of Cobalt in M₆L₃ Nanoprisms with Cobalt-Porphyrin Walls. *Chemical Communications* **2021**, *57* (86), 11342–11345.
- (80) Vaněčková, E.; Bouša, M.; Vivaldi, F.; Gál, M.; Rathouský, J.; Kolivoška, V.; Sebechlebská, T. UV/VIS Spectroelectrochemistry with 3D Printed Electrodes. *Journal of Electroanalytical Chemistry* **2020**, *857*, 113760.
- (81) Munery, S.; Ratel-Ramond, N.; Benjalal, Y.; Vernisse, L.; Guillermet, O.; Bouju, X.; Coratger, R.; Bonvoisin, J. Synthesis and Characterization of a Series of Ruthenium Tris(β -Diketonato) Complexes by an UHV-STM Investigation and Numerical Calculations. *European Journal of Inorganic Chemistry* **2011**, 2698–2705.
- (82) Barlow, J. M.; Clarke, L.; Zhang, Z.; Bím, D.; Ripley, K.; Zito, A.; Brushett, F.; Alexandrova, A. N.; Yang, J. Y. Molecular Design of Redox Carriers for Electrochemical CO₂ Capture and Concentration. *Chemical Society Reviews* **2022**, *51*, 8415–8433.
- (83) Endo, A.; Kajitani, M.; Mukaida, M.; Shimizu, K.; Sato, G. P. A New Synthetic Method for Ruthenium Complexes of β -Diketones from ‘Ruthenium Blue Solution’ and Their Properties. *Inorganica Chimica Acta* **1988**, *150*, 25–34.

- (84) Dubrovina, N. V.; Tararov, V. I.; Monsees, A.; Kadyrov, R.; Fischer, C.; Borner, A. Economic Preparation of 1,3-Diphenyl-1,3-Bis(Diphosphino)Propane: A Versatile Chiral Diphosphine Ligand for Enantioselective Hydrogenations. *Tetrahedron: Asymmetry* **2003**, *14* (18), 2739–2745.
- (85) Hein, R.; Beer, P. D.; Davis, J. J. Electrochemical Anion Sensing: Supramolecular Approaches. *Chemical Reviews* **2020**, *120*, 1888–1935.
- (86) Beer, P. D.; Gale, P. A. Anion Recognition and Sensing: The State of the Art and Future Perspectives. *Angewandte Chemie International Edition* **2001**, *40*, 486–516.
- (87) Hupp, J. T.; Weaver, M. J. Solvent, Ligand, and Ionic Charge Effects on Reaction Entropies for Simple Transition-Metal Redox Couples. *Inorganic Chemistry* **1984**, *23*, 3639–3644.
- (88) Li, H.; Zhang, Z.; Zhou, H.; Zhao, G.; Wang, C. Efficient Annihilation Electrochemiluminescence of [Ru(Bpy)₃]²⁺ within a Deep Eutectic Solvent as Green Electrolyte. *Dyes and Pigments* **2023**, *211*, 111052.
- (89) Zieliński, T.; Jurczak, J. Thioamides versus Amides in Anion Binding. *Tetrahedron* **2005**, *61* (16), 4081–4089.
- (90) Tremlett, W. D. J.; Söhnel, T.; Crowley, J. D.; Wright, J.; Hartinger, C. G. Ferrocene-Derived Palladium(II)-Based Metallosupramolecular Structures: Synthesis, Guest Interaction, and Stimulus- Responsiveness Studies. *Inorganic Chemistry* **2023**, *62*, 3616–3628.
- (91) Zubi, A.; Wragg, A.; Turega, S.; Adams, H.; Costa, P. J.; Félix, V.; Thomas, J. A. Modulating the Electron-Transfer Properties of a Mixed-Valence System through Host–Guest Chemistry. *Chemical Science* **2015**, *6*, 1334.
- (92) Smolenaers, P. J.; Beattie, J. K.; Hutchinson, N. D. Crystal and Molecular Structure of Racemic Tris(Ethylenediamine)Ruthenium(II) Tetrachlorozincate(II). *Inorganic Chemistry* **1981**, *20* (7), 2202–2206.
- (93) Rillema, D. P.; Jones, D. S. Structure of Tris(2,2'-Bipyridyl)Ruthenium(II) Hexafluorophosphate, [Ru(bipy)₃][PF₆]₂; X-Ray Crystallographic Determination. *Journal of the Chemical Society, Chemical Communications* **1979**, No. 19, 849–851.
- (94) Puttreddy, R.; Hutchison, J. A.; Gorodetski, Y.; Harrowfield, J.; Rissanen, K. Enantiomer Separation of Tris(2,2'-Bipyridine)Ruthenium(II): Interaction of a D₃-Symmetric Cation with a C₂-Symmetric Anion. *Crystal Growth & Design* **2015**, *15* (4), 1559–1563.
- (95) Langton, M. J.; Serpell, C. J.; Beer, P. D. Anion Recognition in Water: Recent Advances from a Supramolecular and Macromolecular Perspective. *Angewandte Chemie International Edition* **2016**, *55*, 1974–1987.
- (96) Kubik, S. Anion Recognition in Water. *Chemical Society Reviews* **2010**, *39*, 3648–3663.

- (97) Vasdev, R. A. S.; Findlay, J. A.; Turner, D. R.; Crowley, J. D. Self-Assembly of a Redox Active, Metallosupramolecular $[Pd_3L_6]^{6+}$ Complex Using a Rotationally Flexible Ferrocene Ligand. *Chemistry: An Asian Journal* **2020**, *16*, 39–43.
- (98) Vasdev, R. A. S.; Findlay, J. A.; Garden, A. L.; Crowley, J. D. Redox Active $[Pd_2L_4]^{4+}$ Cages Constructed from Rotationally Flexible 1,10-Disubstituted Ferrocene Ligands. *Chemical Communications* **2019**, *55*, 7506–7509.
- (99) Li, J.; Zhang, G.; Zhang, D.; Zheng, R.; Shi, Q.; Zhu, D. Boron-Containing Monopyrrolo-Annulated Tetra Thiafulvalene Compounds: Synthesis and Absorption Spectral/Electrochemical Responsiveness toward Fluoride Ion. *The Journal of Organic Chemistry* **2010**, *75*, 5330–5333.
- (100) Kirchner, J. G. Modern Techniques in TLC. *Journal of Chromatographic Science* **1975**, *13* (12), 558–563.
- (101) Merritt, L. L.; Lanterman, E. The Crystal Structure of Dimethylglyoxime. *Acta Crystallographica* **1952**, *5* (6), 811–817.
- (102) Shaker, S. A. Preparation and Spectral Properties of Mixed-Ligand Complexes of VO(IV), Ni(II), Zn(II), Pd(II), Cd(II) and Pb(II) with Dimethylglyoxime and N-Acetyl glycine. *Journal of Chemistry* **2010**, *7*, S580–S586.
- (103) Schepartz, A.; McDevitt, J. P. Self-Assembling Ionophores. *Journal of the American Chemical Society* **1989**, *111*, 5977–5978.

Vita

Jasmine Shermaine Sanford was born in Baton Rouge, Louisiana. She received her Bachelor of Science degree in Chemistry from Louisiana State University in 2017. She is currently a candidate for the Doctor of Philosophy degree in the Department of Chemistry at Louisiana State University and Agricultural and Mechanical College with Dr. Andrew W. Maverick as her advisor.